

Beta human papillomavirus E6: a menace to genomic integrity

by

Dalton Dacus

B.S., Kansas State University, 2015

AN ABSTRACT OF A DISSERTATION

submitted in partial fulfillment of the requirements for the degree

DOCTOR OF PHILOSOPHY

Division of Biology
College of Arts and Sciences

KANSAS STATE UNIVERSITY
Manhattan, Kansas

2022

Abstract

Beta genus human papillomaviruses (β -HPV) are associated with the development of cutaneous squamous cell carcinomas (cSCC) by destabilizing the genome. *In vitro and in vivo* studies indicate the β -HPV E6 and E7 proteins act as co-factors with ultraviolet radiation (UV) to cause genome destabilization. However, the E6 protein from β -HPV type 8 (8 E6) induces tumor formation in mice without UV exposure, but the mechanisms driving carcinogenesis are unclear. In this dissertation, we investigated UV-independent mechanisms of HPV8 E6-induced genome destabilization. *In silico* screens validated by cell line characterization showed that 8 E6 deregulated the Hippo pathway by destabilizing the histone acetyltransferase, p300. Hippo pathway disruption increased cell proliferation and attenuated cell death in response to failed cytokinesis. While 8 E6 alone was unable to promote long-term proliferation after cytokinesis failure, we demonstrated that 8 E6 combined with *TERT* expression rescued long-term proliferation. However, this resulted in increased genomic instability in the form of ploidy changes. Furthermore, we showed 8 E6 decreased the abundance of anaphase bridge resolving helicase, Bloom syndrome protein (BLM). The diminished BLM was associated with increased segregation errors and micronuclei. 8 E6 reduced antiproliferative responses to micronuclei and time-lapse imaging revealed 8 E6 promoted cells with micronuclei to complete mitosis. Finally, whole-genome sequencing demonstrated that 8 E6 induced a mutational phenomenon known as chromothripsis, in 9 chromosomes. Overall, the findings from my dissertation provide insight into the processes by which 8 E6 induces genome instability in the absence of UV exposure.

Beta human papillomavirus E6: a menace to genomic integrity

by

Dalton Dacus

B.S., Kansas State University, 2015

A DISSERTATION

submitted in partial fulfillment of the requirements for the degree

DOCTOR OF PHILOSOPHY

Division of Biology
College of Arts and Sciences

KANSAS STATE UNIVERSITY
Manhattan, Kansas

2022

Approved by:

Major Professor
Dr. Nicholas Wallace

Copyright

© Dalton Dacus 2022.

Abstract

Beta genus human papillomaviruses (β -HPV) are associated with the development of cutaneous squamous cell carcinomas (cSCC) by destabilizing the genome. *In vitro and in vivo* studies indicate the β -HPV E6 and E7 proteins act as co-factors with ultraviolet radiation (UV) to cause genome destabilization. However, the E6 protein from β -HPV type 8 (8 E6) induces tumor formation in mice without UV exposure, but the mechanisms driving carcinogenesis are unclear. In this dissertation, we investigated UV-independent mechanisms of HPV8 E6-induced genome destabilization. *In silico* screens validated by cell line characterization showed that 8 E6 deregulated the Hippo pathway by destabilizing the histone acetyltransferase, p300. Hippo pathway disruption increased cell proliferation and attenuated cell death in response to failed cytokinesis. While 8 E6 alone was unable to promote long-term proliferation after cytokinesis failure, we demonstrated that 8 E6 combined with *TERT* expression rescued long-term proliferation. However, this resulted in increased genomic instability in the form of ploidy changes. Furthermore, we showed 8 E6 decreased the abundance of anaphase bridge resolving helicase, Bloom syndrome protein (BLM). The diminished BLM was associated with increased segregation errors and micronuclei. 8 E6 reduced antiproliferative responses to micronuclei and time-lapse imaging revealed 8 E6 promoted cells with micronuclei to complete mitosis. Finally, whole-genome sequencing demonstrated that 8 E6 induced a mutational phenomenon known as chromothripsis, in 9 chromosomes. Overall, the findings from my dissertation provide insight into the processes by which 8 E6 induces genome instability in the absence of UV exposure.

Table of Contents

List of Figures	ix
List of Supplementary Figures.....	x
List of Tables	xi
Glossary	xii
Acknowledgements.....	xv
Dedication.....	xvii
Chapter 1 - Introduction.....	1
Beta human papillomavirus and skin cancer	1
References.....	3
Chapter 2 - Beta-Genus Human Papillomavirus 8 E6 Destabilizes the Host Genome by Promoting p300 Degradation.....	6
Abstract.....	7
Keywords	7
Introduction.....	7
Materials and Methods.....	9
Results.....	9
p300 Is a Master Transcription Regulator and Tumor Suppressor	9
HPV8 E6 Reduces Genome Stability by Destabilizing p300	11
ATR.....	12
ATM.....	12
DNA-PK	13
Double Strand Break Repair	13
Cell-Cycle Checkpoints and Differentiation.....	14
p53.....	15
How Conserved Is p300 Binding among β -HPV E6s.....	16
Confirming the Dependence of a HPV8 E6 Phenotype on p300 Destabilization.....	19
Discussion.....	25
Conclusions and Future Directions.....	26
Author Contributions	28

Funding	28
Acknowledgments	29
References.....	29
Chapter 3 - Beta Human Papillomavirus 8E6 Attenuates LATS Phosphorylation after Failed	
Cytokinesis	41
Abstract.....	42
Importance	42
Introduction.....	42
Results.....	45
Loss of p300 alters Hippo pathway gene expression.....	45
β-HPV E6 expression alters Hippo pathway gene expression.....	47
p300 is necessary for a robust Hippo pathway response to failed cytokinesis.	49
β-HPV 8E6 attenuates LATS2 phosphorylation but does not impede nuclear exclusion of YAP.....	51
β-HPV 8E6 attenuates p53 accumulation after failed cytokinesis.....	52
β-HPV 8E6 does not completely abrogate the Hippo pathway.	56
Discussion.....	59
Materials and Methods.....	60
Acknowledgments	64
Supplementary Data.....	65
References.....	65
Chapter 4 - β-HPV 8E6 combined with TERT expression promotes long-term proliferation and	
genome instability after cytokinesis failure.....	71
Abstract.....	72
Keywords	72
Introduction.....	72
Results.....	75
β-HPV 8E6 exacerbates aneuploidy in <i>TERT</i> -HFKs after recovering from failed cytokinesis	79
Discussion.....	81
Material and methods.....	84
Acknowledgments:	87

Supplementary data.....	87
References.....	88
Chapter 5 - Beta HPV8 E6 Induces Micronuclei Formation and Promotes Chromothripsis	95
Abstract.....	96
Importance	96
Introduction.....	97
Results.....	99
p300-dependent BLM reduction correlates with loss of ATR and Chk1 abundance.	99
8 E6 reduces BLM at anaphase bridges increasing unresolved bridge frequency	102
8 E6 increases micronuclei frequency, in part through BLM reduction.	104
8 E6 reduces Lamin B1 integrity of micronuclei	106
8 E6 promotes some nuclear function despite disrupted micronuclear envelopes	109
8 E6 reduces apoptosis and senescence in response to micronuclei	111
8 E6 promotes chromothripsis events	113
Discussion.....	115
Material and Methods	117
Supplementary Data.....	122
Acknowledgements.....	127
References.....	127
Chapter 6 - Conclusions and Future Directions	135
Chromosomal Instability After Cytokinesis Failure.....	135
Consequences of BLM Reduction	136
Micronucleus Formation.....	138
Mutational Signatures	139
Big Picture Ideas.....	139
References.....	140

List of Figures

Figure 2.1. p300 structural domain and their localization.	10
Figure 2.2. Phylogenetic tree of β -HPV and MmuPV1 based on the E6 nucleotide sequence. ...	19
Figure 3.1. Loss of p300 leads to changes in Hippo pathway gene expression.....	46
Figure 3.2. β -HPV 8E6 alters Hippo pathway gene expression.	49
Figure 3.3. Loss of p300 impedes the Hippo pathway's response to failed cytokinesis.	50
Figure 3.4. β -HPV 8E6 diminishes LATS phosphorylation during failed cytokinesis.	52
Figure 3.5. β -HPV 8E6 attenuates p53 accumulation upon H2CB-induced failed cytokinesis ...	53
Figure 3.6. β -HPV 8E6 hinders LATS phosphorylation and p53 accumulation after failed cytokinesis.....	55
Figure 3.7. β -HPV 8E6 increases SA β -Gal staining and reduces YAP abundance after failed cytokinesis.....	56
Figure 3.8. β -HPV 8E6 does not inhibit the Hippo pathway's response to cellular density.	58
Figure 4.1. H2CB-induced failed cytokinesis prevents long-term proliferation	76
Figure 4.2. TERT expression promotes recovery from failed cytokinesis.	78
Figure 4.3. β -HPV 8E6 and cytokinesis failure induce changes in ploidy.	80
Figure 4.4. β -HPV 8E6 and telomerase activation affect cell fate after failed cytokinesis.	82
Figure 5.1. HPV8 E6 reduces BLM abundance.....	100
Figure 5.2. HPV8 E6 augments segregation error rate independent of p300.	103
Figure 5.3. HPV8 E6 increases micronuclei frequency.....	105
Figure 5.4. HPV8 E6 reduces Lamin B1 integrity of micronuclei.	107
Figure 5.5. Some micronuclear functions changed by HPV8 E6.	110
Figure 5.6. HPV8 E6 reduces a cell's apoptotic and senescent response to micronuclei.....	111
Figure 5.7. HPV8 E6 promotes non-canonical chromothripsis.	114

List of Supplementary Figures

Figures S 4.1. Responses to H2CB-induced failed cytokinesis in TERT-HFK.....	87
Figures S 4.2. TERT-HFK recovering from H2CB-induced cytokinesis failure.	88
Figures S 5.1. p300 level detected by immunoblot.....	122
Figures S 5.2. Time-lapse images of anaphase bridge duration.	123
Figures S 5.3. 8 E6 increases micronuclei frequency in U2OS cells.....	123
Figures S 5.4. Characteristics of micronuclei in E6 expression HFK cells.	124
Figures S 5.5. Representative images of nuclear activity in micronuclei of varying envelope status.	125
Figures S 5.6. Representative chromothripsis plots for each chromothripsis category.	125

List of Tables

Table 2.1 Phenotypes of HPV8 E6 Δ 132-136 that are weaker than those of wild type HPV8 E6.	21
Table 2.2 Phenotypes of HPV8 E6 Δ 132-136 analogous to wild type HPV8 E6.....	21
Table 2.3 . Phenotypes of HPV8 E6 that have been confirmed to be through the destabilization of p300.....	25

Glossary

annexin V – a common marker of apoptosis “see apoptosis”

apoptosis – the process of programmed cell death

centromere – the region of a chromosome to which the microtubules of the spindle attach during cell division

centrosome – an organelle that facilitates the organization of the spindle poles during mitosis

cytokinesis – the cytoplasmic division of a cell at the end of mitosis, bringing about the separation into two daughter cells

differentiation -- the process by which dividing cells change from one cell type to another and serves as a form of cell cycle exit for skin cells

dihydrocytochalasin B – inhibitor of cytokinesis

DNA damage response – a complex network of genes responsible for sensing and responding to specific types of DNA damage as well as repairing said damage to maintain genome integrity

E6 – a beta human papillomavirus gene that encodes a protein of the same name with host pathway altering functions

E7 – a beta human papillomavirus gene that encodes a protein of the same name with host pathway altering functions

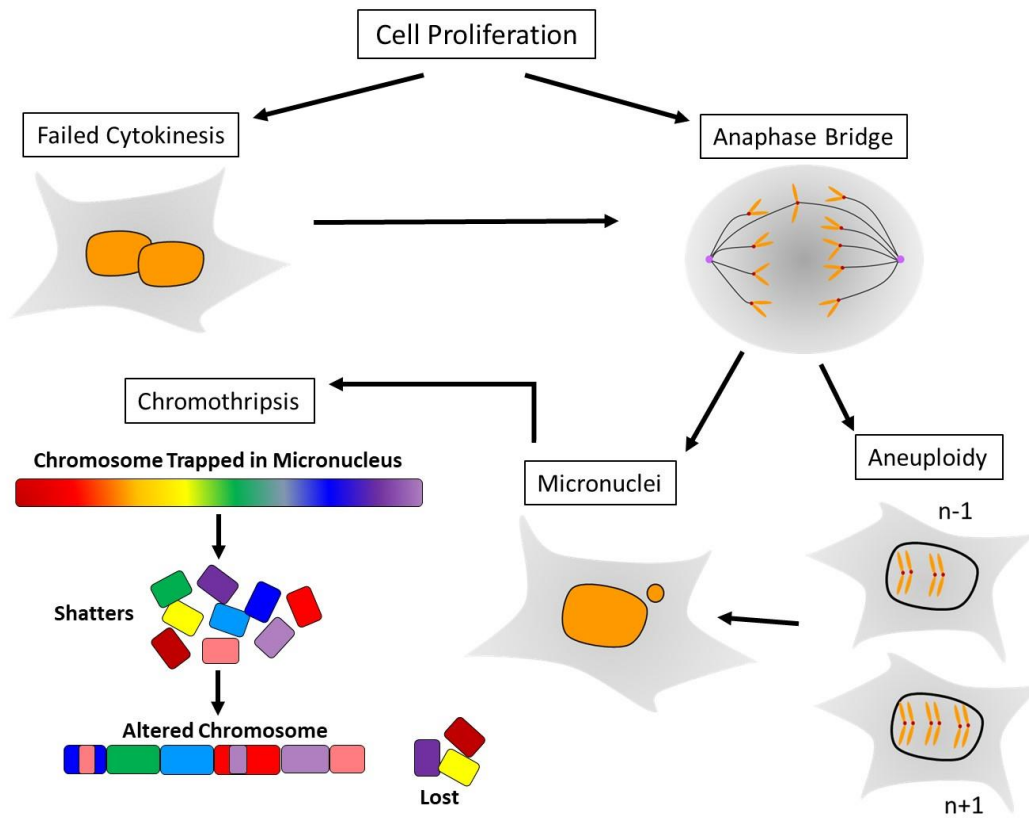
epidermodysplasia verruciformis – a rare autosomal recessive hereditary skin disorder associated with increased beta human papillomavirus infections and high risk of skin cancer

gene knockout – a genetic technique in which one of an organism's genes is made inoperative

gene ontology – a community-based bioinformatics resource that employs ontologies to represent biological knowledge and describes information about gene and gene product function

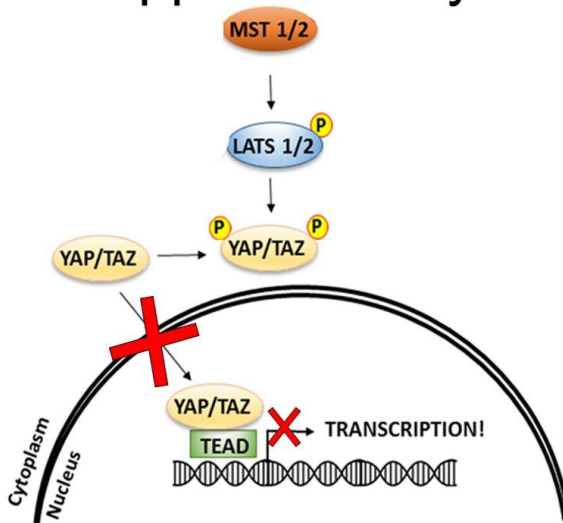
genome instability [See image below] –

- **anaphase bridge** – DNA threads stretching between the two DNA masses as cells attempt to segregate them during anaphase
- **aneuploidy** – having or missing extra chromosomes
- **chromothripsis** – a mutational phenomenon characterized by massive, clustered chromosomal rearrangements that occurs in a single event
- **failed cytokinesis** – cells fail to divide after replicating their DNA
- **micronuclei** – extra-nuclear bodies that contain damaged chromosome fragments and/or whole chromosomes that were not incorporated into the nucleus after cell division



Hippo pathway – an evolutionarily conserved signaling pathway that controls cell proliferation and death. Core proteins in this pathway include mammalian Sterile 20-related 1 and 2 kinases (MST1 and MST2), Large tumor suppressor 1 and 2 kinases (LATS1 and LATS2), Yes-associated protein 1 (YAP), Transcriptional coactivator with PDZ-binding motif (TAZ), and TEA domain family member (TEAD) transcription factors (TEAD1-4) [See image below].

Hippo Pathway



hit-and-run hypothesis – beta human papillomaviruses promote the accumulation of tumor driving mutations that persist after the transient viral lifecycle is complete

immortalization – the manipulation of cells to proliferate indefinitely and can thus be cultured for long periods of time

immunoblot – a technique for analyzing or identifying proteins in a mixture, involving separation by electrophoresis followed by staining with antibodies

in silico – a study performed on computer or via computer simulation

in vitro – studies conducted in with microorganisms, cells, or biological molecules outside their normal biological context

in vivo – research or work is done with or within an entire, living organism

keratinocytes - an epidermal cell which produces keratin

kinase – an enzyme that catalyzes the transfer of a phosphate group from ATP to a specified molecule (or to phosphorylate)

oncogenic – causing development of a tumor or tumors

p300 – a protein with acetyltransferase activity that regulates gene expression

p53 – a transcription factor that suppresses tumor formation by regulating cell division and cell death

phosphomimetic – amino acid substitutions that mimic a phosphorylated protein, thereby activating (or deactivating) the protein

ploidy – the number of sets of chromosomes in a cell, or in the cells of an organism

proliferation - an increase in the number of cells because of cell growth and cell division

propidium iodide – a red fluorescent intercalating agent used to stain dead cells as it does not permeate live cells

senescence – permanent cell cycle arrest driven by different forms of cellular stress

TERT – the gene that encodes the enzyme responsible for maintenance of the length of telomeres

ultraviolet radiation – a form of non-ionizing radiation that is emitted by the sun and artificial sources such as tanning beds

wildtype – a phenotype, genotype, or gene that predominates in a natural population of organisms

Acknowledgements

I would first like to thank my advisor Dr. Nicholas Wallace for not only helping me traverse the cogs in the machine that is science but also for making the journey fun and exciting. Watching you sprint past your goals while simultaneously being there with whole-hearted support for each of us makes it difficult for me to not aspire to become half as great as you.

A large thank you to my committee members over the years. Dr. Zhilong Yang, Dr. Stella Lee, Dr. Jianzhong Yu, Dr. Sherry Fleming, and Dr Ryan Rafferty, you have helped to make me a better scientist. I am thankful for all your feedback over these years. A special shout-out to Zhilong and Shuai for being my first mentors as I baby stepped into science. Your patience, the friendships forged, and the skills you taught me, will never be forgotten.

I want to thank all my lab mates who have all helped make me the man/scientist I am today. Spending time with you wacky folk has been a honor and I will cherish the memories we've made. I thank everyone that I've mentored, each one of you helped me grow and I enjoyed getting to know you all. A special thanks to Sebastian and Changkun for putting up with me for so long and helping expand my tastebuds into new dimensions.

Thank you to the all the wonderful people who make up the Division's Staff. Not only have you made my time here go by more smoothly, but you also helped create memories that I will never forget. Memories of the hundreds of crosswords completed with the ever-rowdy lunch gang, the endless sharing of stories with Matt and Ken, and inspiring nuggets of wisdom from Greg, Melissa, Sarah, and Tari. And a special thanks to Justin for your guidance and friendship. Teaching lab was always a blast thanks to your sage-like wisdom and support.

To my dear friends, thank you for keeping me sane during these years. I wouldn't choose anyone else to trip through life or roll into battle with. You have all truly been a blessing in my

life and I cannot wait to see all of you more often. To Silver, thank you, for all the love and support through the years. To my fellow graduate students who have become my work family, I am grateful for the breaks from science we've enjoyed. From softball and volleyball to BBQs and costume parties, I wish you all the best in your future endeavors.

A huge thank you to my entire family, you have all afforded me a loving, supportive network that allows me to be the best version of myself. No matter the potholes I've encountered you are always there to help me move forward. To my wonderful sister Paige, watching you thrive is inspiring and it pushes me every day to be the best that I can be. To my parents Mark and Brenda Dacus. I am eternally grateful for all you have done for me. Dad, thank you for showing me what it means to work hard, to laugh at yourself even when no one else is, and how to be the foundation for an amazing family. Mom, thank you for the years of unwavering support, tear-jerking love, and showing me what caring for others is all about.

Finally, to the one, the only, Emily Burghardt. My fiancée, my best friend, and the amazing person who I will never stop being thankful for. Your support has been instrumental towards my success. Thank you again and again for all you have done and know that I Love you more than food itself.

Dedication

I dedicate this dissertation to my Uncle Clyde. I hope the beach is relaxing and beer cold.

Chapter 1 - Introduction

Beta human papillomavirus and skin cancer

Human papillomaviruses (HPV) are a large family of small, non-enveloped DNA viruses associated with numerous epithelial malignancies (1). The HPV genome comprises circular double-stranded DNA approximately 8-kb in length. The genome is organized into three distinct regions: i) the long control region, involved in viral transcription and replication; ii) the early region, which encodes the E1-E8 proteins which play a key role in viral gene expression and survival; and iii) the late region, which encodes for the capsid proteins, L1 and L2 (2). These regions are highly conserved among the more than 200 HPV types that have been discovered so far. HPV types are organized into five genera: alpha, beta, gamma, mu, and nu (3). The alpha and beta types have been the most thoroughly studied due to their associations with cancer (4). Alpha-HPVs infect the mucosal epithelia, and a portion of them, classified as the high-risk types, are responsible for virtually all cervical cancers and a subset of head-and-neck cancers (5).

Beta genus HPVs (β -HPV) are ubiquitous in the skin of the general population (6, 7). These cutaneous viruses are subdivided into five different species: beta-1, -2, -3, -4, and -5, with species 1 and 2 being the most prevalent (8). The first β -HPV types, HPV5 and HPV8, were originally found in skin warts and cutaneous squamous cell carcinoma (cSCC) of patients with a rare genetic disorder, epidermodysplasia verruciformis (EV) (9, 10). These patients are more susceptible to β -HPV infections and develop skin lesions from the time they are born. Lesions in 30-60% of EV patients develop into cSCC after a few decades, mostly in sun-exposed areas (9). These tumors harbor high copy numbers of certain β -HPVs and about 90% of the tumors are associated with HPV5 and HPV8, both beta-1 species (11). The International Agency for

Research on Cancer classified these two β -HPVs as "possibly carcinogenic" in EV patients in 2009 (12).

The frequency of β -HPVs in cSCC, however, is lower in the general population than in EV patients (6, 13). While recent analysis demonstrates that certain β -HPV types are associated with an increased risk of cSCC, the viral load in tumor biopsies is less than one copy of viral DNA per cell (14, 15). This is in contrast to alpha-HPVs, which require at least one copy in each malignant cell to maintain tumorigenicity and often have more on average (16, 17). Further, among the few published studies, only one has found evidence of β -HPV transcription in non-EV-associated cSCCs (18), indicating that, unlike alpha-HPVs, β -HPV expression is not required for the malignant phenotype to persist in cSCCs. Taken together, these data indicate that β -HPV is involved in tumor initiation rather than tumor maintenance. The high prevalence (up to 50 copies/cell) of β -HPV DNA in healthy skin and precancerous actinic keratosis lesions, but not cSCC, is consistent with a carcinogenic role for β -HPVs in the early stages of skin cancer development (16). This concept underpins the hypothesis that additional mutagens synergize with β -HPVs to induce genomic instability capable of promoting carcinogenesis after β -HPVs have cleared.

UV exposure has been established as the main risk factor for the development of cSCC (19). β -HPV-related lesions often occur in sun-exposed skin, implicating a synergistic role between UV and β -HPV. Supporting this theory are numerous *in vitro* and *in vivo* studies demonstrating that the β -HPVs proteins, E6 and E7, facilitate the accumulation of UV-induced DNA damage (13, 20). Other studies have found that HPV8 E6 (8 E6) causes tumors in mice without UV exposure, implying a broader role for β -HPV proteins, in which 8 E6 causes genome instability without an exogenous stimulus (21–23).

This dissertation investigates the potential for 8 E6 to destabilize the genome without UV exposure. All HPV E6 proteins lack enzymatic activity and interact with many cellular proteins to dysregulate their functions. p300, a histone acetyltransferase, is one such protein 8 E6 binds to alter cellular activity (24). Chapter 2 of this dissertation contains a thorough review of the consequences to genome integrity due to the interaction between 8 E6 and p300. This review is followed by our findings on how 8 E6 dysregulates the Hippo tumor suppression pathway and promotes proliferation via p300. Chapter 4 details the interaction between 8 E6 and a common cSCC mutation to promote genomic instability. Finally, Chapter 5 of this dissertation discusses our most recent findings of genome destabilization caused by 8 E6.

References

1. Haedicke J, Iftner T. 2013. Human papillomaviruses and cancer. *Radiother Oncol J Eur Soc Ther Radiol Oncol* 108:397–402.
2. Gheit T. 2019. Mucosal and Cutaneous Human Papillomavirus Infections and Cancer Biology. *Front Oncol* 9.
3. Van Doorslaer K, Li Z, Xirasagar S, Maes P, Kaminsky D, Liou D, Sun Q, Kaur R, Huyen Y, McBride AA. 2017. The Papillomavirus Episteme: a major update to the papillomavirus sequence database. *Nucleic Acids Res* 45:D499–D506.
4. Tomaić V. 2016. Functional Roles of E6 and E7 Oncoproteins in HPV-Induced Malignancies at Diverse Anatomical Sites. *Cancers* 8.
5. Donà MG, Tommasino M. 2020. Biological Pathways of HPV-Induced Carcinogenesis, p. 347–362. In Cristaudo, A, Giuliani, M (eds.), *Sexually Transmitted Infections : Advances in Understanding and Management*. Springer International Publishing, Cham.
6. Howley PM, Pfister HJ. 2015. Beta Genus Papillomaviruses and Skin Cancer. *Virology* 0:290–296.
7. Antonsson A, Forslund O, Ekberg H, Sterner G, Hansson BG. 2000. The Ubiquity and Impressive Genomic Diversity of Human Skin Papillomaviruses Suggest a Commensalic Nature of These Viruses. *J Virol* 74:11636–11641.
8. Rollison DE, Viarisio D, Amorrortu RP, Gheit T, Tommasino M. 2019. An Emerging Issue in Oncogenic Virology: the Role of Beta Human Papillomavirus Types in the Development of Cutaneous Squamous Cell Carcinoma. *J Virol* 93:e01003-18.

9. Orth G. 1986. Epidermodysplasia verruciformis: a model for understanding the oncogenicity of human papillomaviruses. *Ciba Found Symp* 120:157–174.
10. Orth G. 2008. Host defenses against human papillomaviruses: lessons from epidermodysplasia verruciformis. *Curr Top Microbiol Immunol* 321:59–83.
11. Dubina M, Goldenberg G. 2009. Viral-associated nonmelanoma skin cancers: A review. *Am J Dermatopathol* 31:561–573.
12. Bouvard V, Baan R, Straif K, Grosse Y, Secretan B, Ghissassi FE, Benbrahim-Tallaa L, Guha N, Freeman C, Galichet L, Cogliano V. 2009. A review of human carcinogens—Part B: biological agents. 4. *Lancet Oncol* 10:321–322.
13. Wendel SO, Wallace NA. 2017. Loss of Genome Fidelity: Beta HPVs and the DNA Damage Response. *Front Microbiol* 8.
14. Meyer T, Arndt R, Christophers E, Nindl I, Stockfleth E. 2001. Importance of human papillomaviruses for the development of skin cancer. 6. *Cancer Detect Prev* 25:533–547.
15. Nindl I, Koehler A, Meyer T, Forschner T, Meijer CJLM, Snijders PJF, Sterry W, Stockfleth E. 2006. Detection of human papillomavirus DNA in primary squamous cell carcinoma and metastases. 4. *Br J Dermatol* 154:797–799.
16. Weissenborn SJ, Nindl I, Purdie K, Harwood C, Proby C, Breuer J, Majewski S, Pfister H, Wieland U. 2005. Human Papillomavirus-DNA Loads in Actinic Keratoses Exceed those in Non-Melanoma Skin Cancers. 1. *J Invest Dermatol* 125:93–97.
17. Li W, Tian S, Wang P, Zang Y, Chen X, Yao Y, Li W. 2019. The characteristics of HPV integration in cervical intraepithelial cells. *J Cancer* 10:2783–2787.
18. Dang C, Koehler A, Forschner T, Sehr P, Michael K, Pawlita M, Stockfleth E, Nindl I. 2006. E6/E7 expression of human papillomavirus types in cutaneous squamous cell dysplasia and carcinoma in immunosuppressed organ transplant recipients. 1. *Br J Dermatol* 155:129–136.
19. Fahradyan A, Howell AC, Wolfswinkel EM, Tsuha M, Sheth P, Wong AK. 2017. Updates on the Management of Non-Melanoma Skin Cancer (NMSC). *Healthcare* 5.
20. Meyers JM, Grace M, Uberoi A, Lambert PF, Munger K. 2018. Inhibition of TGF- β and NOTCH Signaling by Cutaneous Papillomaviruses. *Front Microbiol* 9.
21. Dong W, Kloz U, Accardi R, Caldeira S, Tong W-M, Wang Z-Q, Jansen L, Dürst M, Sylla BS, Gissmann L, Tommasino M. 2005. Skin Hyperproliferation and Susceptibility to Chemical Carcinogenesis in Transgenic Mice Expressing E6 and E7 of Human Papillomavirus Type 38. *J Virol* 79:14899–14908.

22. Marcuzzi GP, Hufbauer M, Kasper HU, Weißenborn SJ, Smola S, Pfister H. 2009. Spontaneous tumour development in human papillomavirus type 8 E6 transgenic mice and rapid induction by UV-light exposure and wounding. *J Gen Virol* 90:2855–2864.
23. Schaper ID, Marcuzzi GP, Weissenborn SJ, Kasper HU, Dries V, Smyth N, Fuchs P, Pfister H. 2005. Development of Skin Tumors in Mice Transgenic for Early Genes of Human Papillomavirus Type 8. *Cancer Res* 65:1394–1400.
24. Howie HL, Koop JI, Weese J, Robinson K, Wipf G, Kim L, Galloway DA. 2011. Beta-HPV 5 and 8 E6 Promote p300 Degradation by Blocking AKT/p300 Association. *PLoS Pathog* 7.

Chapter 2 - Beta-Genus Human Papillomavirus 8 E6 Destabilizes the Host Genome by Promoting p300 Degradation

Dalton Dacus and Nicholas A. Wallace*

Division of Biology, Kansas State University, Manhattan, Kansas, USA

*Corresponding Author: nwallac@ksu.edu

Published as: Dacus D, Wallace NA. 2021. Beta-Genus Human Papillomavirus 8 E6
Destabilizes the Host Genome by Promoting p300 Degradation. 8. *Viruses* 13:1662.

Abstract

The beta genus of human papillomaviruses infects cutaneous keratinocytes. Their replication depends on actively proliferating cells and, thus, they conflict with the cellular response to the DNA damage frequently encountered by these cells. This review focus on one of these viruses (HPV8) that counters the cellular response to damaged DNA and mitotic errors by expressing a protein (HPV8 E6) that destabilizes a histone acetyltransferase, p300. The loss of p300 results in broad dysregulation of cell signaling that decreases genome stability. In addition to discussing phenotypes caused by p300 destabilization, the review contains a discussion of the extent to which E6 from other β -HPVs destabilizes p300, and provides a discussion on dissecting HPV8 E6 biology using mutants.

Keywords

HPV; skin cancer; p300; DNA damage; proliferation; differentiation; UV

Introduction

The stability of our genome is threatened by internal and external hazards [1]. Endogenous sources of genomic destabilization include errors during replication and mitosis, as well as reactive oxygen species resulting from metabolism [2,3]. Exogenous sources are equally prevalent, including ultraviolet radiation (UV), ionizing radiation (IR), and naturally occurring as well as human-made mutagens [4,5]. To minimize the mutations associated with these genotoxic events and agents, cells have evolved an elaborate collection of specific DNA repair and cell cycle arrest signaling pathways. Collectively they are known as the DNA damage response (DDR) and play an integral part in maintaining genome stability [6,7]. When necessary, DDR signaling can also include the induction of apoptosis [8]. The DDR has exquisite specificity as

individual pathways specializing in a single type of damage/challenge occurring in one portion of the cell cycle [9]. Despite this specialization, individual DDR pathways also have an impressive ability to substitute for each other [10]. Together, the DDR minimizes the mutagenic impact of challenges during mitosis and after DNA damage. The importance of the DDR is best illustrated by the striking increases in tumorigenesis that result from deficiencies in one or more of its member pathways [11,12,13].

Understanding how the DDR functions and how defects in the DDR impact genomic integrity has direct implications for improving chemotherapeutics, countering chemoresistance, and genome editing. As a result, there is widespread research interest in the DDR from a diverse set of perspectives. This review discusses how a protein of beta genus of human papillomaviruses (β -HPV) promotes destabilization of the cellular genome by hindering DDR pathways. β -HPVs are small, double-stranded DNA viruses, some of which may contribute to non-melanoma skin cancer in immunocompromised individuals [14,15]. They also commonly infect the general population. Their role in promoting oncogenesis is controversial. While numerous in vitro and in vivo studies have demonstrated oncogenic properties of certain β -HPV proteins [16], the absence of β -HPV gene expression in tumors has caused many to question the physiological relevance of these properties regarding oncogenesis. Further, a recent report suggests that cutaneous HPVs protect against skin carcinogenesis [17]. This controversial claim resulted in an interesting series of articles where the evidence for and against β -HPV infections protecting against skin cancer development was discussed [18,19].

To complete their lifecycle, β -HPVs require skin cells to remain proliferatively active, despite stimuli (e.g., differentiation and UV exposure) that are known to induce cell cycle exit. The E6 protein from β -HPVs (β -HPV E6) plays a notable role in promoting this aberrant

proliferation. All five β -HPV species (beta-1, beta-2, beta-3, beta-4, and beta-5) encode E6 [20]. β -HPV E6 is a small, 150 amino acid protein that contains two zinc-finger domains at its N- and C-termini [21]. The β -HPV E6 from some β -HPVs (e.g., HPV5 and HPV8) binds and destabilizes a cellular histone acetyltransferase, p300, to counter the cell cycle arrest and apoptosis associated with differentiation and DNA damage [22]. It is currently unclear how common p300 binding by β -HPV E6s is because only a few β -HPV types have been thoroughly studied; however, p300 destabilization is not a universal feature of β -HPV E6s. Among the β -HPV E6s that have been well characterized, p300 binding varies from weak/no attachment to robust tethering [23,24]. This review discusses these topics and others, with a particular focus on HPV8 E6. β -HPV E6 functions not related to p300 binding have been extensively reviewed [25,26,27,28] and will not be discussed in this review.

Materials and Methods

The E6 amino acid sequences from 53 beta genus of human papillomaviruses available at PaVE (<https://pave.niaid.nih.gov>, accessed on 14 May 2021) were downloaded and aligned. A phylogenetic tree was constructed using PaVE.

Results

p300 Is a Master Transcription Regulator and Tumor Suppressor

A great deal has been determined about p300 through traditional approaches geared toward dissecting its biology. It is encoded by the gene EP300 and belongs to the type 3 family of lysine acetyltransferases, with homologs found in mammals and other multicellular organisms such as flies, worms, and plants [29,30]. p300 consists of conserved domains, including a central catalytic domain (KAT) responsible for protein acetylation that is adjacent to a bromodomain and PHD finger (CH2), both of which aid in chromatin association and modification [31,32]. The

central domain is flanked by four transactivation domains: (i) the cysteine–histidine-rich region 1 (CH1) that contains a transcriptional adapter zing finger 1 (TAZ1), (ii) a kinase-inducible interacting domain (KIX), (iii) another cysteine–histidine-rich region (CH3) that includes a TAZ2 and a ZZ domain that are known to interact with a wide range of proteins including HPV8 E6, and (iv) a nuclear receptor coactivator binding domain (IBiD) (**Figure 2.1**) [33]. As a transcriptional coactivator, it interacts with over 400 factors, allowing it to regulate physiological processes including the DDR, differentiation, proliferation, and apoptosis [34,35]. p300 also acts as a stabilizing scaffold between transcription machinery and transcription factors that bind through the CH1, CH3, and KIX domains of p300 [36,37]. p300 promotes transcription directly by acetylating histones through its HAT domain [38,39]. It also acetylates non-histone proteins and, as a result, modifies their activities [40].

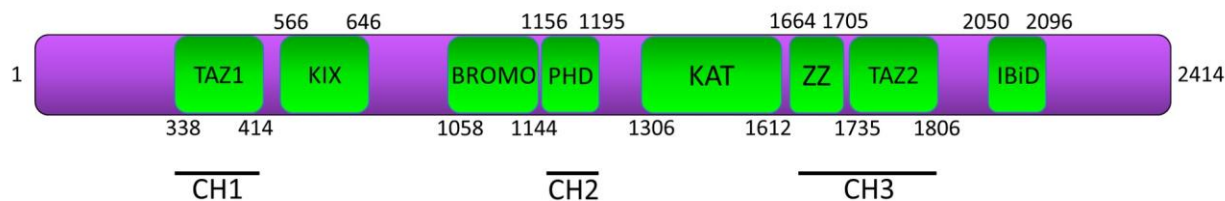


Figure 2.1. p300 structural domain and their localization.

TAZ1 (also known as CH1), KIX, BROMO, PHD (also known as CH2), KAT, ZZ and TAZ2 (together known as CH3), and IBiD. Approximate domain boundaries were taken from the p300 Pfam database entry (Q09472).

While these activities have a wide ranging ability to alter cellular processes, they are closely linked to promoting the DDR [41,42,43]. For example, p300 contributes to the homologous recombination pathway by transcriptionally activating RAD51 and BRCA1 [44]. Additionally, loss of p300 lead to defects in cell cycle arrest induced by DNA replication errors and is correlated with a lack of CHK1 phosphorylation [45]. Cell lines harboring EP300

mutations display faulty base excision repair in response to oxidative damage [46]. Suppression of p300 histone acetyltransferase activity significantly abrogates the recruitment of DDR factors normally seen in response to UV [47]. Additionally, p300 promotes pRB, p53, and TGF- β signaling [48,49,50,51].

Given the established tumor suppressor role of the DDR and its other targets, it is not surprising that p300 mutations are associated with tumorigenesis and act as a tumor suppressor in cutaneous squamous cell carcinoma (cSCC) [52]. EP300 mutations, largely missense point mutations, are found across a wide variety of cancer types [53]. However, mutations were most frequent in cSCC as reported in the COSMIC (Catalogue of Somatic Mutations in Cancer) database [54]. Further, decreased nuclear p300 staining is associated with disease progression in melanoma patients [55]. Finally, a heterozygous germline EP300 mutation results in reduced p300 abundance that manifests as Rubinstein–Taybi syndrome (RSTS), a condition characterized by increased cancer predisposition [56].

HPV8 E6 Reduces Genome Stability by Destabilizing p300

Although multiple β -HPV E6 proteins bind and destabilize p300, HPV8 E6 is the most studied β -HPV E6. Further, because HPV8 infections are hypothesized to promote non-melanoma skin cancer by increasing the mutagenic risk of UV exposure, the ability of HPV8 E6 to hinder the repair of DNA damaged by UV has been a research focus. As a result, characterizations of HPV8 E6 biology have complemented and confirmed more traditional molecular biology studies, dissecting the role of p300 in preserving genome stability. The following sections highlight the known mechanisms by which HPV8 E6-mediated p300 destabilization hinders genome stability.

ATR

ATR is the principal kinase activated in response to UV and replication stress [57]. By destabilizing p300, HPV8 E6 reduces ATR mRNA and protein levels [58]. This demonstrates a role for p300 in ATR transcription, presumably through histone modification. The reduction in ATR abundance results in delayed formation of ATR repair complexes following UV damage. As expected, HPV8 E6 delays the resolution of UV-photolesions and increases the frequency of UV-induced double-stranded breaks in DNA (DSBs). While these studies were conducted in cell line models, similar effects were seen in transgenic mice expressing HPV8 E6 from the K14 promoter. Namely, HPV8 E6 made UV-damage more persistent, made UV-induced DSBs more common, and diminished ATR activation [59]. These repair defects are likely the result of impaired ATR signaling, as HPV8 E6 attenuates the phosphorylation of ATR and its downstream targets CHK1 and CDC25A [59,60]. Unlike the p300-dependent reduction in ATR by HPV8 E6, the role of p300 destabilization in downstream ATR signaling has not been demonstrated. HPV8 E6 also impaired ATR-dependent events critical for the cellular response to UV damage (nuclear localization of XPA and pol η repair complex formation) but, again, the requirement of p300 destabilization in these hindrances was not tested [60,61,62,63].

ATM

ATM is one of the primary kinases responsible for orchestrating the cellular response (i.e., apoptosis, cell cycle checkpoint activation, and DNA repair) to DSBs through phosphorylation of its hundreds of targets [57,64]. HPV8 E6 decreases total ATM protein levels by destabilizing p300 [65]. Following UV damage in cell culture models, HPV8 E6 also diminishes ATM activation (via autophosphorylation) and reduces ATM-mediated phosphorylation of two essential downstream DDR factors, BRCA1 and CHK2 [60]. Further,

HPV8 E6 reduces UV-induced ATM phosphorylation in three-dimensional organotypic raft cultures [59]. As in the repression of ATR signaling by HPV8 E6, while p300 destabilization is the most likely mechanism by which HPV8 E6 attenuates downstream ATM signaling, this has not been demonstrated [60,66].

DNA-PK

DNA-PK is the other principal kinase activated in response to DSBs. DNA-PK is unique compared to ATM and ATR, in that it is a holoenzyme, made up of DNA-dependent protein kinase catalytic subunit (DNA-PKcs) and a heterodimer, of Ku70 and Ku80 [67]. DNA-PK is recruited to DSBs by 53bp1, leading to its autophosphorylation, and ultimately to the phosphorylation of downstream proteins, including Artemis [68]. HPV8 E6 delays the resolution of DNA-PKcs and 53bp1 foci by destabilizing p300 [69,70]. HPV8 E6 also reduced phosphorylation of DNA-PKcs and Artemis [69].

Double Strand Break Repair

The reduction in ATM and DNA-PKcs signaling suggests that HPV8 E6 impairs DSB repair. Homologous recombination (HR) is the primary mechanism for DSB repair, while non-homologous end joining (NHEJ) generally serves as a backup repair mechanism when HR fails [71,72]. HR is usually restricted to cell cycle segments when a homologous template is available (i.e., S and G2 phase), while NHEJ is not restricted to any particular portion of the cell cycle [73,74]. HPV8 E6 delays the repair of DSBs by reducing the efficacy of HR and NHEJ. In both cases, the mechanism of action by which HPV8 E6 attenuates repair is the destabilization of p300. For the HR pathway, destabilization reduces the abundance of p300 at the promoters of two essential HR genes, BRCA1 and BRCA2 [70]. As a result, there are fewer BRCA1 and BRCA2 transcripts, lower protein abundance, and fewer repair complexes formed in response to

DSBs [70]. Despite BRCA1 and BRCA2 facilitating an earlier step in the HR pathway, HPV8 E6 does not prevent RAD51 foci formation [70]. However, the RAD51 foci that form are not resolved, suggesting that the reduction in p300 results in further deregulation of the HR pathway. HPV8 E6 also attenuates the repair of DSBs by NHEJ. NHEJ-requires DNA-PK activity. As described in the previous section, by destabilizing p300, HPV8 E6 hinders DNA-PK autophosphorylation and the phosphorylation of at least one DNA-PK substrate (Artemis). The reduced p300 abundance also delays the resolution of at least two NHEJ repair complexes (DNA-PKcs and 53bp1) [69,70].

Cell-Cycle Checkpoints and Differentiation

Growth arrest is a powerful tool for responding to threats to genome stability [75,76,77]. Preventing growth allows time for repair to occur or missegregated chromosomes to resolve. If the danger is not mitigated, permanent growth arrest assures that cells containing a mutated genome do not propagate. Additionally, differentiation was recently identified as a mechanism by which polyploidy epithelial cells are prevented from growth [78]. Despite the benefits to the cell, pauses to cellular growth run counter to the requirements for β -HPV replication.

The E6 from multiple types of β -HPVs inhibits the cues that normally stop cells from dividing upon UV exposure [79,80]. However, the role of p300 destabilization in escape from UV-induced cell cycle arrest was not tested in these studies. p300 destabilization allows HPV8 E6 to promote proliferation in the face of other genome destabilizing events and reduces differentiation both in vivo and in vitro [81,82,83,84,85]. One mechanism by which reduced p300 availability promotes proliferation is the dysregulation of the Hippo pathway. By destabilizing p300, HPV8 E6 increases the expression and protein levels of pro-proliferative Hippo pathway factors: CTGF, AXL, and SERPINE1 [82]. Altered Hippo pathway signaling has

genome destabilizing consequences, as it allows cells to continue proliferating after failed cytokinesis, leading to viable cells with polyploid genomes [84]. Similarly, HPV8 E6 allows cells with more than three centrosomes to continue to proliferate by destabilizing p300, but a connection to the Hippo pathway has not been examined [84].

HPV8 E6 also reduces differentiation by destabilizing p300 [83]. This occurs at least in part through the downregulation of CCAAT/enhancer-binding protein α (C/EBP α), another p300-responsive gene (24). C/EBP α is a pro-differentiation transcription factor and, by decreasing its availability, HPV8 E6 causes a reduction in the differentiation marker involucrin. The reduced C/EBP α suppresses its transcriptional activator activity on microRNA-203 (miR-203), resulting in increased proliferation. Other differentiation markers (i.e., K1 and K10) are also reduced by HPV8 E6-mediated p300 destabilization, possibly as a result of C/EBP α reduction [83].

p53

p53 is the most commonly mutated tumor suppressor found in human cancer [86]. By acting as a transcription factor, it regulates DNA repair, cell cycle arrest, senescence, angiogenesis, apoptosis, and many other pathways [87,88,89,90]. Unlike high-risk alpha-HPVs, all but one β -HPV E6 (HPV49 E6) are unable to bind and degrade p53 [91,92]. However, HPV8 E6 attenuates p53 signaling by destabilizing p300. p53 binding to chromatin regulates p53 activity in response to DNA damage [93]. p300 facilitates this damage-induced response by acetylating both histones and p53 [48,94,95]. HPV8 E6 reduces p53 acetylation (K382) in response to UVB exposure [58]. p53 is also regulated by ATR via phosphorylation on its serine-15 and -37 residues [96,97]. These post-translational modifications inhibit MDM2-mediated degradation stabilizing p53. This allows p53 to accumulate, prompting activation of DDR genes

and association with p300 [98,99]. Likely by destabilizing p300, HPV8 E6 lessens phosphorylation of p53 at Serines 15 and 37 in response to UV, and limits p53 accumulation [58]. However, the role of p300 destabilization in p53 phosphorylation has not been tested.

The inhibition of p53 signaling by HPV8 E6 is not restricted to the response to damaged DNA. HPV8 E6 also reduces p53 accumulation in response to mitotic errors [84]. The destabilization of p300 by HPV8 E6 lowered p53 levels in the binucleated cells that form as a result of failed cytokinesis [84]. Stabilization of p53 in response to failed cytokinesis requires activation of the Hippo pathway, specifically LATS2 phosphorylation [100]. This causes LATS2 to bind p53 and inhibit MDM-mediated degradation [101,102]. HPV8 E6 reduces LATS2 activation and prevents p53 buildup induced by cytokinesis failure [82]. However, HPV8 E6 does not affect the activation of the Hippo pathway in response to high cell density. Although less mechanistically clear, the destabilization of p300 by HPV8 E6 also prevents p53 accumulation in response to the accumulation of supernumerary centrosomes [84]. Together, these data show that p300 protects against chromosomal instability [103,104,105].

How Conserved Is p300 Binding among β -HPV E6s

Only a handful of the 53 β -HPVs have been studied for their biological function in vitro or in vivo. As a result, little is known about the p300 binding potential of most β -HPV E6 proteins. To this end, the review has focused exclusively on HPV8 E6. However, four other β -HPV E6 proteins (HPV 5, -20, -25, and -38 E6) have been shown to bind p300 by via immunoprecipitation, followed by immunoblot and/or mass spectrometry [83,106,107]. Of these, HPV5 E6 and HPV38 E6 have been the most thoroughly characterized. HPV5 E6 behaves similarly to HPV8 E6 in as much that it binds and destabilizes p300 [83]. As both HPV5 E6 and HPV8 E6 destabilize p300, it is reasonable to assume that the p300 degradation-dependent

phenotypes discovered in one apply to the other. Supporting this idea, HPV5 E6 and HPV8 E6 share many properties. These include: (i) destabilizing p300 [83], (ii) increasing thymine dimer persistence, (iii) increasing DSB prevalence after UVB exposure [58], (iv) decreasing ATR expression and activity [58], (v) reducing post-translational modifications of p53 [58], (vi) reducing ATM protein levels [65], (vii) increasing the frequency of cells with more than two nuclei, (viii) increasing the frequency of cells with more than 4N DNA, (ix) decreasing senescence-associated β -galactosidase levels in late passage primary cells [84], (x) increasing the average number of centrosomes per cell [84], (xi) attenuating p53 signaling in response to failed cytokinesis and supernumerary centrosome [84], and (xii) reducing BRCA1/BRCA2 expression [70]. It should be noted that HPV8 E6's p300 degradation, but not binding, is cell line dependent, as cell lines can harbor a constitutively active AKT [83]. Other groups have also failed to show p300 destabilization in some cell lines, suggesting that there may be additional factors that determine whether HPV8 E6 destabilizes p300 [59].

HPV38 E6 binds p300 less stringently than HPV5 E6 or HPV8 E6. As a result, HPV38 E6 does not appreciably destabilize p300. However, it impacts p300 signaling. For example, HPV38 E6 reduces p53 acetylation at lysine 382 [85]. In addition, p300 binding by HPV38 E6 is likely necessary for HPV38 E6 and E7 to immortalize primary cells [85]. The connection between HPV38 E6 binding p300 and immortalization relies on a mutation in HPV38 E6, and such mutants can produce data that are difficult to interpret (limitations and concerns with β -HPV E6 mutants are discussed further below). While HPV38 E6 shares some phenotypes with HPV8 E6, immortalization is reasonably unique to HPV38 E6, as neither HPV5 E6 nor HPV8 E6 immortalize cells with or without their associated E7 protein. This could be due to HPV38 E6

binding p300 with a different portion of its E6 protein than HPV5 E6 and HPV8 E6. Thus, HPV38 E6 may impact a different subset of p300-dependent signaling events.

Other β -HPV E6 proteins are predicted to destabilize p300 based on amino acid alignment to β -HPV E6s known to destabilize p300 (**Figure 2.2**). The p300 binding domains of HPV5 E6 or HPV 8 E6 are conserved in eight other β -HPV E6s (HPV12, -14, -19, -47, -99, -10, -143, and -203 E6). All of these except HPV206 are members of one of the most prevalent genera of β -HPVs (beta-1 genus), along with HPV5 and HPV8 [108]. HPV206 is currently unclassified [20,108]. Notably, HPV12, -14, and -47, along with HPV5 and HPV8, are associated with skin lesions in people with the rare genetic disorder epidermodysplasia verruciformis [109,110,111]. HPV47 E6 and HPV14 E6 also share significant amino acid sequences with HPV5 E6 and HPV8 E6, beyond the residues required for p300 binding [112]. The *Mus musculus* papillomavirus 1 (MmuPV1) is used as an *in vivo* model for β -HPV, as it shares some biological and biochemical properties with HPV8 E6 [113]. However, MmuPV1 E6 does not bind p300 [114] and does not contain a conserved p300-binding sequence (**Figure 2.2**). Therefore, MmuPV1 is unlikely to fully reproduce the biology of the β -HPVs most closely linked with epidermodysplasia verruciformis. An *in vivo* model system using cottontail rabbit papillomavirus (CRPV) DNA injected into rabbits demonstrated that CRPV E6 mutants deficient in binding p300 did not induce tumor formation, nor did they prevent apoptosis [85]. However, unlike the MmuPV1 model, only DNA of the virus was used instead of an infectious-replicative virus.

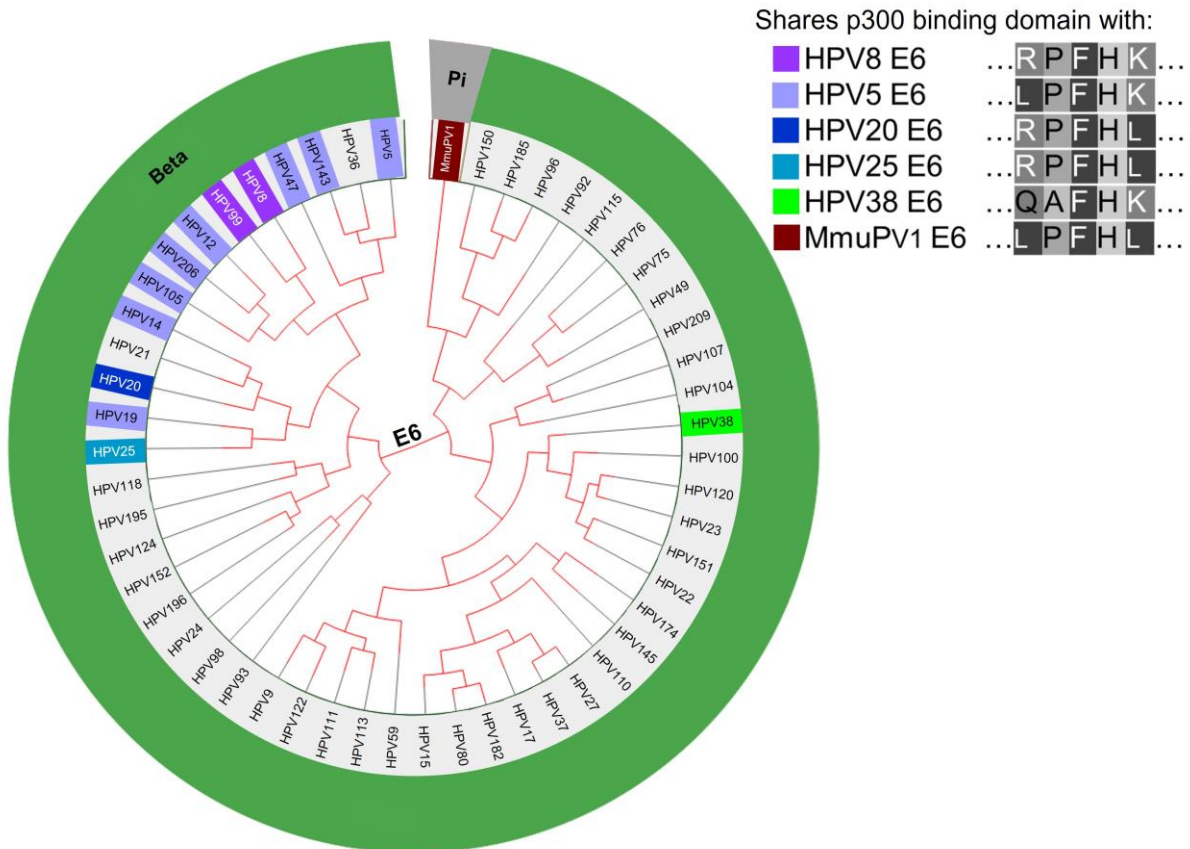


Figure 2.2. Phylogenetic tree of β -HPV and MmuPV1 based on the E6 nucleotide sequence. (<https://pave.niaid.nih.gov/>, accessed on 14 May 2021). E6s with identical amino acid sequence highlighted to match corresponding E6s either known to bind p300 (HPV8, 5, 20, 25, 38) or not bind p300 (MmuPv1).

Confirming the Dependence of a HPV8 E6 Phenotype on p300 Destabilization

While HPV8 E6 clearly alters cell signaling by destabilizing p300, some caution needs to be exercised when determining whether a phenotype is the result of p300 destabilization. The initial screening for identifying phenotypes caused by HPV8 E6-mediated reductions in p300 is typically performed by comparing a vector control cell lines to ones expressing either wild type HPV8 E6 or HPV8 E6, with the residues responsible for p300 binding deleted or mutated (e.g., HPV8 E6 Δ 132-136). Phenotypes seen in cells expressing wild type HPV8 E6 but reduced or

absent in the HPV8 E6 Δ 132-136 are potentially the result of p300 destabilization. However, data from the HPV E6 mutants can easily be misinterpreted because deletions and mutations in the small viral protein frequently disrupt more than one aspect of HPV E6 biology. This is also the case for HPV8 E6 mutants. For example, deletion of the residues of HPV8 E6 that facilitate p300 binding (Δ 132-136) also prevent HPV8 E6 from binding to MAML1, which is critical for HPV8 E6 inhibition of the NOTCH pathway [114]. As a result, comparisons between wildtype and mutant HPV8 E6 cannot distinguish between a phenotype that is the result of p300 destabilization, MAML1 binding, or attributable to a more generalized loss of HPV8 E6 function. This is particularly true for phenotypes that are only reduced (rather than abrogated) in cells expressing HPV8 E6 Δ 132-136. Table 1 lists phenotypes found in cells expressing HPV8 E6 that remain partially intact in cells expressing HPV8 E6 Δ 132-136. While this gives reason for concern that the HPV8 E6 Δ 132-136 mutant might cause entirely non-specific inhibition of HPV8 E6, a subset of phenotypes is not reduced when these residues are deleted. Table 2 contains a list of these phenotypes. Therefore, HPV8 E6 Δ 132-136 is not an entirely functionless protein.

Table 2.1 Phenotypes of HPV8 E6 Δ 132-136 that are weaker than those of wild type HPV8 E6.

Cell lines abbreviations: primary human epidermal keratinocytes (PHEK), human foreskin keratinocyte (HFK). Stable expression via lentiviral transduction.

Cell Type	Expression	Partial Phenotype	Reference
PHEK	Stable	Reduction in Syntenin-2 mRNA and protein levels	[115]
HFK	Stable	Increased persistence of thymine dimers after UVB	[58]
HFK	Stable	Augmented late passage cells with >4 N content	[84]
HFK	Stable	Fewer BRCA1/2 positive cells after IR	[70]
HFK	Stable	Increased sensitivity to PARP1 inhibitor	[70]
HFK	Stable	Delays RAD51 foci resolution after 4 gray of IR	[70]
HFK	Stable	Enhances sensitivity to IR	[70]

Table 2.2 Phenotypes of HPV8 E6 Δ 132-136 analogous to wild type HPV8 E6.

Cell lines abbreviations: human osteosarcoma cell line (U2OS), human foreskin keratinocytes (HFK), HPV-negative cervical carcinoma cell line (C33A), HPV-negative skin squamous cell carcinoma-derived cell line (RTS3b), primary human foreskin keratinocytes (NHK). “Stable” denotes stable expression achieved via lentiviral transduction. “Transient” denotes transient expression achieved via transfection.

Cell Type	Expression	Phenotype	Reference
U2OS	Stable	Inhibits non-homologous end joining	[69]
C33A	Transient	Precipitated with PTPH1	[116]
RTS3b	Transient	Activates early HPV8 promotor	[117]
NHK	Stable	JunB mRNA expression downregulated	[81]
HFK	Stable	Diminishes senescence-associated β -galactosidase staining in late passage binucleated cells	[84]
HFK	Stable	Increases frequency of cell with three centrosomes	[84]
HFK	Stable	Increases growth rate in late passage cells	[84]
U2OS	Stable	Prevented XRCC4 foci in response to DSBs	[69]
U2OS	Stable	Decreases H ₂ O ₂ -induced DNA-PKcs phosphorylation	[69]

More targeted mutations to the p300-binding site are needed to eliminate the concern associated with HPV8 E6 Δ 132-136. However, no consensus has been reached on the efficacy of the currently available alternatives. For example, there are conflicting reports over the extent to which HPV8 E6K136N is deficient for p300-binding [59,114]. These differences may be attributable to differences in experimental approaches. HPV8 E6K136N failed to bind p300 when transiently expressed in RTS3b cells but continued to bind p300 when stably expressed in U2OS cells [59,114]. One other mutation (HPV8 E6H135A) was initially described as having a significantly reduced ability to bind p300 [117]. Unfortunately, the HPV8 E6H135A mutant has not been thoroughly characterized (or used) since it was initially described.

Currently, the best way to validate the p300 dependence of any phenotype caused by β -HPV E6 is to use other molecular techniques as complimentary approaches. To this end, cells expressing β -HPV E6 have been transiently transfected with either phosphomimetic (p300

S1834E) or phospho-dead (p300 S1834A) p300 mutants [58,65,70,83]. Since HPV8 E6 reduces p300 abundance by blocking its phosphorylation by AKT, the phosphomimetic p300 mutant is resistant to HPV8 E6-mediated destabilization [83]. p300 S1834A is catalytically inactive and thus serves as a negative control [118]. In this system, phenotypes that require p300 destabilization are lost in cells transfected with p300 S1834E and maintained in cells transfected with p300 S1834A. A disadvantage of using this approach to confirm the p300 dependence of a phenotype is the transient nature of p300 mutant expression that limits the types of phenotypes that can be examined.

The role of p300 destabilization in phenotypes can also be confirmed using non-viral mechanisms of knocking p300 down or out. siRNA-mediated knockdown of p300 has been used to validate cellular processes identified as likely requiring p300 destabilization [58,65,81,83,85]. Since the knockdown of p300 is transient, this approach is also not ideal for testing phenotypes associated with prolonged HPV8 E6 expression. shRNA may be useful for testing the p300-dependence of phenotypes that take more time to occur. However, RNAi-mediated degradation can result in off-target effects or require multiple siRNAs/shRNAs to be pooled together to reach a significant reduction in p300, further enhancing possible off-targets.

Genetic knockouts have the potential to eliminate these concerns and have been used to test the role of p300 in multiple HPV8 E6-mediated phenotypes [69,82]. Most commonly, colorectal cancer cell lines (HCT116) with and without the p300 gene knocked out are compared [119]. A clear disadvantage of this approach is that the cell type is unlikely to be physiologically relevant to β -HPVs. In the future, it would be useful to knockout the p300 gene in primary or immortalized keratinocytes to overcome this issue.

Small molecule inhibitors of p300 have been developed and offer the ability to impair p300 activity in keratinocytes [120,121,122]. Our unpublished data have confirmed that p300 inhibitor CCS1477 is capable of reproducing aspects of HPV8 E6 biology that require p300 destabilization. One potential advantage of using p300 inhibitors is their ability to target the protein directly. However, because p300 would not be destabilized by a small molecule inhibitor, it could still act as a scaffold. Finally, an untested yet feasible option is to use Rubinstein–Taybi syndrome (RSTS) patient-derived cell lines that have reduced p300 levels and increased genomic instability, attributable to defective DNA repair [46,123].

The concerns about HPV8 E6 mutants necessitate confirming the p300 dependence of any phenotype with these or other approaches. As noted in this section, each of these methods has its limitations. As a result, using multiple confirmatory approaches raises confidence that HPV8 E6 is causing a given phenotype by destabilizing p300. Table 3 lists the phenotypes described in this review and the methods that were used to confirm their dependence on p300 destabilization by HPV8 E6. To the best of our knowledge, the role of p300 in these phenotypes was first identified by studying HPV8 E6.

Table 2.3 . Phenotypes of HPV8 E6 that have been confirmed to be through the destabilization of p300.

p300 mutants include S1834E and S1834A. E6 mutant refers to HPV8 E6 Δ 132-136. Knockout and Knockdown are via siRNA and HCT cells without p300, respectively.

Phenotype	p300 Activity Confirmed via:				Reference
	p300 Mutants	E6 Mutant	Knockout	Knockdown	
Reduction in K1, K10, and involucrin mRNA expression		×		×	[83]
Diminish ATR expression	×	×		×	[58]
Lessen ATM expression	×	×		×	[65]
Inhibit p53 accumulation in binucleated cells	×	×			[84]
Prevent p53 buildup in cells with ≥ 3 centrosomes	×	×			[84]
Allow binucleated cells to proliferate	×	×			[84]
Allow cells with ≥ 3 centrosomes to proliferate	×	×			[84]
Reduce BRCA1 and BRCA2 expression		×	×		[70]
Attenuate DSB repair	×	×	×		[70]
Reduce C/EPB α and miR-203 expression	×			×	[81]
Upregulate expression of pro-proliferative Hippo pathway genes		×	×		[82]
Attenuate DNA-PKcs phosphorylation after DSB induction		×	×		[69]
Decrease phosphorylation of Artemis after DSB induction		×	×		[69]

Discussion

In this review, we aligned β -HPV E6 proteins based on their amino acids. This grouping shows that E6 proteins with proven or putative p300 binding capability cluster together. The extent to which these β -HPV E6 proteins represent a group with unique biology has yet to be

fully determined. Similarly, the extent to which viral life cycle differences exist between β -HPVs that express E6s that can and cannot destabilize p300 has not been explored.

Conclusions and Future Directions

As a transcription factor, p300 regulates the expression or activity of hundreds of genes directly. Many of those genes (e.g., p53, ATM, and ATR) are key factors in other signaling pathways where they control the expression or activity of multiple other genes. This broad influence makes p300 a critically important factor in maintaining genomic stability via the DDR, cell cycle checkpoints, the regulation of p53, and likely other mechanisms. Unsurprisingly, aberrant p300 biology is linked to multiple cancers and disease states [46,53,124,125].

Therefore, it is important to examine p300 biology from multiple angles. Investigations into HPV8 E6 biology represent a markedly different approach. While studies of HPV8 E6 biology are generally not designed to learn about p300, they have nevertheless provided significant insights into p300 biology (Table 3). As well as the potential to learn about p300 by studying HPV8 E6, it is important to note that multiple control and confirmatory experiments are required before strong conclusions about p300 can be made. Furthermore, there are accumulating data that HPV8 E6 reduces the cell's ability to address errors during mitosis, such as failed cytokinesis or centrosome duplication [82,84]. As a result, the genome-destabilizing potential of HPV8 E6 extends beyond the inhibition of UV-damaged DNA.

There are several opportunities to expand our understanding of how the binding of p300 by β -HPVs impacts viral biology. First, sequence alignments suggest that the number of β -HPVs that deregulate p300 activity is higher than what has been demonstrated. These β -HPVs are therefore also likely to impair genomic stability, but this should be confirmed experimentally. Next, it is critical to determine if the disruption of p300 signaling is heightened, diminished, or

unaltered by other β -HPV early proteins (i.e., E1, E2, E7, E8^{E2}) that are expressed alongside β -HPV E6 during naturally occurring infections. Among these, β -HPV E7 demonstrates potential synergy with E6 to disrupt the DDR via its ability to attenuate expression of DDR- and apoptosis-related genes [126] Further, some β -HPV E7s bind and destabilize the tumor suppressor pRB, which could promote UV-damaged cells to bypass cell cycle checkpoints [91,127].

Finally, HPV8 E6 may alter CREB-binding protein (CBP) signaling. CBP shares significant sequence homology with p300 and is also a critical regulator of RNA polymerase II-mediated transcription via histone acetylation [34,128]. Despite their high level of homology, p300 and CBP regulate distinct gene sets and thus are not entirely redundant [129]. It was hypothesized that all mammalian E6 proteins may interfere with CBP/p300 functions through direct interaction or by capturing LxxLL containing CBP/p300 partners [130]. Driving this idea is mammalian E6's ability to recognize LxxLL motifs and CBP/p300's critical role in numerous functions, including a host's innate antiviral response [130,131]. To our knowledge, the only available data regarding HPV8 E6 and CBP come from two separate pulldown mass spectrometry experiments that found CBP peptides to be associated with HPV8 E6 [83,106]. Despite the potential interaction, HPV8 E6 did not reduce CBP levels [83]. While this suggests that HPV8 E6 may not degrade CBP, studies of other viral proteins provide reason to believe the interaction could be significant. The adenoviral protein E1A alters CBP signaling in order to promote S-phase by binding (but not destabilizing) CBP [125,132,133,134]. Given that CBP is a master transcription regulator, akin to p300, dysregulation of CBP signaling would be expected to markedly alter cellular environment.

Clearly, HPV8 E6 did not evolve the ability to destabilize p300 to serve as a tool for gaining insight into DNA repair and cell signaling. Instead, the destabilization of p300 likely provides the virus a replicative advantage. The damaging effect of UV exposure on the skin normally induces cell cycle exit. This would oppose HPV8 replication, as β -HPVs require actively proliferating cells to complete their lifecycle. The destabilization of p300 affords HPV8 the opportunity to attenuate the cell cycle arrest associated with UV and other genome destabilizing events. It also increases the expression of pro-proliferative genes and inhibits differentiation.

Author Contributions

Conceptualization, D.D. and N.A.W.; methodology, D.D.; investigation, D.D.; resources, N.A.W.; writing—original draft preparation, D.D. and N.A.W.; writing—review and editing, D.D. and N.A.W.; visualization, D.D.; supervision, N.A.W.; funding acquisition, N.A.W. All authors have read and agreed to the published version of the manuscript.

Funding

We would like to thank the Terry Johnson Basic Cancer Research Center for their support of this project. We also received support from a career development award provided by the United States' Department of Defense's Congressionally Directed Medical Research Program's Peer Reviewed Cancer Research Program (CMDRP PRCRP CA160224 (NW)) and from the National Institutes of Health (NCI R15 CA242057 01A1). Finally, the research reported in this manuscript was supported by the National Institute of General Medical Sciences (NIGMS) of the National Institutes of Health under award number P20GM130448. The content is solely the responsibility of the authors and does not necessarily represent the official views of the National Institutes of Health.

Acknowledgments

We thank Rose Pollina for her grammatical editing of the manuscript.

References

1. Jackson, S.P.; Bartek, J. The DNA-Damage Response in Human Biology and Disease. *Nature* 2009, 461, 1071–1078.
2. Caldecott, K.W. Mammalian Single-Strand Break Repair: Mechanisms and Links with Chromatin. *DNA Repair* 2007, 6, 443–453.
3. Lans, H.; Hoeijmakers, J.H.J.; Vermeulen, W.; Marteijn, J.A. The DNA Damage Response to Transcription Stress. *Nat. Rev. Mol. Cell Biol.* 2019, 20, 766–784.
4. Ciccia, A.; Elledge, S.J. The DNA Damage Response: Making It Safe to Play with Knives. *Mol. Cell* 2010, 40, 179–204.
5. Ghosal, G.; Chen, J. DNA Damage Tolerance: A Double-Edged Sword Guarding the Genome. *Transl Cancer Res.* 2013, 2, 107–129.
6. Knijnenburg, T.A.; Wang, L.; Zimmermann, M.T.; Chambwe, N.; Gao, G.F.; Cherniack, A.D.; Fan, H.; Shen, H.; Way, G.P.; Greene, C.S.; et al. Genomic and Molecular Landscape of DNA Damage Repair Deficiency across The Cancer Genome Atlas. *Cell Rep.* 2018, 23, 239–254.e6.
7. Alhmoud, J.F.; Woolley, J.F.; Al Moustafa, A.-E.; Malki, M.I. DNA Damage/Repair Management in Cancers. *Cancers* 2020, 12, 1050.
8. Norbury, C.J.; Zhivotovsky, B. DNA Damage-Induced Apoptosis. *Oncogene* 2004, 23, 2797–2808.
9. Branzei, D.; Foiani, M. Regulation of DNA Repair throughout the Cell Cycle. *Nat. Rev. Mol. Cell Biol.* 2008, 9, 297–308.
10. Campos, A.; Clemente-Blanco, A. Cell Cycle and DNA Repair Regulation in the Damage Response: Protein Phosphatases Take Over the Reins. *Int. J. Mol. Sci.* 2020, 21, 446.
11. Kiwerska, K.; Szyfter, K. DNA Repair in Cancer Initiation, Progression, and Therapy—a Double-Edged Sword. *J. Appl. Genet.* 2019, 60, 329–334.
12. Van Gent, D.C.; Kanaar, R. Exploiting DNA Repair Defects for Novel Cancer Therapies. *Mol. Biol. Cell* 2016, 27, 2145–2148.

13. Hoeijmakers, J.H. Genome Maintenance Mechanisms for Preventing Cancer . *Nature* 2001, 411, 366–374. Available online: <https://www.nature.com/articles/35077232> (accessed on 19 May 2021).
14. Pfister, H. Chapter 8: Human Papillomavirus and Skin Cancer. *J. Natl. Cancer Inst. Monogr.* 2003, 2003, 52–56.
15. Tommasino, M. HPV and Skin Carcinogenesis. *Papillomavirus Res.* 2019, 7, 129–131.
16. Rollison, D.E.; Viariso, D.; Amorrortu, R.P.; Gheit, T.; Tommasino, M. An Emerging Issue in Oncogenic Virology: The Role of Beta Human Papillomavirus Types in the Development of Cutaneous Squamous Cell Carcinoma. *J. Virol.* 2019, 93, e01003-18.
17. Strickley, J.D.; Messerschmidt, J.L.; Awad, M.E.; Li, T.; Hasegawa, T.; Ha, D.T.; Nabeta, H.W.; Bevins, P.A.; Ngo, K.H.; Asgari, M.M.; et al. Immunity to Commensal Papillomaviruses Protects against Skin Cancer. *Nature* 2019, 575, 519–522.
18. Lambert, P.F.; Münger, K.; Rösl, F.; Hasche, D.; Tommasino, M. Beta Human Papillomaviruses and Skin Cancer. *Nature* 2020, 588, E20–E21.
19. Strickley, J.D.; Messerschmidt, J.L.; Jenson, A.B.; Joh, J.; Demehri, S. Reply to: Beta Human Papillomaviruses and Skin Cancer. *Nature* 2020, 588, E22–E23.
20. Van Doorslaer, K.; Li, Z.; Xirasagar, S.; Maes, P.; Kaminsky, D.; Liou, D.; Sun, Q.; Kaur, R.; Huyen, Y.; McBride, A.A. The Papillomavirus Episteme: A Major Update to the Papillomavirus Sequence Database. *Nucleic Acids Res.* 2017, 45, D499–D506.
21. Tommasino, M. The Biology of Beta Human Papillomaviruses. *Virus Res.* 2017, 231, 128–138.
22. Wendel, S.O.; Wallace, N.A. Loss of Genome Fidelity: Beta HPVs and the DNA Damage Response. *Front. Microbiol.* 2017, 8.
23. Tahseen, D.; Rady, P.L.; Tyring, S.K. Effects of β -HPV on DNA Damage Response Pathways to Drive Carcinogenesis: A Review. *Virus Genes* 2021, 57, 23–30.
24. Hasche, D.; Vinzón, S.E.; Rösl, F. Cutaneous Papillomaviruses and Non-Melanoma Skin Cancer: Causal Agents or Innocent Bystanders? *Front. Microbiol.* 2018, 9, 874.
25. Meyers, J.M.; Grace, M.; Uberoi, A.; Lambert, P.F.; Munger, K. Inhibition of TGF- β and NOTCH Signaling by Cutaneous Papillomaviruses. *Front. Microbiol.* 2018, 9, 874.
26. Howley, P.M.; Pfister, H.J. Beta Genus Papillomaviruses and Skin Cancer. *Virology* 2015, 479, 290–296.

27. Assunta, V.; Stefan, L.; Massimo, T.; Sigrun, S. Cross-Talk of Cutaneous Beta Human Papillomaviruses and the Immune System: Determinants of Disease Penetrance. *Philos. Trans. R. Soc. B Biol. Sci.* 2019, 374, 20180287.
28. Sichero, L.; Rollison, D.E.; Amorrortu, R.P.; Tommasino, M. Beta Human Papillomavirus and Associated Diseases. *Acta Cytol.* 2019, 63, 100–108.
29. Yuan, L.W.; Giordano, A. Acetyltransferase Machinery Conserved in P300/CBP-Family Proteins. *Oncogene* 2002, 21, 2253–2260. Available online: <https://www.nature.com/articles/1205283> (accessed on 6 May 2021).
30. Bordoli, L.; Netsch, M.; Lüthi, U.; Lutz, W.; Eckner, R. Plant Orthologs of P300/CBP: Conservation of a Core Domain in Metazoan P300/CBP Acetyltransferase-Related Proteins. *Nucleic Acids Res.* 2001, 29, 589–597.
31. Delvecchio, M.; Gaucher, J.; Aguilar-Gurrieri, C.; Ortega, E.; Panne, D. Structure of the P300 Catalytic Core and Implications for Chromatin Targeting and HAT Regulation. *Nat. Struct. Mol. Biol.* 2013, 20, 1040–1046.
32. Kraus, W.L.; Manning, E.T.; Kadonaga, J.T. Biochemical Analysis of Distinct Activation Functions in P300 That Enhance Transcription Initiation with Chromatin Templates. *Mol. Cell. Biol.* 1999, 19, 8123.
33. Dyson, H.J.; Wright, P.E. Role of Intrinsic Protein Disorder in the Function and Interactions of the Transcriptional Coactivators CREB-Binding Protein (CBP) and P300. *J. Biol. Chem.* 2016, 291, 6714–6722.
34. Kalkhoven, E. CBP and P300: HATs for Different Occasions. *Biochem. Pharmacol.* 2004, 68, 1145–1155.
35. Goodman, R.H.; Smolik, S. CBP/P300 in Cell Growth, Transformation, and Development. *Genes Dev.* 2000, 14, 1553–1577.
36. Giordano, A.; Avantaggiati, M.L. P300 and CBP: Partners for Life and Death. *J. Cell. Physiol.* 1999, 181, 218–230. Available online: [https://onlinelibrary.wiley.com/doi/10.1002/\(SICI\)1097-4652\(199911\)181:2%3C218::AID-JCP4%3E3.0.CO;2-5](https://onlinelibrary.wiley.com/doi/10.1002/(SICI)1097-4652(199911)181:2%3C218::AID-JCP4%3E3.0.CO;2-5) (accessed on 6 May 2021).
37. Chan, H.M.; Thangue, N.B.L. P300/CBP Proteins: HATs for Transcriptional Bridges and Scaffolds. *J. Cell Sci.* 2001, 114, 2363–2373.

38. Dancy, B.M.; Cole, P.A. Protein Lysine Acetylation by P300/CBP. *Chem. Rev.* 2015, 115, 2419–2452.
39. Bannister, A.J.; Kouzarides, T. The CBP Co-Activator Is a Histone Acetyltransferase. *Nature* 1996, 384, 641–643.
40. Narita, T.; Weinert, B.T.; Choudhary, C. Functions and Mechanisms of Non-Histone Protein Acetylation. *Nat. Rev. Mol. Cell Biol.* 2019, 20, 156–174.
41. Dutto, I.; Scalera, C.; Prosperi, E. CREBBP and P300 Lysine Acetyl Transferases in the DNA Damage Response. *Cell. Mol. Life Sci.* 2018, 75, 1325–1338.
42. Ogiwara, H.; Ui, A.; Otsuka, A.; Satoh, H.; Yokomi, I.; Nakajima, S.; Yasui, A.; Yokota, J.; Kohno, T. Histone Acetylation by CBP and P300 at Double-Strand Break Sites Facilitates SWI/SNF Chromatin Remodeling and the Recruitment of Non-Homologous End Joining Factors. *Oncogene* 2011, 30, 2135–2146.
43. Hasan, S.; Hottiger, M.O. Histone Acetyl Transferases: A Role in DNA Repair and DNA Replication. *J. Mol. Med.* 2002, 80, 463–474.
44. Ogiwara, H.; Kohno, T. CBP and P300 Histone Acetyltransferases Contribute to Homologous Recombination by Transcriptionally Activating the BRCA1 and RAD51 Genes. *PLoS ONE* 2012, 7, e52810.
45. Stauffer, D.; Chang, B.; Huang, J.; Dunn, A.; Thayer, M. P300/CREB-Binding Protein Interacts with ATR and Is Required for the DNA Replication Checkpoint. *J. Biol. Chem.* 2007, 282, 9678–9687.
46. Dutto, I.; Scalera, C.; Tillhon, M.; Ticali, G.; Passaniti, G.; Cazzalini, O.; Savio, M.; Stivala, L.A.; Gervasini, C.; Larizza, L.; et al. Mutations in CREBBP and EP300 Genes Affect DNA Repair of Oxidative Damage in Rubinstein-Taybi Syndrome Cells. *Carcinogenesis* 2020, 41, 257–266.
47. Kim, M.-K.; Shin, J.-M.; Eun, H.C.; Chung, J.H. The Role of P300 Histone Acetyltransferase in UV-Induced Histone Modifications and MMP-1 Gene Transcription. *PLoS ONE* 2009, 4, e4864.
48. Grossman, S.R. P300/CBP/P53 Interaction and Regulation of the P53 Response. *Eur. J. Biochem.* 2001, 268, 2773–2778.
49. Dai, C.; Gu, W. P53 Post-Translational Modification: Deregulated in Tumorigenesis. *Trends Mol. Med.* 2010, 16, 528–536.

50. Chan, H.M.; Krstic-Demonacos, M.; Smith, L.; Demonacos, C.; La Thangue, N.B. Acetylation Control of the Retinoblastoma Tumour-Suppressor Protein. *Nat. Cell Biol* 2001, 3, 667–674.
51. Nishihara, A.; Hanai, J.I.; Okamoto, N.; Yanagisawa, J.; Kato, S.; Miyazono, K.; Kawabata, M. Role of P300, a Transcriptional Coactivator, in Signalling of TGF-Beta. *Genes Cells* 1998, 3, 613–623.
52. Iyer, N.G.; Özdag, H.; Caldas, C. P300/CBP and Cancer. *Oncogene* 2004, 23, 4225–4231.
53. Attar, N.; Kurdistani, S.K. Exploitation of EP300 and CREBBP Lysine Acetyltransferases by Cancer. *Cold Spring Harb. Perspect. Med.* 2017, 7, a026534.
54. Forbes, S.A.; Beare, D.; Gunasekaran, P.; Leung, K.; Bindal, N.; Boutselakis, H.; Ding, M.; Bamford, S.; Cole, C.; Ward, S.; et al. COSMIC: Exploring the World’s Knowledge of Somatic Mutations in Human Cancer. *Nucleic Acids Res.* 2015, 43, D805-811.
55. Rotte, A.; Bhandaru, M.; Cheng, Y.; Sjoestroem, C.; Martinka, M.; Li, G. Decreased Expression of Nuclear P300 Is Associated with Disease Progression and Worse Prognosis of Melanoma Patients. *PLoS ONE* 2013, 8, e75405.
56. Giles, R.H.; Peters, D.J.M.; Breuning, M.H. Conjunction Dysfunction: CBP/P300 in Human Disease. *Trends Genet.* 1998, 14, 178–183.
57. Blackford, A.N.; Jackson, S.P. ATM, ATR, and DNA-PK: The Trinity at the Heart of the DNA Damage Response. *Mol. Cell* 2017, 66, 801–817.
58. Wallace, N.A.; Robinson, K.; Howie, H.L.; Galloway, D.A. HPV 5 and 8 E6 Abrogate ATR Activity Resulting in Increased Persistence of UVB Induced DNA Damage. *PLoS Pathog.* 2012, 8, e1002807.
59. Hufbauer, M.; Cooke, J.; van der Horst, G.T.J.; Pfister, H.; Storey, A.; Akgül, B. Human Papillomavirus Mediated Inhibition of DNA Damage Sensing and Repair Drives Skin Carcinogenesis. *Mol. Cancer* 2015, 14, 183.
60. Snow, J.A.; Murthy, V.; Dacus, D.; Hu, C.; Wallace, N.A. β -HPV 8E6 Attenuates ATM and ATR Signaling in Response to UV Damage. *Pathogens* 2019, 8, 267.
61. Göhler, T.; Sabbioneda, S.; Green, C.M.; Lehmann, A.R. ATR-Mediated Phosphorylation of DNA Polymerase η Is Needed for Efficient Recovery from UV Damage. *J. Cell Biol.* 2011, 192, 219–227.

62. Curtis, M.J.; Hays, J.B. Cooperative Responses of DNA-Damage-Activated Protein Kinases ATR and ATM and DNA Translesion Polymerases to Replication-Blocking DNA Damage in a Stem-Cell Niche. *DNA Repair (Amst.)* 2011, 10, 1272–1281.
63. Lee, T.-H.; Park, J.-M.; Leem, S.-H.; Kang, T.-H. Coordinated Regulation of XPA Stability by ATR and HERC2 during Nucleotide Excision Repair. *Oncogene* 2014, 33, 19–25.
64. Cheng, Q.; Chen, J. Mechanism of P53 Stabilization by ATM after DNA Damage. *Cell Cycle* 2010, 9, 472–478.
65. Wallace, N.A.; Gasior, S.L.; Faber, Z.J.; Howie, H.L.; Deininger, P.L.; Galloway, D.A. HPV 5 and 8 E6 Expression Reduces ATM Protein Levels and Attenuates LINE-1 Retrotransposition. *Virology* 2013, 443, 69–79.
66. Dickson, M.A.; Hahn, W.C.; Ino, Y.; Ronfard, V.; Wu, J.Y.; Weinberg, R.A.; Louis, D.N.; Li, F.P.; Rheinwald, J.G. Human Keratinocytes That Express HTERT and Also Bypass a P16INK4a-Enforced Mechanism That Limits Life Span Become Immortal yet Retain Normal Growth and Differentiation Characteristics. *Mol. Cell Biol.* 2000, 20, 1436–1447.
67. Mohiuddin, I.S.; Kang, M.H. DNA-PK as an Emerging Therapeutic Target in Cancer. *Front. Oncol.* 2019, 9.
68. Shibata, A.; Jeggo, P.A. Roles for the DNA-PK Complex and 53BP1 in Protecting Ends from Resection during DNA Double-Strand Break Repair. *J. Radiat. Res.* 2020, 61, 718–726.
69. Hu, C.; Bugbee, T.; Gamez, M.; Wallace, N.A. Beta Human Papillomavirus 8E6 Attenuates Non-Homologous End Joining by Hindering DNA-PKcs Activity. *Cancers* 2020, 12, 2356.
70. Wallace, N.A.; Robinson, K.; Howie, H.L.; Galloway, D.A. β -HPV 5 and 8 E6 Disrupt Homology Dependent Double Strand Break Repair by Attenuating BRCA1 and BRCA2 Expression and Foci Formation. *PLoS Pathog.* 2015, 11, e1004687.
71. Bakr, A.; Oing, C.; Köcher, S.; Borgmann, K.; Dornreiter, I.; Petersen, D.; Dikomey, E.; Mansour, W.Y. Involvement of ATM in Homologous Recombination after End Resection and RAD51 Nucleofilament Formation. *Nucleic Acids Res.* 2015, 43, 3154–

3166. Available online: <https://academic.oup.com/nar/article/43/6/3154/2453440> (accessed on 17 June 2021).
72. Ceccaldi, R.; Rondinelli, B.; D'Andrea, A.D. Repair Pathway Choices and Consequences at the Double-Strand Break. *Trends Cell Biol.* 2016, 26, 52–64.
 73. Mao, Z.; Bozzella, M.; Seluanov, A.; Gorbunova, V. Comparison of Nonhomologous End Joining and Homologous Recombination in Human Cells. *DNA Repair (Amst.)* 2008, 7, 1765–1771.
 74. Du, J.; Yin, N.; Xie, T.; Zheng, Y.; Xia, N.; Shang, J.; Chen, F.; Zhang, H.; Yu, J.; Liu, F. Quantitative Assessment of HR and NHEJ Activities via CRISPR/Cas9-Induced Oligodeoxynucleotide-Mediated DSB Repair. *DNA Repair* 2018, 70, 67–71.
 75. Kastan, M.B.; Bartek, J. Cell-Cycle Checkpoints and Cancer. *Nature* 2004, 432, 316–323.
 76. Hayashi, M.T.; Karlseder, J. DNA Damage Associated with Mitosis and Cytokinesis Failure. *Oncogene* 2013, 32, 4593–4601.
 77. Storchova, Z.; Kuffer, C. The Consequences of Tetraploidy and Aneuploidy. *J. Cell Sci.* 2008, 121, 3859–3866.
 78. Sanz-Gómez, N.; de Pedro, I.; Ortigosa, B.; Santamaría, D.; Malumbres, M.; de Cárcer, G.; Gandarillas, A. Squamous Differentiation Requires G2/Mitosis Slippage to Avoid Apoptosis. *Cell Death Differ.* 2020, 27, 2451–2467.
 79. Jackson, S.; Harwood, C.; Thomas, M.; Banks, L.; Storey, A. Role of Bak in UV-Induced Apoptosis in Skin Cancer and Abrogation by HPV E6 Proteins. *Genes Dev.* 2000, 14, 3065–3073.
 80. Giampieri, S.; Storey, A. Repair of UV-Induced Thymine Dimers Is Compromised in Cells Expressing the E6 Protein from Human Papillomaviruses Types 5 and 18. *Br. J. Cancer* 2004, 90, 2203–2209.
 81. Marthaler, A.M.; Podgorska, M.; Feld, P.; Fingerle, A.; Knerr-Rupp, K.; Grässer, F.; Smola, H.; Roemer, K.; Ebert, E.; Kim, Y.-J.; et al. Identification of C/EBP α as a Novel Target of the HPV8 E6 Protein Regulating MiR-203 in Human Keratinocytes. *PLoS Pathog.* 2017, 13, e1006406.
 82. Dacus, D.; Cotton, C.; McCallister, T.X.; Wallace, N.A. β -HPV 8E6 Attenuates LATS Phosphorylation After Failed Cytokinesis. *J. Virol.* 2020.

83. Howie, H.L.; Koop, J.I.; Weese, J.; Robinson, K.; Wipf, G.; Kim, L.; Galloway, D.A. Beta-HPV 5 and 8 E6 Promote P300 Degradation by Blocking AKT/P300 Association. *PLoS Pathog.* 2011, 7, e1002211.
84. Wallace, N.A.; Robinson, K.; Galloway, D.A. Beta Human Papillomavirus E6 Expression Inhibits Stabilization of P53 and Increases Tolerance of Genomic Instability. *J. Virol.* 2014, 88, 6112–6127.
85. Muench, P.; Probst, S.; Schuetz, J.; Leiprecht, N.; Busch, M.; Wesselborg, S.; Stubenrauch, F.; Iftner, T. Cutaneous Papillomavirus E6 Proteins Must Interact with P300 and Block P53-Mediated Apoptosis for Cellular Immortalization and Tumorigenesis. *Cancer Res.* 2010, 70, 6913–6924.
86. Ozaki, T.; Nakagawara, A. Role of P53 in Cell Death and Human Cancers. *Cancers (Basel)* 2011, 3, 994–1013.
87. Chen, J. The Cell-Cycle Arrest and Apoptotic Functions of P53 in Tumor Initiation and Progression. *Cold Spring Harb. Perspect. Med.* 2016, 6, a026104.
88. Zhu, G.; Pan, C.; Bei, J.-X.; Li, B.; Liang, C.; Xu, Y.; Fu, X. Mutant P53 in Cancer Progression and Targeted Therapies. *Front. Oncol.* 2020, 10, 2418.
89. Pucci, B.; Kasten, M.; Giordano, A. Cell Cycle and Apoptosis. *Neoplasia* 2000, 2, 291–299.
90. Lakin, N.D.; Jackson, S.P. Regulation of P53 in Response to DNA Damage. *Oncogene* 1999, 18, 7644–7655.
91. Cornet, I.; Bouvard, V.; Campo, M.S.; Thomas, M.; Banks, L.; Gissmann, L.; Lamartine, J.; Sylla, B.S.; Accardi, R.; Tommasino, M. Comparative Analysis of Transforming Properties of E6 and E7 from Different Beta Human Papillomavirus Types. *J. Virol.* 2012, 86, 2366–2370.
92. Huibregtse, J.M.; Scheffner, M.; Howley, P.M. A Cellular Protein Mediates Association of P53 with the E6 Oncoprotein of Human Papillomavirus Types 16 or 18. *EMBO J.* 1991, 10, 4129–4135.
93. Hafner, A.; Bulyk, M.L.; Jambhekar, A.; Lahav, G. The Multiple Mechanisms That Regulate P53 Activity and Cell Fate. *Nat. Rev. Mol. Cell Biol.* 2019, 20, 199–210.
94. Saeed, S.; Logie, C.; Francoijs, K.-J.; Frigè, G.; Romanenghi, M.; Nielsen, F.G.; Raats, L.; Shahhoseini, M.; Huynen, M.; Altucci, L.; et al. Chromatin Accessibility, P300, and

- Histone Acetylation Define PML-RAR α and AML1-ETO Binding Sites in Acute Myeloid Leukemia. *Blood* 2012, 120, 3058–3068.
95. Sakamoto, S.; Wakae, K.; Anzai, Y.; Murai, K.; Tamaki, N.; Miyazaki, M.; Miyazaki, K.; Romanow, W.J.; Ikawa, T.; Kitamura, D.; et al. E2A and CBP/P300 Act in Synergy To Promote Chromatin Accessibility of the Immunoglobulin κ Locus. *J. Immunol.* 2012, 188, 5547–5560.
 96. Tibbetts, R.S.; Brumbaugh, K.M.; Williams, J.M.; Sarkaria, J.N.; Cliby, W.A.; Shieh, S.-Y.; Taya, Y.; Prives, C.; Abraham, R.T. A Role for ATR in the DNA Damage-Induced Phosphorylation of P53. *Genes Dev.* 1999, 13, 152–157.
 97. Lakin, N.D.; Hann, B.C.; Jackson, S.P. The Ataxia-Telangiectasia Related Protein ATR Mediates DNA-Dependent Phosphorylation of P53. *Oncogene* 1999, 18, 3989–3995.
 98. Meek, D.W. Tumour Suppression by P53: A Role for the DNA Damage Response? *Nat. Rev. Cancer* 2009, 9, 714–723.
 99. Loughery, J.; Cox, M.; Smith, L.M.; Meek, D.W. Critical Role for P53-Serine 15 Phosphorylation in Stimulating Transactivation at P53-Responsive Promoters. *Nucleic Acids Res.* 2014, 42, 7666–7680.
 100. Ganem, N.J.; Cornils, H.; Chiu, S.-Y.; O'Rourke, K.P.; Arnaud, J.; Yimlamai, D.; Théry, M.; Camargo, F.D.; Pellman, D. Cytokinesis Failure Triggers Hippo Tumor Suppressor Pathway Activation. *Cell* 2014, 158, 833–848.
 101. Furth, N.; Aylon, Y.; Oren, M. P53 Shades of Hippo. *Cell Death Differ.* 2018, 25, 81.
 102. Aylon, Y.; Michael, D.; Shmueli, A.; Yabuta, N.; Nojima, H.; Oren, M. A Positive Feedback Loop between the P53 and Lats2 Tumor Suppressors Prevents Tetraploidization. *Genes Dev.* 2006, 20, 2687–2700.
 103. Davoli, T.; de Lange, T. The Causes and Consequences of Polyploidy in Normal Development and Cancer. *Annu. Rev. Cell Dev. Biol.* 2011, 27, 585–610.
 104. Ganem, N.J.; Godinho, S.A.; Pellman, D. A Mechanism Linking Extra Centrosomes to Chromosomal Instability. *Nature* 2009, 460, 278–282.
 105. Krämer, A.; Neben, K.; Ho, A.D. Centrosome Replication, Genomic Instability and Cancer. *Leukemia* 2002, 16, 767–775.
 106. White, E.A.; Kramer, R.E.; Tan, M.J.A.; Hayes, S.D.; Harper, J.W.; Howley, P.M. Comprehensive Analysis of Host Cellular Interactions with Human Papillomavirus E6

- Proteins Identifies New E6 Binding Partners and Reflects Viral Diversity. *J. Virol.* 2012, 86, 13174–13186.
107. Rozenblatt-Rosen, O.; Deo, R.C.; Padi, M.; Adelmant, G.; Calderwood, M.A.; Rolland, T.; Grace, M.; Dricot, A.; Askenazi, M.; Tavares, M.; et al. Interpreting Cancer Genomes Using Systematic Host Perturbations by Tumour Virus Proteins. *Nature* 2012, 487, 491–495.
 108. Hampras, S.S.; Rollison, D.E.; Giuliano, A.R.; McKay-Chopin, S.; Minoni, L.; Sereday, K.; Gheit, T.; Tommasino, M. Prevalence and Concordance of Cutaneous Beta Human Papillomavirus Infection at Mucosal and Cutaneous Sites. *J. Infect. Dis.* 2017, 216, 92–96.
 109. Patel, T.; Morrison, L.K.; Rady, P.; Tyring, S. Epidermodysplasia Verruciformis and Susceptibility to HPV. *Dis. Markers* 2010, 29, 199–206.
 110. Emsen, I.M.; Kabalar, M.E. Epidermodysplasia Verruciformis: An Early and Unusual Presentation. *Can. J. Plast Surg.* 2010, 18, 21–24.
 111. Lane, J.E.; Bowman, P.H.; Cohen, D.J. Epidermodysplasia Verruciformis. *South. Med. J.* 2003, 96, 613–615.
 112. Kiyono, T.; Hiraiwa, A.; Ishibashi, M. Differences in Transforming Activity and Coded Amino Acid Sequence among E6 Genes of Several Papillomaviruses Associated with Epidermodysplasia Verruciformis. *Virology* 1992, 186, 628–639.
 113. Cladel, N.M.; Budgeon, L.R.; Cooper, T.K.; Balogh, K.K.; Hu, J.; Christensen, N.D. Secondary Infections, Expanded Tissue Tropism, and Evidence for Malignant Potential in Immunocompromised Mice Infected with Mus Musculus Papillomavirus 1 DNA and Virus. *J. Virol.* 2013, 87, 9391–9395.
 114. Meyers, J.M.; Uberoi, A.; Grace, M.; Lambert, P.F.; Munger, K. Cutaneous HPV8 and MmuPV1 E6 Proteins Target the NOTCH and TGF- β Tumor Suppressors to Inhibit Differentiation and Sustain Keratinocyte Proliferation. *PLoS Pathog.* 2017, 13, e1006171.
 115. Lazić, D.; Hufbauer, M.; Zigrino, P.; Buchholz, S.; Kazem, S.; Feltkamp, M.C.W.; Mauch, C.; Steger, G.; Pfister, H.; Akgül, B. Human Papillomavirus Type 8 E6 Oncoprotein Inhibits Transcription of the PDZ Protein Syntenin-2. *J. Virol.* 2012, 86, 7943–7952.

116. Töpffer, S.; Müller-Schiffmann, A.; Matentzoglou, K.; Scheffner, M.; Steger, G. 2007 Protein Tyrosine Phosphatase H1 Is a Target of the E6 Oncoprotein of High-Risk Genital Human Papillomaviruses. *J. Gen. Virol.* 2007, 88, 2956–2965.
117. Müller-Schiffmann, A.; Beckmann, J.; Steger, G. The E6 Protein of the Cutaneous Human Papillomavirus Type 8 Can Stimulate the Viral Early and Late Promoters by Distinct Mechanisms. *J. Virol.* 2006, 80, 8718–8728.
118. Huang, W.-C.; Chen, C.-C. Akt Phosphorylation of P300 at Ser-1834 Is Essential for Its Histone Acetyltransferase and Transcriptional Activity. *Mol. Cell. Biol.* 2005, 25, 6592–6602.
119. Iyer, N.G.; Chin, S.-F.; Ozdag, H.; Daigo, Y.; Hu, D.-E.; Cariati, M.; Brindle, K.; Aparicio, S.; Caldas, C. P300 Regulates P53-Dependent Apoptosis after DNA Damage in Colorectal Cancer Cells by Modulation of PUMA/P21 Levels. *Proc. Natl. Acad. Sci. USA* 2004, 101, 7386–7391.
120. He, Z.-X.; Wei, B.-F.; Zhang, X.; Gong, Y.-P.; Ma, L.-Y.; Zhao, W. Current Development of CBP/P300 Inhibitors in the Last Decade. *Eur. J. Med. Chem.* 2021, 209, 112861.
121. Yang, Y.; Zhang, R.; Li, Z.; Mei, L.; Wan, S.; Ding, H.; Chen, Z.; Xing, J.; Feng, H.; Han, J.; et al. Discovery of Highly Potent, Selective, and Orally Efficacious P300/CBP Histone Acetyltransferases Inhibitors. *J. Med. Chem.* 2020, 63, 1337–1360.
122. Brooks, N.; Raja, M.; Young, B.W.; Spencer, G.J.; Somerville, T.C.; Pegg, N.A. CCS1477: A Novel Small Molecule Inhibitor of P300/CBP Bromodomain for the Treatment of Acute Myeloid Leukaemia and Multiple Myeloma. *Blood* 2019, 134, 2560.
123. Alari, V.; Russo, S.; Rovina, D.; Gowran, A.; Garzo, M.; Crippa, M.; Mazzanti, L.; Scalera, C.; Prosperi, E.; Giardino, D.; et al. Generation of the Rubinstein-Taybi Syndrome Type 2 Patient-Derived Induced Pluripotent Stem Cell Line (IAli001-A) Carrying the EP300 Exon 23 Stop Mutation c.3829A > T, p.(Lys1277*). *Stem Cell Res.* 2018, 30, 175–179.
124. Gayther, S.A.; Batley, S.J.; Linger, L.; Bannister, A.; Thorpe, K.; Chin, S.-F.; Daigo, Y.; Russell, P.; Wilson, A.; Sowter, H.M.; et al. Mutations Truncating the EP300 Acetylase in Human Cancers. *Nat. Genet.* 2000, 24, 300–303.

125. Turnell, A.S.; Mymryk, J.S. Roles for the Coactivators CBP and P300 and the APC/C E3 Ubiquitin Ligase in E1A-Dependent Cell Transformation. *Br. J. Cancer* 2006, 95, 555–560.
126. Saidj, D.; Cros, M.-P.; Hernandez-Vargas, H.; Guarino, F.; Sylla, B.S.; Tommasino, M.; Accardi, R. Oncoprotein E7 from Beta Human Papillomavirus 38 Induces Formation of an Inhibitory Complex for a Subset of P53-Regulated Promoters. *J. Virol.* 2013, 87, 12139–12150.
127. Yamashita, T.; Segawa, K.; Fujinaga, Y.; Nishikawa, T.; Fujinaga, K. Biological and Biochemical Activity of E7 Genes of the Cutaneous Human Papillomavirus Type 5 and 8. *Oncogene* 1993, 8, 2433–2441.
128. Von Mikecz, A.; Zhang, S.; Montminy, M.; Tan, E.M.; Hemmerich, P. Creb-Binding Protein (Cbp/P300) and RNA Polymerase II Colocalize in Transcriptionally Active Domains in the Nucleus. *J. Cell Biol.* 2000, 150, 265–274.
129. Fauquier, L.; Azzag, K.; Parra, M.A.M.; Quillien, A.; Boulet, M.; Diouf, S.; Carnac, G.; Waltzer, L.; Gronemeyer, H.; Vandell, L. CBP and P300 Regulate Distinct Gene Networks Required for Human Primary Myoblast Differentiation and Muscle Integrity. *Sci. Rep.* 2018, 8, 12629.
130. Suarez, I.; Trave, G. Structural Insights in Multifunctional Papillomavirus Oncoproteins. *Viruses* 2018, 10, 37.
131. Zanier, K.; Charbonnier, S.; Sidi, A.O.M.O.; McEwen, A.G.; Ferrario, M.G.; Poussin-Courmontagne, P.; Cura, V.; Brimer, N.; Babah, K.O.; Ansari, T.; et al. Structural Basis for Hijacking of Cellular LxxLL Motifs by Papillomavirus E6 Oncoproteins. *Science* 2013, 339, 694–698.
132. Mo, M.; Shahar, S.; Fleming, S.B.; Mercer, A.A. How Viruses Affect the Cell Cycle through Manipulation of the APC/C. *Trends Microbiol.* 2012, 20, 440–448.
133. Lundblad, J.R.; Kwok, R.P.S.; Lurance, M.E.; Harter, M.L.; Goodman, R.H. Adenoviral E1A-Associated Protein P300 as a Functional Homologue of the Transcriptional Co-Activator CBP. *Nature* 1995, 374, 85–88.
134. O'Connor, M.J.; Zimmermann, H.; Nielsen, S.; Bernard, H.-U.; Kouzarides, T. Characterization of an E1A-CBP Interaction Defines a Novel Transcriptional Adapter Motif (TRAM) in CBP/P300. *J. Virol.* 1999, 73, 3574–3581.

Chapter 3 - Beta Human Papillomavirus 8E6 Attenuates LATS

Phosphorylation after Failed Cytokinesis

Dalton Dacus¹, Celeste Cotton^{1,2}, Tristan X. McCallister¹, Nicholas A. Wallace^{1*}

1. Division of Biology, Kansas State University, Manhattan, Kansas, USA
2. Langston University, Langston, OK, USA

*Corresponding Author: nwallac@ksu.edu

Published as: Dacus D, Cotton C, McCallister TX, Wallace NA. 2020. β -HPV 8E6 Attenuates LATS Phosphorylation After Failed Cytokinesis. *J Virol* <https://doi.org/10.1128/JVI.02184-19>.

Abstract

β -HPVs contribute to cSCC development in immunocompromised populations. However, it is unclear if these common cutaneous viruses are tumorigenic in the general population. Thus, a more thorough investigation of β -HPV biology is warranted. If β -HPV infections do promote cSCCs, they are hypothesized to destabilize the cellular genome. *In vitro* data support this idea by demonstrating the ability of the β -HPV E6 protein to disrupt DNA repair signaling events following UV exposure. We show that β -HPV E6 more broadly impairs cellular signaling, indicating that the viral protein dysregulates the HP. The HP protects genome fidelity by regulating cell growth and apoptosis in response to a myriad of deleterious stimuli, including failed cytokinesis. After failed cytokinesis, β -HPV 8E6 attenuates phosphorylation of the HP kinase (LATS). This decreases some, but not all, HP signaling events. Notably, β -HPV 8E6 does not limit senescence associated with failed cytokinesis.

Importance

The human papillomavirus (HPV) family includes over 200 double-stranded DNA viruses that are divided into five genera, all of which infect human epithelia (1). Upon infecting mucosal or cutaneous tissue, members of each genus can cause a broad array of pathologies. Of these, the most prominent diseases are the anogenital and oropharyngeal carcinomas caused by alpha genus HPVs (2, 3). Cutaneous beta genus HPVs (β -HPVs) have also been linked to tumorigenesis via high viral DNA loads in cutaneous squamous cell carcinomas (cSCCs) of immunocompromised patients, primarily in sun-exposed skin (4–6).

Introduction

While β -HPV infections are common in immunocompetent individuals, their contribution to cSCCs is less clear. The main etiological factor in skin cancer pathogenesis is UV. Further, the

characterizations of cSCCs in the general population do not include continued β -HPV expression (7–9). Viral loads decrease as lesions progress from precancerous actinic keratosis (AK) to cSCC (10–12). These data have led to the hypothesized “hit-and-run” mechanism of oncogenesis, where β -HPVs cooperate with UV to enhance genomic instability in the early stages of carcinogenesis (10, 13, 14). This elevated mutational load then increases the chances of tumor progression independent of continued viral gene expression.

While it is hard to prove the role of a transient viral infection in persistent cancer, β -HPVs are also a common resident of our skin and are frequently found in AKs. Despite the billions of dollars spent on sun care products annually, 58 million Americans still have one or more AKs. Moreover, over \$1 billion is spent during 5.2 million outpatient visits each year for AK treatment (15, 16). The cost of these AKs for the patient, both financial and emotional, increases if these lesions develop into malignancies. Within 1 year of diagnosis, an estimated 0.6% of AKs progress to cSCCs. This progression expands to 2.6% of AKs 5 years after diagnosis (17). Because β -HPV infections are quite common, even a mild increase in cancer risk would be notable. Thus, it is important to understand their potential contribution to the genome instability that drives cSCC progression.

A great deal is known about the tumorigenic potential of β -HPV proteins, particularly the E6 protein. The presence of the putative oncogene E6 from β -HPV 8 (β -HPV 8E6) is enough to cause cancers in mice without UV exposure (18, 19). β -HPV 8E6 inhibits differentiation and promotes proliferation by targeting the NOTCH and TGF- β signaling pathways (20). Another central theme of β -HPV E6 proteins is their ability to bind the cellular histone acetyltransferase p300 (21–24). β -HPV 8E6 and the E6 from β -HPV 5 bind p300 strongly, leading to its destabilization and decreasing DNA damage repair (DDR) gene expression (22, 25, 26). β -HPV

type 38's E6 protein has a lower p300-binding affinity and cannot destabilize the cellular protein (27). Nevertheless, binding p300 is essential for HPV38-induced immortalization of human foreskin keratinocytes (HFKs) (28). This suggests that p300 binding may be a shared factor in β -HPV-promoted oncogenesis. Because p300 is a master regulator of gene expression (29, 30), other signaling pathways are likely to be altered by β -HPV 8E6's destabilization of the histone acetyltransferase.

Approximately 10% of skin cells do not divide after entering mitosis (25, 31). β -HPV 8E6 allows these cells to divide by preventing p53 stabilization in a p300-dependent manner (25). p53 accumulation requires the activation of large tumor suppressor kinase (LATS), a kinase in the Hippo signaling pathway (HP) (32). This suggests that β -HPV 8E6 may attenuate LATS activity. The HP also prevents growth by inhibiting the proproliferative activity of YAP/TAZ (32–34). Our analysis of transcriptomic data from cell lines segregated by their relative p300 expression was consistent with p300 acting as a negative regulator of HP and HP-responsive gene expression. We confirm that p300 modulates HP gene expression using HCT 116 cells with and without the p300 gene locus. Expressing β -HPV 8E6 in HFKs recapitulated some, but not all, of these effects. p300 is also important for responding to dihydrocytochalasin B (H2CB)-induced failed cytokinesis. HCT 116 cells without p300 had reduced LATS activation and p53 accumulation. β -HPV 8E6's destabilization of p300 similarly hindered LATS phosphorylation and p53 accumulation. Despite p53's role in apoptosis, elevated p53 levels did not correlate with increased apoptosis until the drug was washed off and the cells were allowed to recover. During this recovery period, β -HPV 8E6 displayed some ability to reduce markers of apoptosis. β -HPV 8E6 did not completely abrogate the HP's response to failed cytokinesis, as YAP was still

excluded from the nucleus. β -HPV 8E6 also did not impede the HP induction in cells grown to a high density.

Results

Loss of p300 alters Hippo pathway gene expression.

Animal models show that certain β -HPV E6 genes can contribute to UV-associated carcinogenesis (18, 19, 23). *In vitro* studies from our group and others have added molecular details by describing β -HPV E6's ability to impair the DDR by destabilizing p300 (18, 22, 27, 28, 35, 36). Despite this focus on repair, there are DDR-independent pathways that protect genome fidelity (37–39). To identify p300-regulated pathways that could contribute to β -HPV E6-associated genome destabilization, we performed an *in silico* screen comparing RNA sequencing data among 1,020 cancer cell lines grouped by their relative p300 expression levels (**Data Set S3.1** in the Supplementary Data) (40–42). The rationale for this approach is based on our prior observations that reducing p300 expression via RNA interference (RNAi) phenocopies β -HPV 8E6's p300-dependent reduction of gene expression (22, 26). We compared expression in cell lines with and without low p300 expression (*Z* scores of less than -1.64 and greater than -1.64 , respectively). Of the cell lines screened, 71 had low p300 expression. The remaining 949 cell lines were considered as not having low p300 expression. This identified 4,211 genes that had altered expression in cells with lower p300 expression. Next, gene ontology (GO) analysis was performed using Gene Ontology enRIchment anaLysis and visuaLizAtion tool (GORilla) to identify pathways that were significantly altered when p300 expression was reduced (43, 44). Notably, HP was the only pathway identified by GORilla as significantly changed (**Fig. 3.1A**). We then performed a more detailed analysis of HP, using the Kyoto Encyclopedia of Genes and Genomes (KEGG) to provide an unbiased definition of the pathway's members. When p300

expression was reduced, many canonical HP genes were upregulated. However, the most striking changes occurred in proliferative TEAD-responsive genes (e.g., CYR61, CTGF, AXL, and SERPINE1) (Fig. 3.1B). As expected, there was a significant reduction in the expression of genes (ATM, BRCA1, and BRCA2) that are dependent on p300 for robust transcription (26, 45, 46).

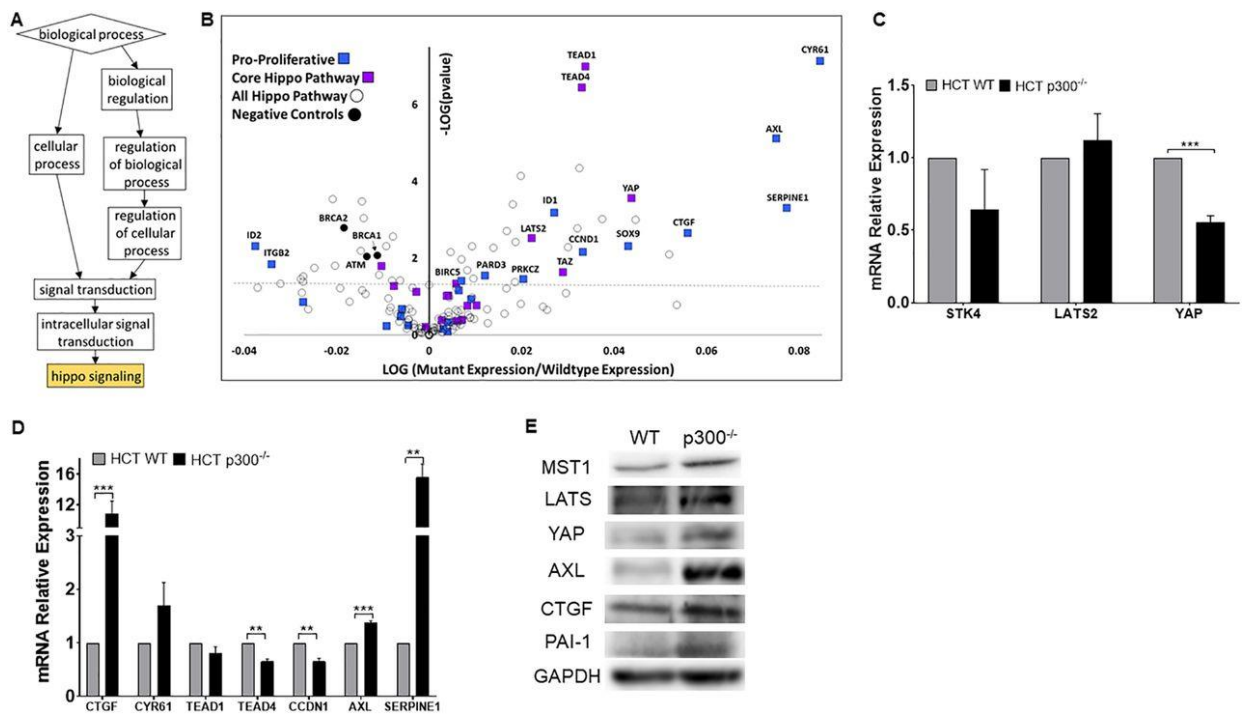


Figure 3.1. Loss of p300 leads to changes in Hippo pathway gene expression.

(A) Gene ontology of 1,020 cancer cell lines via GOrilla. Boxes show GO biological process terms. Boxes descend from general to specific functions. Gold color indicates $P \leq 0.001$. (B) Volcano plot of 154 HP genes in 1,020 cancer cell lines with decreased EP300 expression. The colors blue, purple, and black represent proliferative TEAD targets, core HP genes, and p300-negative controls, respectively. The horizontal line denotes $P = 0.05$. (C and D) Canonical HP genes (C) and TEAD-regulated mRNA expression (D) in HCT 116 WT and -p300^{-/-} measured by RT-qPCR and normalized to β -actin mRNA. (E) Representative immunoblots of HP and TEAD-regulated proteins in HCT 116 WT and -p300^{-/-}. Figures depict the mean \pm the standard

error of the mean; $n \geq 3$. *, significant difference between indicated samples; *, $P \leq 0.05$; **, $P \leq 0.01$; ***, $P \leq 0.001$ (Student's *t* test).

We used isogenic HCT 116 cells with (WT) or without the p300 gene (p300^{-/-}) deleted to confirm our *in silico* analysis (47). The p300 status of these cells was verified by immunoblot (data not shown) before the expression of canonical HP genes (LATS2, STK4, and YAP1) was measured by quantitative real-time PCR (RT-qPCR). Note, STK4 is the gene that encodes the HP kinase, MST1. Of the three HP genes analyzed, the expression of YAP was significantly decreased by p300 loss (**Fig. 3.1C**). Next, we defined the abundance of TEAD and TEAD-responsive gene transcripts by RT-qPCR. Seven genes (CTGF, CYR61, TEAD1, TEAD4, CCND1, AXL, and SERPINE1) were chosen based on indications that they were negatively regulated by p300 in our computational screen. Some of these transcripts were more abundant in HCT 116 cells that lacked p300, with increased expression of CTGF, AXL, and SERPINE1 reaching statistical significance (**Fig. 3.1D**). Next, we turned to immunoblots to determine if p300 loss leads to changes at the protein level. These data show that increased canonical HP proteins are increased in the absence of p300 (**Fig. 3.1E**). The elevated levels extended to AXL, CTGF, and PAI-1 (the protein encoded by the SERPINE1 gene).

β-HPV E6 expression alters Hippo pathway gene expression.

β-HPV 8E6 destabilizes p300, but this does not result in complete loss of the histone acetyltransferase. We questioned if this decrease in p300 was enough to dysregulate the HP. To determine the extent that the reduction of p300 by β-HPV 8E6 increased HP gene expression, we defined the expression of canonical HP genes using RT-qPCR. β-HPV 8E6 did not increase expression of the canonical HP genes in human foreskin keratinocytes or HFKs (**Fig. 3.2A**).

Immunoblots of these cells were consistent with these results except for LATS, which was more abundant when β -HPV 8E6 was expressed (**Fig. 3.2B**). We continued this analysis by defining the amount of TEAD and TEAD-responsive genes in HFKs expressing β -HPV 8E6. RT-qPCR comparing expression between vector control (LXSN) and β -HPV E6-expressing HFKs found β -HPV E6 increased expression of some TEAD-responsive genes (CTGF, CYR61, CCND1, AXL, and SERPINE1) (**Fig. 3.2C**). This was similar to our results in HCT 116 cells except for CCND1. Immunoblots were used to compare protein levels for TEAD-responsive genes, with elevated expression in HFKs expression in β -HPV 8E6. This demonstrated that β -HPV 8E6 increases CTGF, PAI-1, and AXL protein (**Fig. 3.2D**). A luciferase reporter assay showed a small but reproducible increase in luciferase expression driven from a TEAD-responsive promoter (data not shown). The increased expression of proliferative TEAD-responsive genes correlated with increased proliferation (**Fig. 3.2E**). Consistent with a p300-dependent mechanism, β -HPV 8E6-driven changes in the HP were abrogated by the deletion of the p300-binding domain in a previously characterized mutant, β -HPV Δ 8E6 (**Fig. 3.2**).

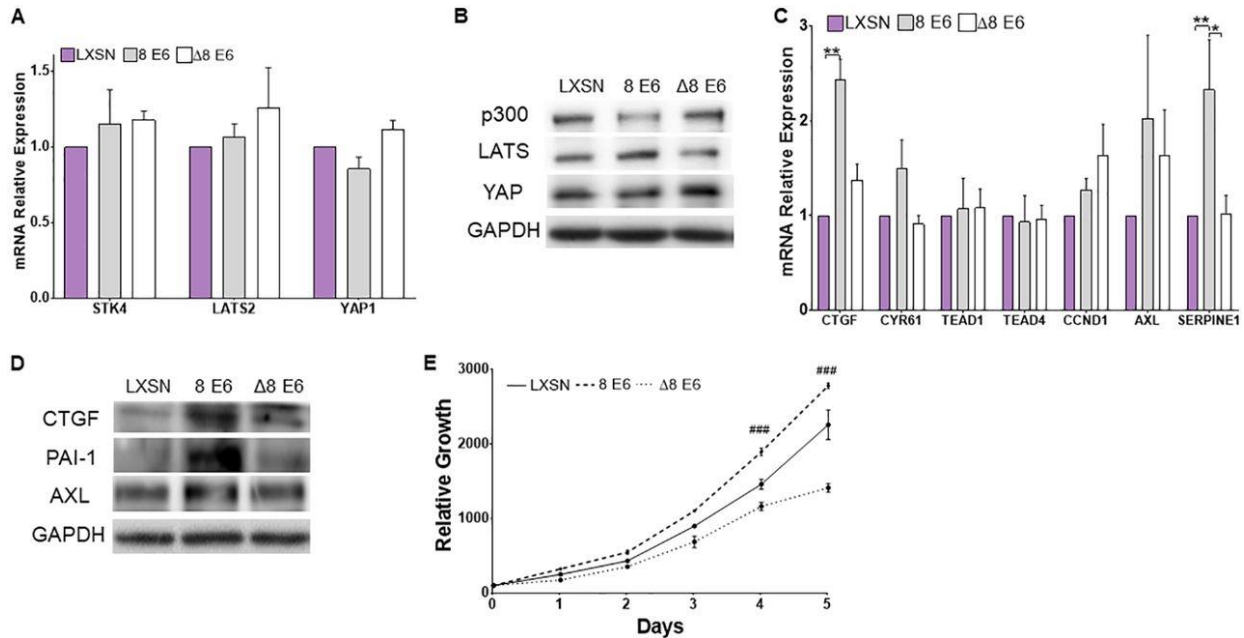


Figure 3.2. β-HPV 8E6 alters Hippo pathway gene expression.

Canonical HP genes (A) and TEAD-regulated mRNA expression (C) in HFKs LXSNS, β-HPV 8E6, and β-HPV Δ8E6 measured by RT-qPCR and normalized to β-actin mRNA. Representative immunoblots of HP (B) and TEAD-regulated proteins (D) in HFKs LXSNS, β-HPV 8E6, and β-HPV Δ8E6. (E) Relative growth recorded over a 5-day period. Figures depict mean ± standard error of the mean; $n \geq 3$. *, significant difference between indicated samples; #, significant difference from LXSNS; one symbol (* or #), $P \leq 0.05$; two symbols (** or ##), $P \leq 0.01$; three symbols (***) or ###), $P \leq 0.001$ (Student's t test). In β-HPV Δ8E6, residues 132 to 136 were deleted.

p300 is necessary for a robust Hippo pathway response to failed cytokinesis.

The HP typically restricts growth in response to adverse conditions. This includes failed cytokinesis, induced by dihydrocytochalasin B (H2CB), an inhibitor of actin polymerization (48). Because the loss of p300 promoted proliferation gene expression and dysregulated the HP, we hypothesized that p300 was required for the cellular response to H2CB exposure. Confirming previous data, LATS phosphorylation increased in HCT 116 cells with exposure to 4 μM H2CB (Fig. 3.3A and B). YAP phosphorylation was similarly elevated by H2CB treatment (Fig. 3.3A

and C). Loss of p300 in HCT 116 cells reduced LATS in response to H2CB (**Fig. 3.3A and B**). When cells are treated with H2CB, LATS activation leads to p53 accumulation (32). To determine if p300 was necessary for this response, we used immunofluorescence microscopy to detect p53 in wild-type (WT) and p300 knockout (p300^{-/-}) HCT 116 cells grown in H2CB-containing media. We were able to confirm previous reports of p53 buildup in response to the drug in WT HCT 116 cells (**Fig. 3.3D and E**). However, p53 did not accumulate in HCT 116 cells lacking p300.

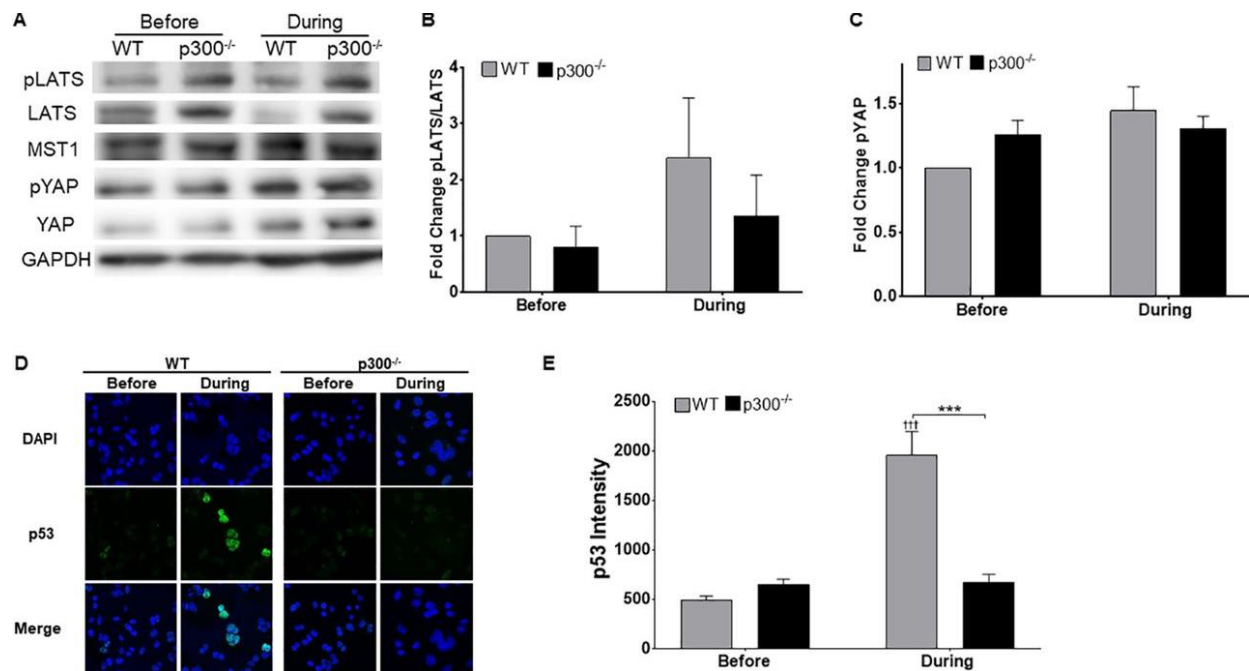


Figure 3.3. Loss of p300 impedes the Hippo pathway's response to failed cytokinesis.

(A) Representative immunoblot of HP proteins before and during H2CB treatment. (B and C) Densitometry of immunoblots described in panel A. GAPDH was used as a loading control. (D) Representative images of p53 (green)- and DAPI (blue)-stained HCT 116 cells before and during H2CB exposure. (E) Relative p53 intensity in HCT 116 cells. At least 150 cells/line were imaged across three independent experiments. Figures depict mean \pm standard error of the mean; $n \geq 3$. *, significant difference between indicated samples; †, significant difference relative to before H2CB; one symbol (* or †), $P \leq 0.05$; two symbols (** or ††), $P \leq 0.01$; three symbols (***) or †††), $P \leq 0.001$ (Student's *t* test). In β -HPV Δ 8E6, residues 132 to 136 were deleted.

β -HPV 8E6 attenuates LATS2 phosphorylation but does not impede nuclear exclusion of YAP.

These data suggest that β -HPV 8E6 alters H2CB induction of the HP. Before evaluating this possibility, we needed to confirm that β -HPV 8E6 did not impede H2CB-induced failed cytokinesis. The visualization of cells with more than one nucleus provides a straightforward measure of failed cytokinesis. We used bright-field and immunofluorescence microscopy to detect the presence of two or more nuclei in cells grown in media containing H2CB (**Fig. 3.4A to D**). The percentage of cells with supernumerary nuclei increased as a function of time in H2CB. This was true in both HFK and U2OS cells. The frequency of these abnormal cells was also not notably altered by β -HPV 8E6 or β -HPV Δ 8E6. H2CB increased STK4 and YAP1 gene expression. Neither β -HPV 8E6 nor β -HPV Δ 8E6 changed this (**Fig. 3.4E**). Consistent with our observations in HCT 116 cells, β -HPV 8E6 reduced LATS phosphorylation in cells exposed to H2CB (**Fig. 3.4F**). β -HPV Δ 8E6 did not attenuate LATS phosphorylation. β -HPV 8E6's restriction of HP signaling may be limited to reducing LATS phosphorylation. β -HPV 8E6 did not change YAP phosphorylation or the abundance of other HP proteins (data not shown). Moreover, immunofluorescence microscopy of YAP shows that β -HPV 8E6 did not hinder the nuclear exclusion of YAP associated with the protein's phosphorylation (**Fig. 3.4G**) (49). As expected from these results, H2CB reduced TEAD-responsive promoter activity. β -HPV 8E6 did not prevent this decrease (data not shown).

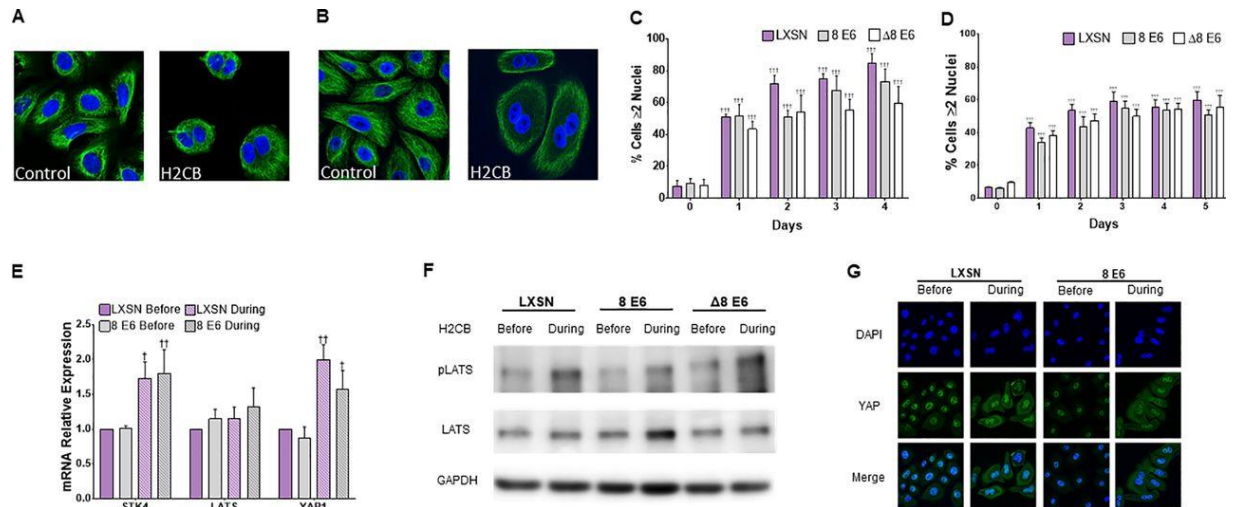


Figure 3.4. β -HPV 8E6 diminishes LATS phosphorylation during failed cytokinesis. Representative images of U2OS (A) and HFK (B) cells before and during H2CB exposure. Green and blue represent α -tubulin and DAPI, respectively. Quantification of U2OS (C) and HFK (D) cells with 2 or more nuclei as a function of time in H2CB. (E) STK4, LATS, and YAP1 expression before and after H2CB exposure measured by RT-qPCR; $n = 2$. (F) Representative immunoblot of pLATS and totals LATS protein levels in HFK cells before and during H2CB exposure. (G) Representative images of YAP (green)- and DAPI (blue)-stained HFK cells before and during H2CB treatment. At least 200 cells/line were imaged from three independent experiments. Figures depict mean \pm standard error of the mean; $n \geq 3$. †, significant difference relative to before H2CB; †, $P \leq 0.05$; ††, $P \leq 0.01$; †††, $P \leq 0.001$ (Student's t test). In β -HPV $\Delta 8E6$, residues 132 to 136 were deleted.

β -HPV 8E6 attenuates p53 accumulation after failed cytokinesis.

Seeing β -HPV 8E6 reduce LATS phosphorylation led us to hypothesize that β -HPV 8E6 would also reduce p53 accumulation in response to H2CB. To test this, we used immunofluorescence microscopy to detect p53 in U2OS grown in media containing H2CB. Consistent with our previous observations, H2CB increased the frequency of cells with more than one nucleus. H2CB increased p53 levels in vector control cells but not in cells expressing β -HPV E6 (Fig. 3.5A and B). This abrogation of p53 accumulation is likely dependent on p300

degradation, as β -HPV Δ 8E6 expressing U2OS and vector control had a similar frequency of p53-stained cells. To validate these results, we used immunoblotting to detect p53 levels in cells grown in H2CB. These experiments also demonstrated that β -HPV 8E6 can repress p53 buildup in response to H2CB. Again, vector control U2OS and β -HPV Δ 8E6-expressing U2OS behaved similarly in this assay (**Fig. 3.5C and D**). We speculated that the additional p53 found in cells grown with H2CB would result in apoptosis. Fluorescence-based detection of two apoptosis markers (propidium iodide and annexin V) were used to test this idea (50, 51). Surprisingly, we did not see exposure to H2CB associated with an increase in either of these apoptosis markers (**Fig. 3.5E and F**). There were also no differences in staining among vector control HFKs and HFKs expressing β -HPV 8E6 or β -HPV Δ 8E6.

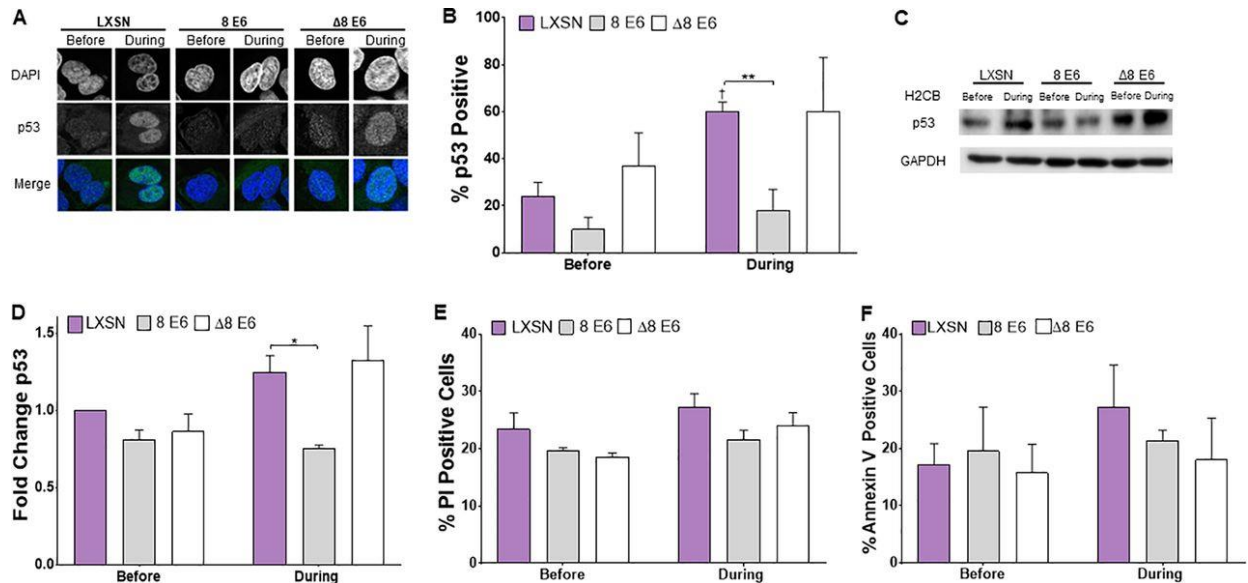


Figure 3.5. β -HPV 8E6 attenuates p53 accumulation upon H2CB-induced failed cytokinesis

(A) Representative images of p53 and DAPI staining in cells before and during H2CB treatment. (B) Percent of p53-positive U2OS cells. (C) Representative immunoblot of p53 before and during H2CB exposure. (D) Densitometry of immunoblots described in panel C. GAPDH was used as a loading control. Data were normalized to p53 levels in untreated LXSN cells (set to 1). (E) Percent of propidium iodide-stained HFK cells before and during H2CB exposure. (F)

Percent of annexin V-stained HFK cells before and during H2CB treatment. At least 200 cells/line were imaged from three independent experiments. Figures depict mean \pm standard error of the mean; $n \geq 3$. *, significant difference between indicated samples; †, significant difference relative to before H2CB; one symbol (* or †), $P \leq 0.05$; two symbols (** or ††), $P \leq 0.01$; three symbols (***) or †††), $P \leq 0.001$ (Student's *t* test). In β -HPV Δ 8E6, residues 132 to 136 were deleted.

H2CB stalls cytokinesis. It was important to understand if/how those cells recover once the drug is removed and cytokinesis is again possible. To this end, we compared HFKs grown in three conditions: without H2CB (before), grown with 4 days of continual H2CB (during), and grown in H2CB for 4 days followed by 3 additional days without H2CB (after). **Figure 3.6A** depicts our experimental setup. We used microscopy to determine the frequency of HFKs with supernumerary nuclei (two or more) in each of these conditions. β -HPV 8E6 did not make supernumerary nuclei less prevalent before or during H2CB exposure (**Fig. 3.6B**). However, β -HPV 8E6 decrease supernumerary nuclei after H2CB. This appears to be dependent on p300 destabilization, as supernumerary nuclei were similarly prevalent in HFKs with β -HPV Δ 8E6 or vector control. We next used immunoblots to determine if β -HPV 8E6 maintained its ability to attenuate LATS phosphorylation after H2CB. While LATS phosphorylation was elevated in vector control HFKs after H2CB, they remained low in HFKs expressing β -HPV 8E6. This phenotype was not seen in HFKs expressing β -HPV Δ 8E6. We used immunofluorescence microscopy as an additional way of detecting p53. These experiments complement the results from immunoblotting, as p53-positive cells were more frequent after H2CB in the vector control but not β -HPV 8E6-expressing HFKs (**Fig. 3.6D and E**). We repeated the detection of propidium iodide (PI) and annexin described in **Fig. 3.5** after H2CB. β -HPV 8E6 reduced the percentage of

PI-positive HFKs after H2CB compared to vector control and β -HPV Δ 8E6-expressing HFKs (Fig. 3.6F). Annexin V staining was also reduced, but this change did not reach statistical

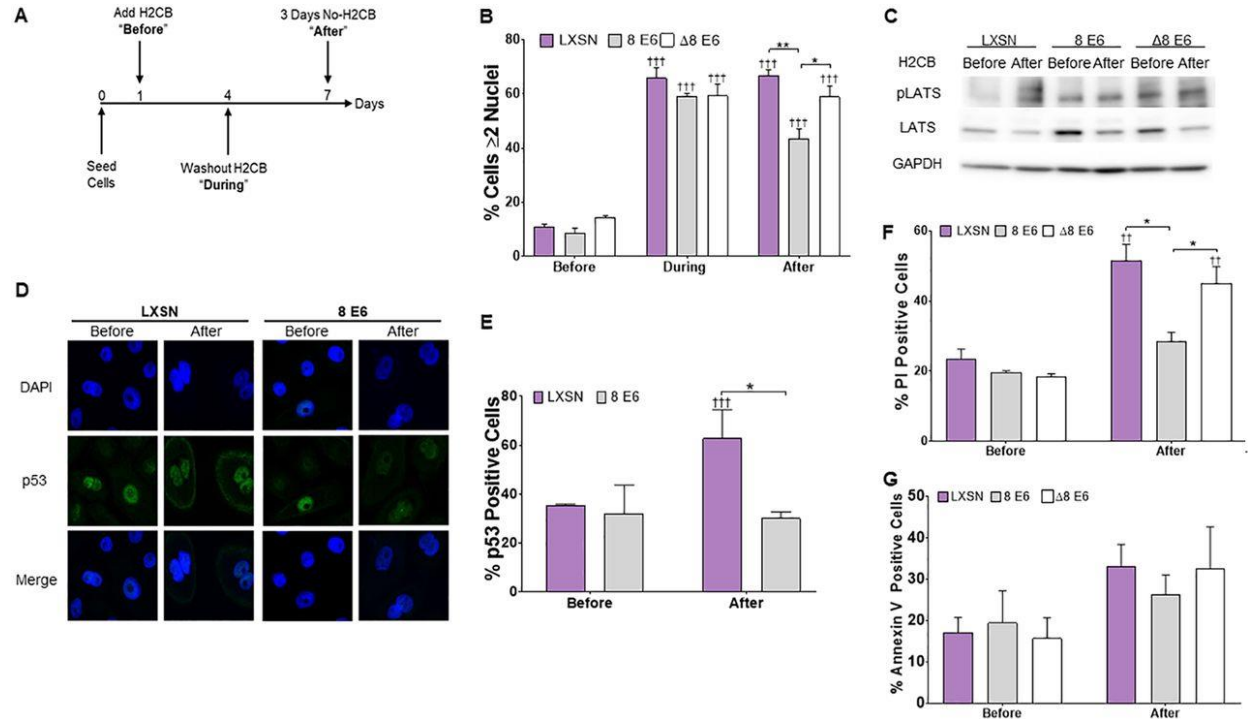


Figure 3.6. β -HPV 8E6 hinders LATS phosphorylation and p53 accumulation after failed cytokinesis.

(A) Timeline for administration and removal of H2CB. (B) Percent of HFK cells with ≥ 2 nuclei per cell before, during, and after H2CB treatment. (C) Representative immunoblots of pLATS and totals LATS in HFKs before and after H2CB exposure. (D) Representative images of p53 and DAPI staining in cells before and after H2CB exposure. (E) Percent of p53-stained HFK cells before and after H2CB exposure. At least 200 cells/line were imaged across three independent experiments. (F) Percent of propidium iodide stained HFK cells before and after H2CB exposure. (G) Percent of annexin V-stained HFK cells before and after H2CB treatment. Figures depict mean \pm standard error of the mean; $n \geq 3$. *, significant difference between indicated samples; †, significant difference relative to before H2CB; one symbol (* or †), $P \leq 0.05$; two symbols (** or ††), $P \leq 0.01$; three symbols (***) or †††), $P \leq 0.001$ (Student's t test). In β -HPV Δ 8E6, residues 132 to 136 were deleted.

β -HPV 8E6 does not completely abrogate the Hippo pathway.

Having seen diminished LATS activation, we queried whether β -HPV 8E6 prevented the HP from restricting growth after H2CB was removed. We used immunofluorescence microscopy to detect Ki67, an established marker of proliferation. While we readily detected Ki67 in both vector control and β -HPV 8E6-expressing HFKs before H2CB, Ki67 was notably less abundant during and after H2CB (**Fig. 3.7A**). Ki67 staining intensity was also lower in HFKs expressing β -HPV 8E6 (**Fig. 3.7B**). Consistent with these results, HFKs were not capable of long-term proliferation with or without β -HPV 8E6 (data not shown). To understand what was happening to HFKs after H2CB, we stained for senescence-associated beta-galactosidase (SA β -Gal) activity as an indicator of cellular senescence. These data were consistent with our Ki67 staining experiments (**Fig. 3.7C and D**). HFKs were more likely to have SA β -Gal activity after H2CB, and β -HPV 8E6 expression amplified this phenotype.

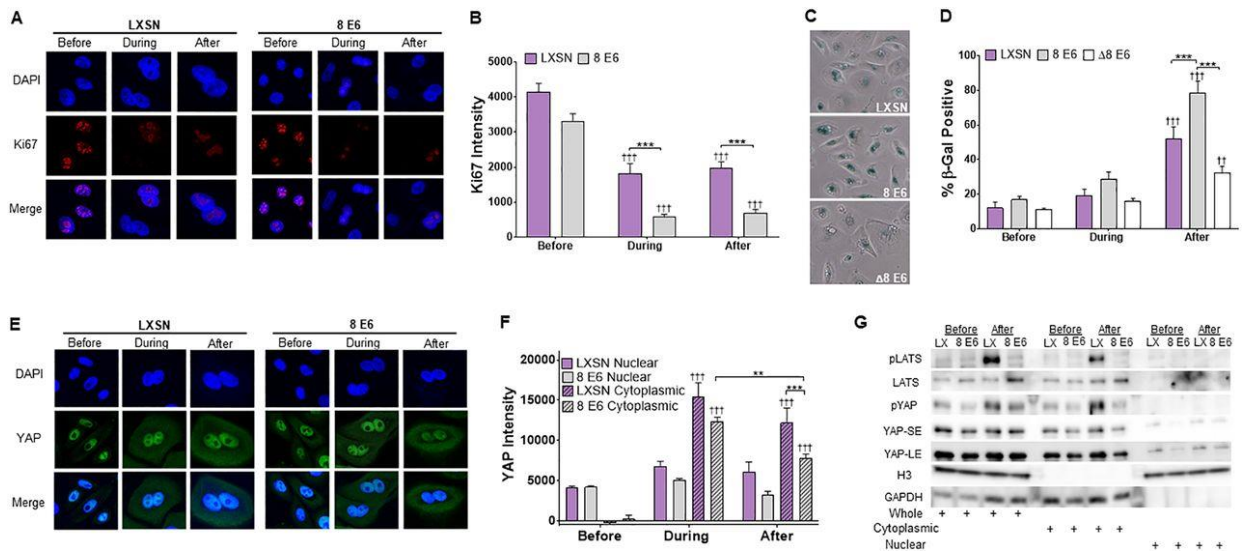


Figure 3.7. β -HPV 8E6 increases SA β -Gal staining and reduces YAP abundance after failed cytokinesis.

(A) Representative images of Ki67 (red) and DAPI (blue) staining in HFK cells before, during, and after H2CB treatment. (B) Relative KI67 intensity in HFK cells before, during, and after

H2CB treatment. At least 150 cells/line were imaged across three independent experiments. (C) Representative images of HFK cells stained for SA β -Gal activity (blue). (D) Percent of SA β -Gal-positive HFK cells before, during, and after H2CB exposure. (E) Representative images of HFK cells stained for YAP (green) and DAPI (blue). (F) Cytoplasmic and nuclear YAP intensity in HFK cells before, during, and after H2CB treatment. At least 205 images were imaged across three independent experiments. (G) Subcellular fractionation of HFKs harvested before and after H2CB treatment. Hippo pathway proteins were probed via immunoblotting. GAPDH and histone H3 serve as cytoplasmic and nuclear loading controls, respectively. YAP-SE and YAP-LE indicate short- and long-term exposure of YAP, respectively. Figures depict mean \pm standard error of the mean; $n \geq 3$. *, significant difference between indicated samples; †, significant difference relative to before H2CB; one symbol (* or †), $P \leq 0.05$, two symbols (** or ††), $P \leq 0.01$; three symbols (***) or †††, $P \leq 0.001$ (Student's *t* test). In β -HPV Δ 8E6, residues 132 to 136 were deleted.

The HP restricts growth by relocating YAP from the nucleus to the cytoplasm. We used immunofluorescence microscopy to define the subcellular localization of YAP in HFKs before, during, and after H2CB (**Fig. 3.7E and F**). Cytoplasmic YAP increased in HFKs during and after H2CB as expected. β -HPV 8E6 attenuated this only after H2CB exposure (**Fig. 3.7F**). Additionally, we saw a nominal decrease in nuclear-located YAP in HFKs expressing β -HPV 8E6 alone after H2CB treatment. To more precisely define YAP localization, we performed subcellular fractionation on HFKs before and after H2CB (**Fig. 3.7G**). Immunoblotting demonstrated that phosphorylated YAP was more abundant in the cytoplasm, particularly after H2CB. This was also true for phosphorylated LATS. After H2CB, β -HPV 8E6 decreased the amount of total YAP in the nuclear fraction, despite reducing total and cytoplasmic phospho-LATS1/2 (pLATS).

We wanted to determine the extent that β -HPV 8E6 could attenuate LATS phosphorylation in response to other stimuli. Because cell density is a commonly used activator

of the HP, we compared LATS and YAP phosphorylation in confluent and subconfluent HFKs (**Fig. 3.8A and B**). Immunoblots of these cells demonstrate increased YAP phosphorylation in confluent HFKs compared to subconfluent HFKs. The phosphorylation of LATS did not increase under these conditions. Next, we used immunofluorescence microscopy to determine if HFKs increased p53 levels when grown to high confluence (**Fig. 3.8C and D**). As expected, p53 staining was more intense in confluent compared to subconfluent HFKs. In general, neither β -HPV 8E6 nor β -HPV Δ 8E6 changed these responses. However, β -HPV Δ 8E6 decreased p53 staining. We have no explanation of this observation, but it does demonstrate that β -HPV Δ 8E6 is not universally inactive.

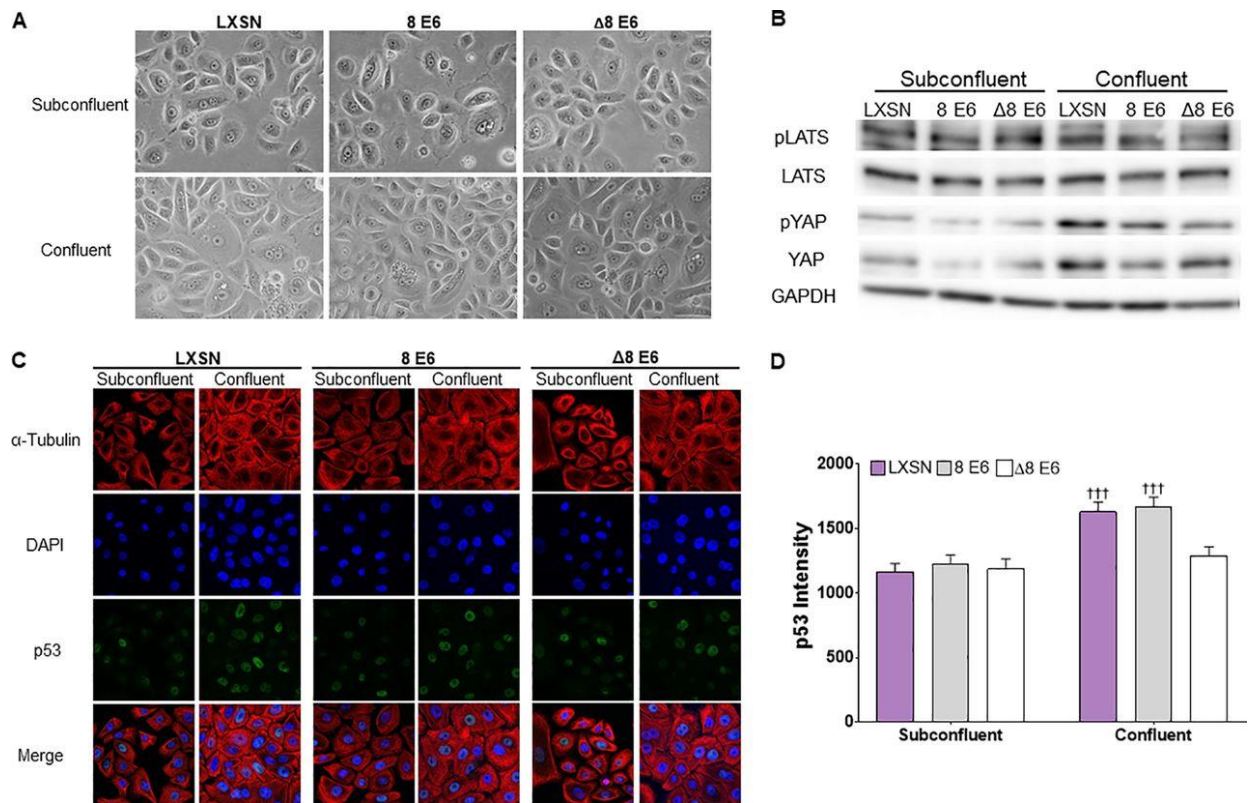


Figure 3.8. β -HPV 8E6 does not inhibit the Hippo pathway's response to cellular density.

(A) Representative images of subconfluent and confluent HFKs. (B) Representative immunoblot of HP proteins in confluent and subconfluent HFKs. (C) Representative images of α -tubulin

(red)-, p53 (green)-, and DAPI (blue)-stained subconfluent and confluent HFK cells. (D) Mean p53 intensity in HFK cells before and after confluence. At least 200 cells/line were imaged across 3 independent experiments; $n = 2$ for β -HPV Δ 8E6. Figures depict mean \pm standard error of the mean; $n \geq 3$. †, significant difference relative to before H2CB; †, $P \leq 0.05$; ††, $P \leq 0.01$; †††, $P \leq 0.001$ (Student's t test). In β -HPV Δ 8E6, residues 132 to 136 were deleted.

Discussion

Tumorigenesis is among the grave consequences associated with changes in ploidy. HP activation is one of the cellular mechanisms that prevents polyploidy by halting the proliferation of cells that do not divide after replication (32, 52). Despite the high stakes, cytokinesis fails in approximately 10% of skin cells that enter mitosis (25, 31). As a result, the HP may play an important role in preventing cSCCs. The growth arrest associated with HP activation is likely refractory to β -HPV replication, as HPV replicates in actively proliferating cells (53). Our work suggests that β -HPV 8E6 helps binucleated cells survive by mitigating HP activation. Presumably limiting HP signaling is beneficial to papillomaviruses in general, as genus α HPV oncogenes also dysregulate the Hippo pathway (54, 55).

The “evolutionary motivation” behind this could stem from the modest growth advantage that we report. However, this weak phenotype seems unlikely to drive convergent evolution toward HP dysregulation. Given the HP’s role in immunity, it is more enticing to speculate that targeting the HP helps HPVs avoid an immune response (56, 57). Indeed, an MST1 deficiency increased β -HPV infections (58). Since the HP was only discovered 14 years ago (59), there could also be other currently unknown advantages to be gained by disrupting the pathway.

Less speculatively, we extend the understanding of β -HPV 8E6 biology. β -HPV E6 disrupts multiple cell signaling pathways necessary for DNA repair and regulating differentiation. Much of β -HPV E6’s ability to disrupt DNA repair is linked to p300

destabilization. We demonstrate that changes in signaling associated with reduced p300 extend to the HP, as LATS phosphorylation is attenuated following failed cytokinesis. β -HPV 8E6 also displays some antiapoptotic properties in response to H2CB-induced failed cytokinesis.

Together, these data demonstrate that β -HPV 8E6 is a versatile protein capable of a striking reprogramming of cellular signaling. We also extend the long history of using viral oncogenes to learn about cell biology by linking p300 to the HP- and TEAD-responsive gene expression.

The fact that most people get infected with β -HPV, but a significantly lower number of those infections become cSCCs causes many to doubt that the virus is tumorigenic. β -HPV 8E6 may be more mutagenic in certain genetic backgrounds. For instance, β -HPV 8E6 reduces LATS phosphorylation after failed cytokinesis, but the cells still senesce. This suggests that mutations that help cells avoid senescence would augment β -HPVs tumorigenic potential. One could imagine any number of additional mutations that might synergize with β -HPV 8E6 to promote mutagenesis. Genetic landscapes where the opposite is true seem equally likely. Moreover, β -HPV E6 could also be more or less harmful when coexpressed with other β -HPV genes. Future studies are needed to evaluate these complexities.

Materials and Methods

Cell cultures.

U2OS and HCT 116 cells were maintained in Dulbecco modified Eagle medium (DMEM) supplemented with 10% fetal bovine serum (FBS) and penicillin-streptomycin. Primary HFKs were derived from neonatal human foreskins. HFKs were grown in EpiLife medium supplemented with calcium chloride (60 μ M), human keratinocyte growth supplement (Thermo Fisher Scientific), and penicillin-streptomycin. HPV genes were cloned, transfected, and confirmed as previously described (25). We carefully monitored cell density in all

experiments. To avoid confounding our experiments by activating the Hippo pathway via contact inhibition, experiments were aborted if unintended differences in seeding resulted in cell densities that were more than 10% different among cell lines at the beginning of an experiment.

Proliferation assays and H2CB cell viability assays.

Cells were counted, and 4.0×10^4 cells were plated into 6 wells per cell line of 6-well tissue culture dishes. One well was trypsinized, resuspended, and counted 3 times via hemocytometer with trypan blue. For dihydrocytochalasin B (H2CB) cell viability assays, cells were grown for 24 h and then treated with $2/4 \mu\text{M}$ H2CB, and fresh H2CB was readministered every 2 days while cells were trypsinized and counted 3 times via hemocytometer with trypan blue.

RT-qPCR.

Cell were lysed using TRIzol (Invitrogen) and RNA isolated with the RNeasy kit (Qiagen). Two micrograms of RNA were reverse transcribed using the iScript cDNA synthesis kit (Bio-Rad). Quantitative real-time PCR (RT-qPCR) was performed in triplicate with the TaqMan FAM-MGB gene expression assay (Applied Biosystems) and C1000 touch thermal cycler (Bio-Rad). The following probes (Thermo Scientific) were used: ACTB (Hs01060665_g1), STK4 (Hs00178979_m1), LATS2 (referred to as LATS in the text) (Hs01059009_m1), YAP1 (Hs00902712_g1), CTGF (Hs00170014_m1), CYR61 (Hs00155479_m1), TEAD4 (Hs01125032_m1), TEAD1 (Hs00173359_m1), CCND1 (Hs00765553_m1), AXL (Hs01064444_m1), and SERPINE1 (Hs00167155_m1).

Immunoblotting.

After being washed with ice-cold phosphate-buffered saline (PBS), cells were lysed with radioimmunoprecipitation assay (RIPA) lysis buffer (VWR Life Science) supplemented with

Phosphatase inhibitor cocktail 2 (Sigma) and protease inhibitor cocktail (Bimake). The Pierce bicinchoninic acid (BCA) protein assay kit (Thermo Scientific) was used to determine protein concentration. Equal protein lysates were run on Novex 4-12% Tris-Glycine WedgeWell mini gels (Invitrogen) and transferred to Immobilon-P membranes (Millipore). Membranes were then probed with the following primary antibodies: glyceraldehyde-3-phosphate dehydrogenase (GAPDH) (Santa Cruz Biotechnologies; catalog no. sc-47724), LATS2 (Cell Signaling Technologies; clone D83D6), phospho-LATS1/2 (Ser909) (referred to as pLATS in the text) (Cell Signaling Technologies; product no. 9157), YAP (Cell Signaling Technologies; product no. 4912S), phospho-YAP (Ser127) (Referred to pYAP in the text) (Cell Signaling Technologies; product no. 4911S), MST1 (Cell Signaling Technologies; product no. 3682S), AXL (Cell Signaling Technologies; product no. 8661S), CTGF (Abcam; catalog no. ab6692), PAI-1 (Cell Signaling Technologies; product no. 11907S), p53 (Calbiochem; catalog no. OP43; 100 µg), p300 (Santa Cruz Biotechnologies; catalog no. sc-584), and histone H3 (Abcam; catalog no. ab1791). After exposure to the matching horseradish peroxidase (HRP)-conjugated secondary antibody, cells were visualized using SuperSignal West Femto maximum sensitivity substrate (Thermo Scientific).

cBioPortal and gene ontology analysis.

Software from www.cbioportal.org was used to recognize, analyze, and categorize mutations and transcriptomic data from over 1,000 cancer cell lines (40–42) and cutaneous squamous cell carcinomas (60, 61). Gene Ontology enRIchment anaLysis and visuaLizAtion tool (GORilla) identified and visualized enriched GO terms from these data (43, 44). The Kyoto Encyclopedia of Genes and Genomes (KEGG) was used to identify genes specific to the Hippo signaling pathway (hsa04390).

Senescence-associated β -galactosidase staining.

Cells were seeded onto three 6-well plates and were grown for 24 h. Then, they were treated with 4 μ M H2CB for stated times, after which cells were fixed and stained for senescence-associated β -galactosidase (β -Gal) expression according to the manufacturer's protocol (Cell Signaling Technologies).

Immunofluorescence microscopy.

Cells were seeded onto either 96-well glass-bottom plates (Cellvis) or coverslips and grown overnight. Cells treated with H2CB for a specified time and concentration were fixed with 4% formaldehyde. Then, 0.1% Triton-X solution in PBS was used to permeabilize the cells, followed by blocking with 3% bovine serum albumin in PBS for 30 min. Cells were then incubated with the following: p53 (Cell Signaling Technologies; clone 1C12), YAP (Cell Signaling Technologies; product no. 4912S), Ki67 (Abcam; catalog no. ab15580), alpha-tubulin (Abcam; catalog no. ab18251), and α -tubulin (Cell Signaling Technologies; product no. 3873S). The cells were washed and stained with the appropriate secondary antibodies: Alexa Fluor 594 goat anti-rabbit (Thermo Scientific; catalog no. A11012) and Alexa Fluor 488 goat anti-mouse (Thermo Scientific A11001). After washing, the cells were stained with 28 μ M 4',6-diamidino-2-phenylindole (DAPI) in PBS and visualized with the Zeiss LSM 770 microscope. Images were analyzed using ImageJ techniques previously described in reference 62.

Apoptosis assay.

After H2CB treatment, HFKs were harvested via trypsinization and then counted while incubating at 37°C for 30 min. After incubation, cells were resuspended to 1×10^6 cells/ml. Next, cells were stained with 100 μ g/ml of propidium iodide (PI) and $1 \times$ annexin-binding buffer following the protocol from Dead Cell apoptosis kit (Invitrogen; catalog no. V13242). Stained

cells were imaged with the Countess II FL automated cell counter (Invitrogen). Images were processed using ImageJ software.

Subcellular fractionation.

Cells were seeded at 5.0×10^5 cells/10 cm² plate and grown for 24 h. Cells were then treated with 4 μ M H2CB for 3 days, washed with PBS, and recovered in fresh EpiLife for 3 days (after H2CB treatment). Before and after H2CB exposure, cells were washed with ice-cold PBS and divided into cytosolic and nuclear fractions via Abcam's subcellular fractionation protocol. Afterward, lysates were treated the same as in the Immunoblotting section.

Statistical analysis.

Unless otherwise noted, statistical significance was determined by an unpaired Student's *t* test and was confirmed when appropriate by two-way analysis of variance (ANOVA) with Turkey's correction. Only *P* values of less than 0.05 were reported as significant.

Acknowledgments

We thank and acknowledge the Kansas State University College of Veterinary Medicine (KSU-CVM) Confocal Core, especially Joel Sanneman, for assisting with our immunofluorescence imaging, Michael Underbrink for providing the telomerase reverse transcriptase (TERT)-immortalized HFKs, Stefano Piccolo for gifting the 8 \times GT1C plasmid, along with Emily Burghardt and Jazmine Snow for their constructive criticism of the manuscript. Also, we thank members of the Zhilong Yang lab for their support.

This work was supported by Department of Defense grant CMDRP PRCRP CA160224 (to N.A.W.) and was made possible by generous support from the Les Clow family and the Johnson Cancer Research Center at Kansas State University.

Supplementary Data

Data Set S3.1

[File \(jvi.02184-19-sd001.xlsx\)](#)

References

1. Van Doorslaer K, Li Z, Xirasagar S, Maes P, Kaminsky D, Liou D, Sun Q, Kaur R, Huyen Y, McBride AA. 2017. The Papillomavirus Episteme: a major update to the papillomavirus sequence database. *Nucleic Acids Res* 45:D499–D506. 10.1093/nar/gkw879.
2. Zur Hausen H. 2002. Papillomaviruses and cancer: from basic studies to clinical application. *Nat Rev Cancer* 2:342–350. 10.1038/nrc798.
3. Cogliano V, Baan R, Straif K, Grosse Y, Secretan B, El Ghissassi F, WHO International Agency for Research on Cancer. 2005. Carcinogenicity of human papillomaviruses. *Lancet Oncol* 6:204. 10.1016/S1470-2045(05)70086-3.
4. Orth G, Jablonska S, Favre M, Croissant O, Jarzabek-Chorzelska M, Rzeska G. 1978. Characterization of two types of human papillomaviruses in lesions of Epidermodysplasia verruciformis. *Proc Natl Acad Sci U S A* 75:1537–1541. 10.1073/pnas.75.3.1537.
5. Purdie KJ, Suretheran T, Sterling JC, Bell L, McGregor JM, Proby CM, Harwood CA, Breuer J. 2005. Human papillomavirus gene expression in cutaneous squamous cell carcinomas from immunosuppressed and immunocompetent individuals. *J Invest Dermatol* 125:98–107. 10.1111/j.0022-202X.2005.23635.x.
6. Harwood CA, McGregor JM, Proby CM, Breuer J. 1999. Human papillomavirus and the development of non-melanoma skin cancer. *J Clin Pathol* 52:249–253. 10.1136/jcp.52.4.249.
7. Chahoud J, Semaan A, Chen Y, Cao M, Rieber AG, Rady P, Tyring SK. 2016. Association between β -genus human papillomavirus and cutaneous squamous cell carcinoma in immunocompetent individuals—a meta-analysis. *JAMA Dermatol* 152:1354–1364. 10.1001/jamadermatol.2015.4530.
8. Masini C, Fuchs PG, Gabrielli F, Stark S, Sera F, Ploner M, Melchi CF, Primavera G, Pirchio G, Picconi O, Petasecca P, Cattaruzza MS, Pfister HJ, Abeni D. 2003. Evidence for the association of human papillomavirus infection and cutaneous squamous cell carcinoma in immunocompetent individuals. *Arch Dermatol* 139:890–894. 10.1001/archderm.139.7.890.
9. Chitsazzadeh V, Coarfa C, Drummond JA, Nguyen T, Joseph A, Chilukuri S, Charpiot E, Adelman CH, Ching G, Nguyen TN, Nicholas C, Thomas VD, Migden M, MacFarlane

- D, Thompson E, Shen J, Takata Y, McNiece K, Polansky MA, Abbas HA, Rajapakshe K, Gower A, Spira A, Covington KR, Xiao W, Gunaratne P, Pickering C, Frederick M, Myers JN, Shen L, Yao H, Su X, Rapini RP, Wheeler DA, Hawk ET, Flores ER, Tsai KY. 2016. Cross-species identification of genomic drivers of squamous cell carcinoma development across preneoplastic intermediates. *Nat Commun* 7:12601. 10.1038/ncomms12601.
10. Weissenborn SJ, Nindl I, Purdie K, Harwood C, Proby C, Breuer J, Majewski S, Pfister H, Wieland U. 2005. Human papillomavirus-DNA loads in actinic keratoses exceed those in non-melanoma skin cancers. *J Invest Dermatol* 125:93–97. 10.1111/j.0022-202X.2005.23733.x.
 11. Howley PM, Pfister HJ. 2015. Beta genus papillomaviruses and skin cancer. *Virology* 479–480:290–296. 10.1016/j.virol.2015.02.004.
 12. Weissenborn SJ, De Koning MNC, Wieland U, Quint WGV, Pfister HJ. 2009. Intrafamilial transmission and family-specific spectra of cutaneous betapapillomaviruses. *J Virol* 83:811–816. 10.1128/JVI.01338-08.
 13. Akgül B, Cooke JC, Storey A. 2006. HPV-associated skin disease. *J Pathol* 208:165–175. 10.1002/path.1893.
 14. Aldabagh B, Angeles JGC, Cardones AR, Arron ST. 2013. Cutaneous squamous cell carcinoma and human papillomavirus: is there an association? *Dermatol Surg* 39:1–23. 10.1111/j.1524-4725.2012.02558.x.
 15. Rosen T, Lebwohl MG. 2013. Prevalence and awareness of actinic keratosis: barriers and opportunities. *J Am Acad Dermatol* 68:S2–9. 10.1016/j.jaad.2012.09.052.
 16. Warino L, Tusa M, Camacho F, Teuschler H, Fleischer AB, Feldman SR. 2006. Frequency and cost of actinic keratosis treatment. *Dermatol Surg* 32:1045–1049. 10.1111/j.1524-4725.2006.32228.x.
 17. Criscione VD, Weinstock MA, Naylor MF, Luque C, Eide MJ, Bingham SF, Department of Veteran Affairs Topical Tretinoin Chemoprevention Trial Group. 2009. Actinic keratoses: natural history and risk of malignant transformation in the Veterans Affairs Topical Tretinoin Chemoprevention Trial. *Cancer* 115:2523–2530. 10.1002/cncr.24284.
 18. Marcuzzi GP, Hufbauer M, Kasper HU, Weißenborn SJ, Smola S, Pfister H. 2009. Spontaneous tumour development in human papillomavirus type 8 E6 transgenic mice and rapid induction by UV-light exposure and wounding. *J Gen Virol* 90:2855–2864. 10.1099/vir.0.012872-0.
 19. Schaper ID, Marcuzzi GP, Weissenborn SJ, Kasper HU, Dries V, Smyth N, Fuchs P, Pfister H. 2005. Development of skin tumors in mice transgenic for early genes of human papillomavirus type 8. *Cancer Res* 65:1394–1400. 10.1158/0008-5472.CAN-04-3263.

20. Meyers JM, Uberoi A, Grace M, Lambert PF, Munger K. 2017. Cutaneous HPV8 and MmuPV1 E6 proteins target the NOTCH and TGF- β tumor suppressors to inhibit differentiation and sustain keratinocyte proliferation. *PLoS Pathog* 13:e1006171. 10.1371/journal.ppat.1006171.
21. Underbrink MP, Howie HL, Bedard KM, Koop JI, Galloway DA. 2008. E6 proteins from multiple human betapapillomavirus types degrade Bak and protect keratinocytes from apoptosis after UVB irradiation. *J Virol* 82:10408–10417. 10.1128/JVI.00902-08.
22. Wallace NA, Robinson K, Howie HL, Galloway DA. 2012. HPV 5 and 8 E6 abrogate ATR activity resulting in increased persistence of UVB induced DNA damage. *PLoS Pathog* 8:e1002807. 10.1371/journal.ppat.1002807.
23. Viarisio D, Mueller-Decker K, Kloz U, Aengeneyndt B, Kopp-Schneider A, Gröne H-J, Gheit T, Flechtenmacher C, Gissmann L, Tommasino M. 2011. E6 and E7 from beta HPV38 cooperate with ultraviolet light in the development of actinic keratosis-like lesions and squamous cell carcinoma in mice. *PLoS Pathog* 7:e1002125. 10.1371/journal.ppat.1002125.
24. Deshmukh J, Pofahl R, Pfister H, Haase I. 2016. Deletion of epidermal Rac1 inhibits HPV-8 induced skin papilloma formation and facilitates HPV-8- and UV-light induced skin carcinogenesis. *Oncotarget* 7:57841–57850. 10.18632/oncotarget.11069.
25. Wallace NA, Robinson K, Galloway DA. 2014. Beta human papillomavirus E6 expression inhibits stabilization of p53 and increases tolerance of genomic instability. *J Virol* 88:6112–6127. 10.1128/JVI.03808-13.
26. Wallace NA, Gasior SL, Faber ZJ, Howie HL, Deininger PL, Galloway DA. 2013. HPV 5 and 8 E6 expression reduces ATM protein levels and attenuates LINE-1 retrotransposition. *Virology* 443:69–79. 10.1016/j.virol.2013.04.022.
27. Howie HL, Koop JI, Weese J, Robinson K, Wipf G, Kim L, Galloway DA. 2011. Beta-HPV 5 and 8 E6 promote p300 degradation by blocking AKT/p300 association. *PLoS Pathog* 7:e1002211. 10.1371/journal.ppat.1002211.
28. Muench P, Probst S, Schuetz J, Leiprecht N, Busch M, Wesselborg S, Stubenrauch F, Iftner T. 2010. Cutaneous papillomavirus E6 proteins must interact with p300 and block p53-mediated apoptosis for cellular immortalization and tumorigenesis. *Cancer Res* 70:6913–6924. 10.1158/0008-5472.CAN-10-1307.
29. Dancy BM, Cole PA. 2015. Protein lysine acetylation by p300/CBP. *Chem Rev* 115:2419–2452. 10.1021/cr500452k.
30. Chan HM, Thangue N. 2001. p300/CBP proteins: HATs for transcriptional bridges and scaffolds. *J Cell Sci* 114:2363–2373.

31. Soto M, García-Santisteban I, Krenning L, Medema RH, Raaijmakers JA. 2018. Chromosomes trapped in micronuclei are liable to segregation errors. *J Cell Sci* 131:jcs214742. 10.1242/jcs.214742.
32. Ganem NJ, Cornils H, Chiu S-Y, O'Rourke KP, Arnaud J, Yimlamai D, Théry M, Camargo FD, Pellman D. 2014. Cytokinesis failure triggers Hippo tumor suppressor pathway activation. *Cell* 158:833–848. 10.1016/j.cell.2014.06.029.
33. Stukenberg PT. 2004. Triggering p53 after cytokinesis failure. *J Cell Biol* 165:607–608. 10.1083/jcb.200405089.
34. Shinmura K, Bennett RA, Tarapore P, Fukasawa K. 2007. Direct evidence for the role of centrosomally localized p53 in the regulation of centrosome duplication. *Oncogene* 26:2939–2944. 10.1038/sj.onc.1210085.
35. Wallace NA, Robinson K, Howie HL, Galloway DA. 2015. β -HPV 5 and 8 E6 disrupt homology dependent double strand break repair by attenuating BRCA1 and BRCA2 expression and foci formation. *PLoS Pathog* 11:e1004687. 10.1371/journal.ppat.1004687.
36. Snow JA, Murthy V, Dacus D, Hu C, Wallace NA. 2019. β -HPV 8E6 attenuates ATM and ATR signaling in response to UV damage. *Pathogens* 8:267. 10.3390/pathogens8040267.
37. Ganem NJ, Storchova Z, Pellman D. 2007. Tetraploidy, aneuploidy and cancer. *Curr Opin Genet Dev* 17:157–162. 10.1016/j.gde.2007.02.011.
38. Sen S. 2000. Aneuploidy and cancer. *Curr Opin Oncol* 12:82–88. 10.1016/j.gde.2007.02.011.
39. Meyers JM, Spangle JM, Munger K. 2013. The human papillomavirus type 8 E6 protein interferes with NOTCH activation during keratinocyte differentiation. *J Virol* 87:4762–4767. 10.1128/JVI.02527-12.
40. Barretina J, Caponigro G, Stransky N, Venkatesan K, Margolin AA, Kim S, Wilson CJ, Lehár J, Kryukov GV, Sonkin D, Reddy A, Liu M, Murray L, Berger MF, Monahan JE, Morais P, Meltzer J, Korejwa A, Jané-Valbuena J, Mapa FA, Thibault J, Bric-Furlong E, Raman P, Shipway A, Engels IH, Cheng J, Yu GK, Yu J, Aspesi P, de Silva M, Jagtap K, Jones MD, Wang L, Hatton C, Palesscandolo E, Gupta S, Mahan S, Sougnez C, Onofrio RC, Liefeld T, MacConaill L, Winckler W, Reich M, Li N, Mesirov JP, Gabriel SB, Getz G, Ardlie K, Chan V, Myer VE, et al.. 2012. The Cancer Cell Line Encyclopedia enables predictive modelling of anticancer drug sensitivity. *Nature* 483:603–607. 10.1038/nature11003.
41. Gao J, Aksoy BA, Dogrusoz U, Dresdner G, Gross B, Sumer SO, Sun Y, Jacobsen A, Sinha R, Larsson E, Cerami E, Sander C, Schultz N. 2013. Integrative analysis of complex cancer genomics and clinical profiles using the cBioPortal. *Sci Signal* 6:pl1. 10.1126/scisignal.2004088.

42. Cerami E, Gao J, Dogrusoz U, Gross BE, Sumer SO, Aksoy BA, Jacobsen A, Byrne CJ, Heuer ML, Larsson E, Antipin Y, Reva B, Goldberg AP, Sander C, Schultz N. 2012. The cBio Cancer Genomics Portal: an open platform for exploring multidimensional cancer genomics data. *Cancer Discov* 2:401–404. 10.1158/2159-8290.CD-12-0095.
43. Eden E, Navon R, Steinfeld I, Lipson D, Yakhini Z. 2009. GOrilla: a tool for discovery and visualization of enriched GO terms in ranked gene lists. *BMC Bioinformatics* 10:48. 10.1186/1471-2105-10-48.
44. Eden E, Lipson D, Yogev S, Yakhini Z. 2007. Discovering motifs in ranked lists of DNA sequences. *PLoS Comput Biol* 3:e39. 10.1371/journal.pcbi.0030039.
45. Stauffer D, Chang B, Huang J, Dunn A, Thayer M. 2007. p300/CREB-binding protein interacts with ATR and is required for the DNA replication checkpoint. *J Biol Chem* 282:9678–9687. 10.1074/jbc.M609261200.
46. Ogiwara H, Kohno T. 2012. CBP and p300 histone acetyltransferases contribute to homologous recombination by transcriptionally activating the BRCA1 and RAD51 genes. *PLoS One* 7:e52810. 10.1371/journal.pone.0052810.
47. Iyer NG, Chin S-F, Ozdag H, Daigo Y, Hu D-E, Cariati M, Brindle K, Aparicio S, Caldas C. 2004. p300 regulates p53-dependent apoptosis after DNA damage in colorectal cancer cells by modulation of PUMA/p21 levels. *Proc Natl Acad Sci U S A* 101:7386–7391. 10.1073/pnas.0401002101.
48. Maness PF, Walsh RC. Jr., 1982. Dihydrocytochalasin B disorganizes actin cytoarchitecture and inhibits initiation of DNA synthesis in 3T3 cells. *Cell* 30:253–262. 10.1016/0092-8674(82)90031-9.
49. Zhao B, Li L, Tumaneng K, Wang C-Y, Guan K-L. 2010. A coordinated phosphorylation by Lats and CK1 regulates YAP stability through SCF β -TRCP. *Genes Dev* 24:72–85. 10.1101/gad.1843810.
50. Cornelissen M, Philippé J, De Sitter S, De Ridder L. 2002. Annexin V expression in apoptotic peripheral blood lymphocytes: an electron microscopic evaluation. *Apoptosis* 7:41–47. 10.1023/a:1013560828090.
51. Riccardi C, Nicoletti I. 2006. Analysis of apoptosis by propidium iodide staining and flow cytometry. *Nat Protoc* 1:1458–1461. 10.1038/nprot.2006.238.
52. Senovilla L, Vitale I, Martins I, Tailler M, Pailleret C, Michaud M, Galluzzi L, Adjemian S, Kepp O, Niso-Santano M, Shen S, Marino G, Criollo A, Boileve A, Job B, Ladoire S, Ghiringhelli F, Sistigu A, Yamazaki T, Rello-Varona S, Locher C, Poirier-Colame V, Talbot M, Valent A, Berardinelli F, Antoccia A, Ciccocanti F, Fimia GM, Piacentini M, Fueyo A, Messina NL, Li M, Chan CJ, Sigl V, Pourcher G, Ruckenstein C, Carmona-Gutierrez D, Lazar V, Penninger JM, Madeo F, Lopez-Otin C, Smyth MJ, Zitvogel L, Castedo M, Kroemer G. 2012. An immunosurveillance mechanism controls cancer cell ploidy. *Science* 337:1678–1684. 10.1126/science.1224922.

53. McBride AA. 2008. Replication and Partitioning of Papillomavirus Genomes. *Adv Virus Res* 72:155–205. 10.1016/S0065-3527(08)00404-1.
54. He C, Mao D, Hua G, Lv X, Chen X, Angeletti PC, Dong J, Remmenga SW, Rodabaugh KJ, Zhou J, Lambert PF, Yang P, Davis JS, Wang C. 2015. The Hippo/YAP pathway interacts with EGFR signaling and HPV oncoproteins to regulate cervical cancer progression. *EMBO Mol Med* 7:1426–1449. 10.15252/emmm.201404976.
55. Morgan E, Patterson M, Lee SY, Wasson C, Macdonald A. 2018 High-risk human papillomaviruses down-regulate expression of the Ste20 family kinase MST1 to inhibit the Hippo pathway and promote transformation. *bioRxiv* 10.1101/369447.
56. Cheng J, Jing Y, Kang D, Yang L, Li J, Yu Z, Peng Z, Li X, Wei Y, Gong Q, Miron RJ, Zhang Y, Liu C. 2018. The role of MstI in lymphocyte homeostasis and function. *Front Immunol* 9:149. 10.3389/fimmu.2018.00149.
57. Zhang Y, Zhang H, Zhao B. 2018. Hippo signaling in the immune system. *Trends Biochem Sci* 43:77–80. 10.1016/j.tibs.2017.11.009.
58. Crequer A, Picard C, Patin E, D'Amico A, Abhyankar A, Munzer M, Debré M, Zhang S-Y, Saint-Basile G. d, Fischer A, Abel L, Orth G, Casanova J-L, Jouanguy E. 2012. Inherited MST1 deficiency underlies susceptibility to EV-HPV infections. *PLoS One* 7:e44010. 10.1371/journal.pone.0044010.
59. Pan D. 2010. The Hippo signaling pathway in development and cancer. *Dev Cell* 19:491–505. 10.1016/j.devcel.2010.09.011.
60. Li YY, Hanna GJ, Laga AC, Haddad RI, Lorch JH, Hammerman PS. 2015. Genomic analysis of metastatic cutaneous squamous cell carcinoma. *Clin Cancer Res off J Am Assoc Cancer Res* 21:1447–1456. 10.1158/1078-0432.CCR-14-1773.
61. Pickering CR, Zhou JH, Lee JJ, Drummond JA, Peng SA, Saade RE, Tsai KY, Curry JL, Tetzlaff MT, Lai SY, Yu J, Muzny DM, Doddapaneni H, Shinbrot E, Covington KR, Zhang J, Seth S, Caulin C, Clayman GL, El-Naggar AK, Gibbs RA, Weber RS, Myers JN, Wheeler DA, Frederick MJ. 2014. Mutational landscape of aggressive cutaneous squamous cell carcinoma. *Clin Cancer Res off J Am Assoc Cancer Res* 20:6582–6592. 10.1158/1078-0432.CCR-14-1768.
62. Murthy V, Dacus D, Gamez M, Hu C, Wendel SO, Snow J, Kahn A, Walterhouse SH, Wallace NA. 2018. Characterizing DNA repair processes at transient and long-lasting double-strand DNA breaks by immunofluorescence microscopy. *JoVE* e57653. 10.3791/57653.

**Chapter 4 - β -HPV 8E6 combined with TERT expression promotes
long-term proliferation and genome instability after cytokinesis
failure**

Dalton Dacus, Elizabeth Riforgiate, Nicholas A. Wallace*

Division of Biology, Kansas State University, Manhattan, Kansas, USA

*Corresponding Author: nwallac@ksu.edu

Published as: Dacus D, Riforgiate E, Wallace NA. 2020. β -HPV 8E6 combined with TERT expression promotes long-term proliferation and genome instability after cytokinesis failure.

Virology <https://doi.org/10.1016/j.virol.2020.07.016>.

Abstract

Human papillomavirus (HPV) is a family of viruses divided into five genera: alpha, beta, gamma, mu, and nu. There is an ongoing discussion about whether beta genus HPVs (β -HPVs) contribute to cutaneous squamous cell carcinoma (cSCC). The data presented here add to this conversation by determining how a β -HPV E6 protein (β -HPV 8E6) alters the cellular response to cytokinesis failure. Specifically, cells were observed after cytokinesis failure was induced by dihydrocytochalasin B (H2CB). β -HPV 8E6 attenuated the immediate toxicity associated with H2CB but did not promote long-term proliferation after H2CB. Immortalization by telomerase reverse transcriptase (*TERT*) activation also rarely allowed cells to sustain proliferation after H2CB exposure. In contrast, *TERT* expression combined with β -HPV 8E6 expression allowed cells to proliferate for months following cytokinesis failure. However, this continued proliferation comes with genome destabilizing consequences. Cells that survived H2CB-induced cytokinesis failure suffered from changes in ploidy.

Keywords

Aneuploid, Polyploid, Chromosome, Skin cancer, β -HPV, Telomerase

Introduction

Cutaneous squamous cell carcinoma (cSCC) is one of the most common malignancies worldwide (Lomas et al., 2012; Alam and Ratner, 2001). The annual rate of cSCC has risen for thirty straight years (Hollestein et al., 2014). These malignancies represent a tremendous financial burden, especially in fair-skinned populations. As a result, the United States currently spends \$3.8 billion annually on treatments (Deady et al., 2014). UV radiation, light skin color, and immunosuppression are the major risk factors implicated in the development of cSCC (Fahradyan et al., 2017). Additionally, it has been hypothesized that cutaneous human

papillomavirus of the beta genus (β -HPV) may be another factor in cSCC progression (Howley and Pfister, 2015a; McLaughlin-Drubin, 2015; Tommasino, 2017).

β -HPV types 5 and 8 were first isolated from sun-exposed skin lesions found in individuals with the rare genetic disorder, epidermodysplasia verruciformis (EV) (Orth, 2008). People with EV are prone to β -HPV infections and cSCC (Orth, 2008; Nunes et al., 2018). A similar association has been observed in people taking immunosuppressive drugs after organ transplants (Genders et al., 2015; Boyle et al., 1984; Boxman et al., 1997). Further, animal and epidemiological studies also suggest β -HPV infections are associated with cSCC (Tommasino, 2017; Chahoud et al., 2016; Patel et al., 2008). Yet β -HPV expression in immunocompetent individuals drops significantly as healthy skin progresses to precancerous actinic keratosis (AK), then onto cSCC (Nunes et al., 2018; Winer et al., 2017; Hampras et al., 2017; Weissenborn et al., 2005, 2009; Howley and Pfister, 2015b). *In vitro* assays suggest that β -HPV proteins, particularly β -HPV E6, alter cell signaling to promote proliferation, impairing genome stability in the process (Wendel and Wallace, 2017; Rollison et al., 2019). These data have led some to hypothesize that β -HPV augments the mutational burden associated with UV, promoting the early stages of malignant conversion. In what has been called the “hit-and-run” model of viral oncogenesis, these mutations result in a tumor that no longer relies on continued viral gene expression (Aldabagh et al., 2013; Hufbauer and Akgül, 2017; de Koning et al., 2007). While this model has merit, other factors seem to dictate the oncogenic potential of β -HPV infections. For example, a recent publication from Strickley et al. helped solidify the growing consensus that immune status is a central determinant of the oncogenic potential associated with β -HPV infections (Strickley et al., 2019). Other factors may also increase or decrease the risk associated

with these infections. Given how widespread β -HPV infections are, it remains important to understand the genetic changes that could augment their deleterious characteristics.

The work described here focuses on the maintenance of genome fidelity during cell division. Live cell microscopy and brightfield microscopy demonstrate that failed cytokinesis occurs about 10% of the time that skin cells enter mitosis (Wallace et al., 2014; Dacus et al., 2020). When this occurs, if the cells continue proliferating, they will suffer changes in ploidy (Hayashi and Karlseder, 2013; Alonso-Lecue et al., 2017; Lens and Medema, 2019). Responses to failed cytokinesis are often studied after induction by dihydrocytochalasin B (H2CB). H2CB causes cytokinesis failure by inhibiting actin polymerization. One study used this approach to show that the Hippo pathway kinase LATS was responsible for orchestrating the cellular response to failed cytokinesis, by inducing p53 accumulation and preventing further proliferation (Ganem et al., 2014). β -HPV 8E6 expression inhibits this buildup of p53 by attenuating LATS activation in a p300-dependent manner (Dacus et al., 2020). Despite the impairment of relevant signaling events, β -HPV 8E6 only imparted transient protection from failed cytokinesis. While β -HPV 8E6 expressing cells tolerated the immediate impact of failed cytokinesis, they were not capable of sustained proliferation. Mutations that activate telomerase are common in cSCC and are associated with growth advantages (Cheng et al., 2015; Griewank et al., 2013; Pópulo et al., 2014). Like β -HPV 8E6 expression, *TERT* expression had a limited ability to promote proliferation after failed cytokinesis. However, expression of β -HPV 8E6 in cells immortalized by telomerase activation promoted short- and long-term proliferation after failed cytokinesis. The survival of H2CB-induced failed cytokinesis was associated with increased aneuploidy.

Results

β -HPV 8E6 expressing HFK cannot sustain proliferation after H2CB-induced failed cytokinesis. β -HPV 8E6 hinders the cellular response to genome destabilizing events, including DNA damage and failed cytokinesis (Wendel and Wallace, 2017; Dacus et al., 2020). This study examines the consequences of β -HPV 8E6's impairment of signaling events stemming from H2CB-induced cytokinesis failure. β -HPV 8E6 reduces H2CB-induced activation of a Hippo tumor suppressor pathway kinase (LATS), p53 stabilization, and the accumulation of apoptotic markers. β -HPV 8E6 also increases the expression of pro-proliferative TEAD-responsive genes. To determine if these alterations allowed cells to survive H2CB-induced failed cytokinesis, we exposed vector control human foreskin keratinocytes (HFK LXS_N) and β -HPV 8E6 expressing HFK (HFK β -HPV 8E6) to media containing 4 μ M of H2CB for 6 days (Ganem et al., 2014). Cells counted on day 0 are referred to as 'before' H2CB. After 6 days of H2CB exposure, cells were counted and are referred to as 'during'. H2CB was washed out and cells were placed in growth media. Cells were monitored until they reached approximately 90% confluency or stopped proliferating (referred to as 'after'). At this point, viable cultures were counted, passaged, and considered to have recovered (recovered-HFK LXS_N or recovered-HFK β -HPV 8E6) from H2CB exposure. Three independent biological replicates found similar results. β -HPV 8E6 attenuated the immediate consequences of H2CB-associated toxicity (compare the number of HFK LXS_N and HFK β -HPV 8E6 after 6 days of H2CB exposure in **Fig. 4.1A**). However, neither cell line was capable of sustained proliferation after H2CB (**Fig. 4.1A**).

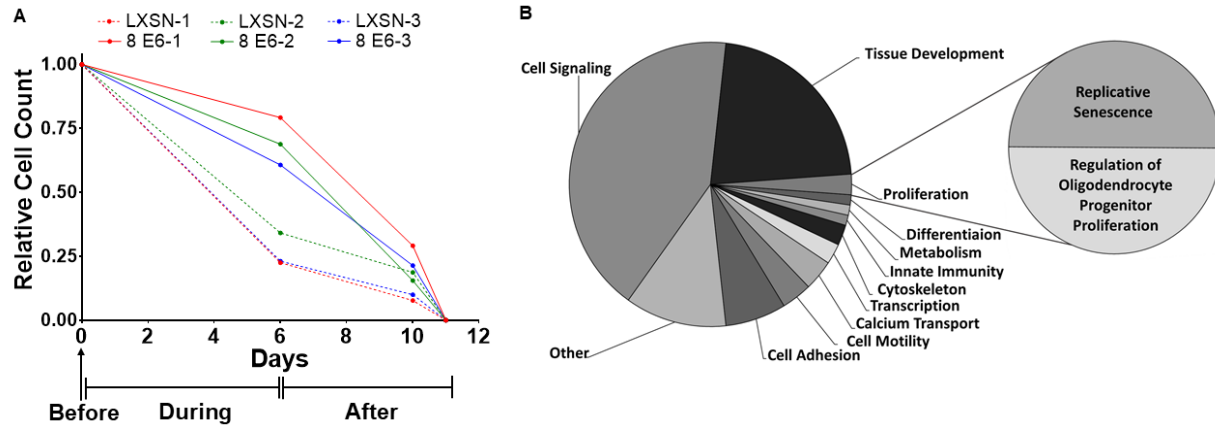


Figure 4.1. H2CB-induced failed cytokinesis prevents long-term proliferation

(A) Three growth curves (biological replicates) comparing HFK LXSN and β -HPV 8E6 cells before, during, and after 6 days of H2CB exposure in 6-well tissue culture plates. HFK LXSN (dashed) and β -HPV 8E6 (solid) data with the same color and number (red, 1; green, 2; and blue, 3) were treated in parallel. (B) Two charts representing GO analysis of common mutations in cSCC. The larger chart on the left represents nodes of similar GO: biological process terms. The smaller chart represents the two GO: biological process terms within the “Proliferation” node. *TERT* expression allows β -HPV 8E6 HFKs growth after H2CB-induced failed cytokinesis. (For interpretation of the references to color in this figure legend, the reader is referred to the Web version of this article.)

β -HPV infections occur in different genetic backgrounds, some of which could act synergistically with β -HPV 8E6 to allow cells to recover from H2CB-induced failed cytokinesis (Martincorena et al., 2015). Given the links between β -HPV and cSCC development, recurrent genetic contributors to cSCC development were examined to identify candidate alterations. Specifically, common mutations from sequencing data of 68 cSCC were ranked by their frequency (Pickering et al., 2014; Li et al., 2015; Gao et al., 2013; Cerami et al., 2012) (**Data Set S4.1** in Supplementary Data). Then, a gene ontology analysis was performed on the top 10% of mutations using the web-based gene ontology software, PANTHER (Mi et al., 2017; The Gene Ontology Resourc, 2019; Ashburner et al., 2000) (**Fig. 4.1B**). The biological process “replicative

senescence” contained within the “proliferation” node contained commonly mutated genes in cSCC. A complementary gene ontology software also identified “replicative senescence” among the cellular responses enriched within cSCC mutated genes (data not shown). This broad unbiased approach was complimented with a literature-based prioritization of the mutated genes. Among the genes in the “replicative senescence” node, mutations in *TERT* (the gene encoding telomerase reverse transcriptase, a component of telomerase) were notable. Multiple other studies have identified telomerase activating mutations within *TERT* promoter region in cSCC (Cheng et al., 2015; Griewank et al., 2013; Pópulo et al., 2014; Scott et al., 2014). Enhanced telomerase activity can promote proliferation despite damage and stress that would normally remove cells from the cell cycle (Urquidi et al., 2000; Victorelli and Passos, 2017; Davoli et al., 2010). It also allows cells immortalized by telomerase activation to continue growing after exposure to cytochalasin B, an unsaturated derivative of H2CB, which shares the ability to inhibit cell division, but unlike H2CB, it affects sugar transport (31, 48–51). These observations suggest that *TERT* activation is a relevant alteration in cSCC and that it could act on its own or synergize with β -HPV 8E6 to promote growth after cytokinesis failure.

To determine if *TERT* activation could promote survival from H2CB, β -HPV 8E6 expression was examined in HFK immortalized by telomerase activation (*TERT*-HFK). Specifically, the effects of H2CB on long term proliferation were studied in previously characterized HA-tagged β -HPV 8E6 and vector control *TERT*-HFKs (*TERT*-HFK β -HPV 8E6 and *TERT*-HFK LXS_N, respectively) (Wang et al., 2016; Dickson et al., 2000). β -HPV 8E6 maintained its previously reported ability to alter the response to H2CB and increase TEAD-responsive gene expression in this genetic background (**Fig. S.41A–C**). Further, H2CB exposure was more effective at inducing binucleation and senescence (indicated by senescence-associated

β -Galactosidase or SA β -Gal staining) in *TERT*-HFK cells (**Fig. S4.1D,E**). These data confirmed that both β -HPV 8E6 and H2CB retained their reported activities in *TERT*-HFK cells. Next, the impact of H2CB exposure (6 days of 4 μ M H2CB) on long-term proliferation was defined for three biological replicates using the growth conditions described in **Fig. 4.1A**. β -HPV 8E6 continued to reduce cell death in *TERT*-HFKs during H2CB exposure (compare cell lines at day 6 in **Fig. 4.2A**). However, β -HPV 8E6 was also able to promote recovery from H2CB-induced failed cytokinesis in this genetic background (recovered-*TERT*-HFK β -HPV 8E6). In each of these long-term growth assays, *TERT*-HFK β -HPV 8E6 survived for at least 17 days after H2CB exposure (**Fig. 4.2A**). Unfortunately, one repeat was contaminated and could not be expanded after survival. In contrast, none of the attempts to grow *TERT*-HFK LXSN after H2CB exposure were successful (recovered-*TERT*-HFK LXSN).

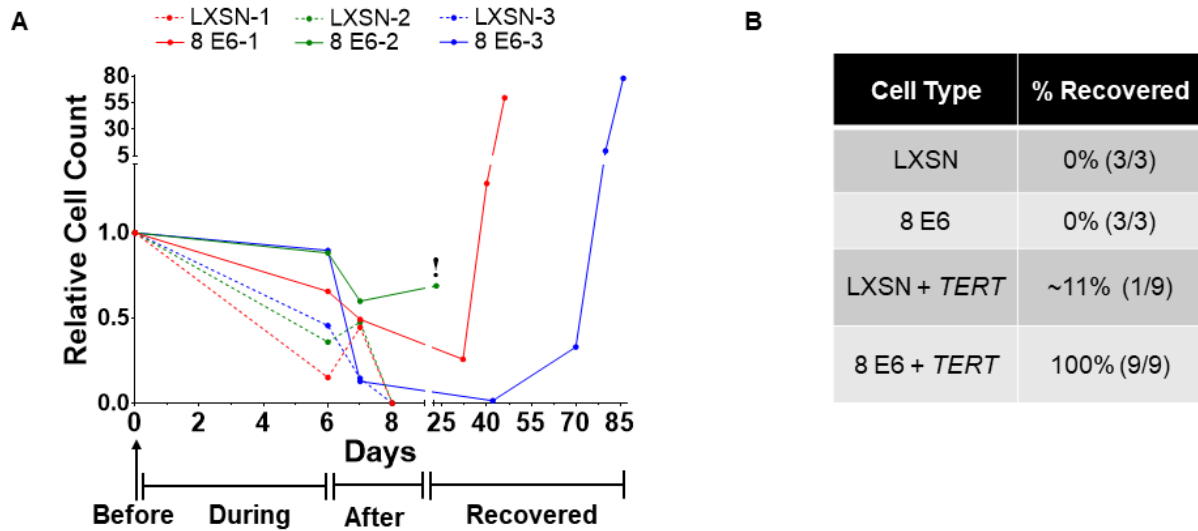


Figure 4.2. *TERT* expression promotes recovery from failed cytokinesis.

(A) Three growth curves (biological replicates) comparing *TERT*-HFK LXSN and β -HPV 8E6 cells before, during, after, and recovered from 6 days of H2CB exposure in 6-well tissue culture plates. LXSN (dashed) and β -HPV 8E6 (solid) data with the same color and number (red, 1; green, 2; and blue, 3) were treated in parallel. ! signifies the premature end of the long-term

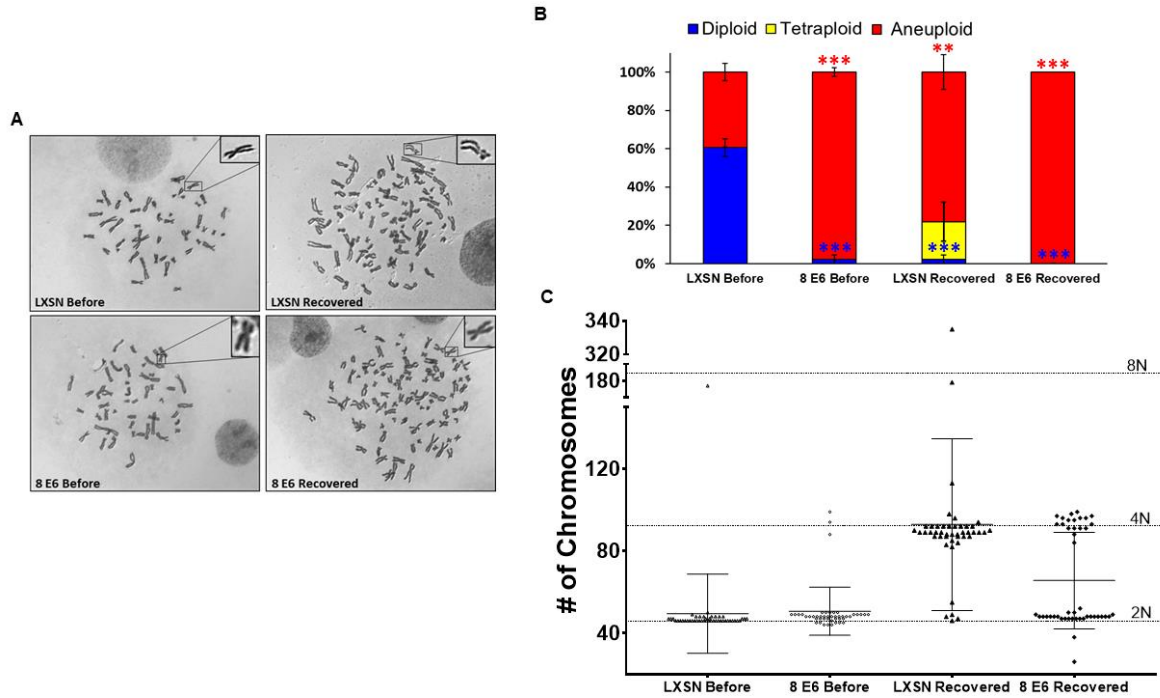
cultivation due to bacterial contamination. (B) Percent of HFK and *TERT*-HFK cells capable of long-term growth after 6 days in H2CB. (For interpretation of the references to color in this figure legend, the reader is referred to the Web version of this article.)

To obtain recovered-*TERT*-HFK LXSNS to compare to recovered-*TERT*-HFK β -HPV 8E6 cells, 6 additional replicates were performed in a format with a larger initial population of cells (expansion from a 6-well to 10-cm plate format). In these conditions, only one of the *TERT*-HFK LXSNS cell lines survived (See **Fig. 4.2B**). *TERT*-HFK β -HPV 8E6 cells also survived in each of the experiments conducted in 10-cm plates. Representative growth data for these cells can be found in Supplementary **Figure 4.2**. Recovered-*TERT*-HFK cells were expanded to determine the genomic consequences of surviving H2CB.

β -HPV 8E6 exacerbates aneuploidy in *TERT*-HFKs after recovering from failed cytokinesis

Failed cytokinesis jeopardizes genome integrity, particularly when cells continue to proliferate afterward (Hayashi and Karlseder, 2013; Storchova and Kuffer, 2008; Ganem et al., 2007). To determine if the cells that survived H2CB-induced failed cytokinesis had impaired genomic instability, differential interference contrast microscopy of condensed chromosomes from metaphase spreads was used to compare the ploidy of *TERT*-HFK LXSNS to recovered-*TERT*-HFK LXSNS cells (**Fig. 4.3A**). While most *TERT*-HFK LXSNS were diploid before H2CB treatment, many recovered-*TERT*-HFK LXSNS cells had aneuploid genomes. A small subset of recovered-*TERT*-HFK LXSNS cells had tetraploid genomes (**Fig. 4.3B**). Chromosome abnormalities were exacerbated by β -HPV 8E6 in the cell line paired with the only recovered-*TERT*-HFK LXSNS cell line. Most *TERT*-HFK β -HPV 8E6 cells had aneuploid genomes before H2CB exposure and all the recovered-*TERT*-HFK β -HPV 8E6 were aneuploid (**Fig. 4.3B, C**).

The length of time in passage is unlikely to explain these data as the cells were analyzed after a similar time in culture. Further, the results were nearly identical when ploidy was determined immediately after recovery or several passages later (data not shown).



Discussion

β -HPVs promote the proliferation of damaged skin cells (Howley and Pfister, 2015a; Tommasino, 2017; Rollison et al., 2019; Wallace et al., 2014; Dacus et al., 2020). β -HPV 8E6 is a critical contributor to this phenotype and acts at least in part by suppressing apoptotic responses (Dacus et al., 2020; Underbrink et al., 2008). As a result, β -HPV infections have been hypothesized to allow the accumulation of potentially tumorigenic mutations. Here, we examine the ability of β -HPV 8E6 to act along with *TERT* expression to facilitate the survival of cells that do not divide after replicating their genomes. We summarize our observations in **Fig. 4.4**. When cytokinesis failure was induced by H2CB, HFK were unable to sustain long-term growth (**Fig. 4.4A**). β -HPV 8E6 did not change this outcome (**Fig. 4.4B**). Immortalization by telomerase activation rarely allowed cells to recover from.

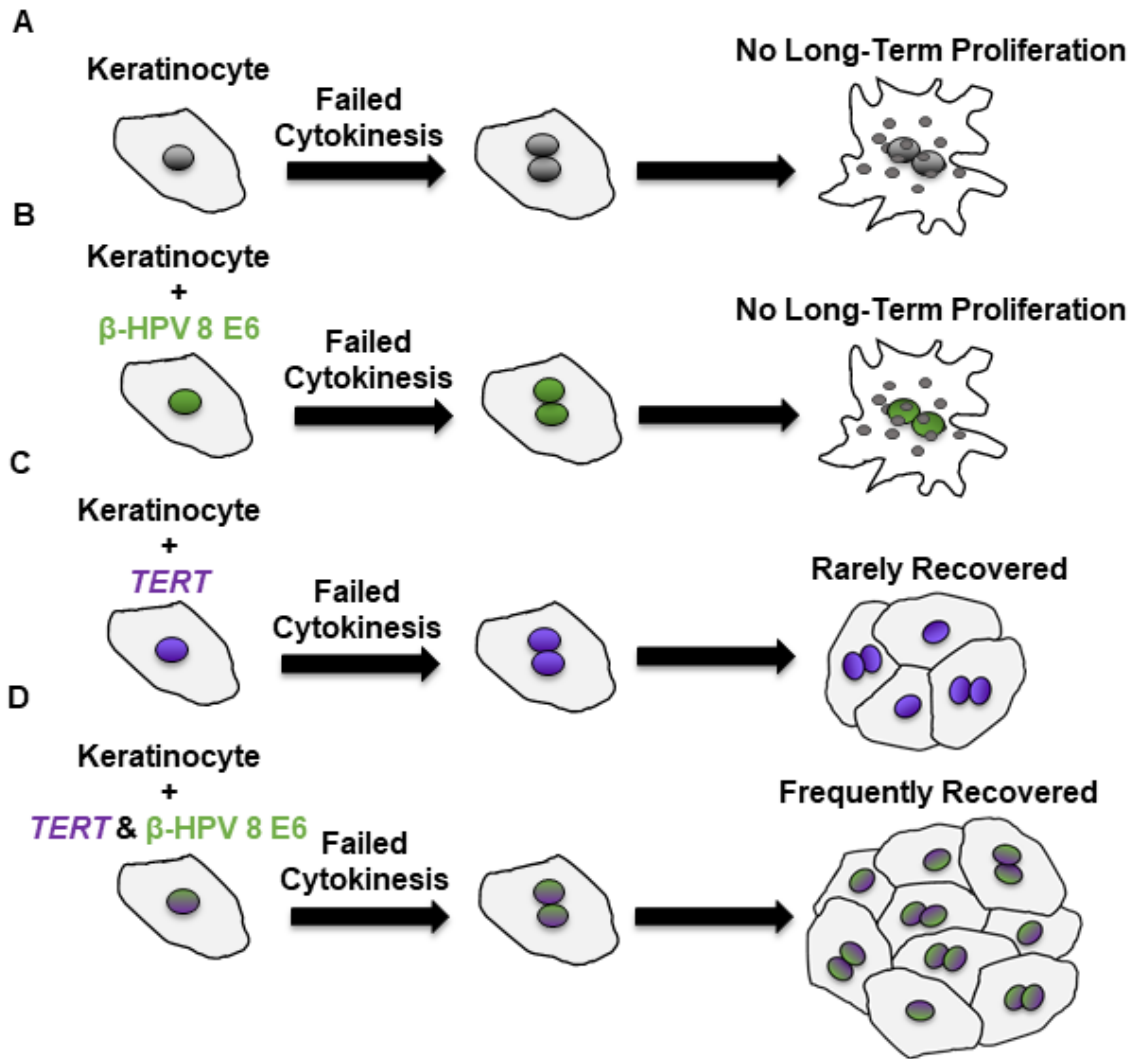


Figure 4.4. β -HPV 8E6 and telomerase activation affect cell fate after failed cytokinesis.

(A) Keratinocytes that experience H2CB-induced cytokinesis failure become binucleated (indicated by two nuclei inside the cell) resulting in cell death and inhibition of long-term proliferation. (B) β -HPV 8E6 (indicated by green nuclei) reduces the death associated with cytokinesis failure but cells remain unable to sustain long-term proliferation. (C) Keratinocytes immortalized by *TERT* activation (indicated by purple nuclei) experience H2CB-associated binucleation and toxicity, but unlike primary keratinocytes, a small number recover. (D) *TERT* immortalized keratinocytes that co-express β -HPV 8E6 (indicated by green/purple nuclei) regularly survive H2CB-exposure but have high levels of aneuploidy. (For interpretation of the references to color in this figure legend, the reader is referred to the Web version of this article.)

H2CB exposure (**Fig. 4.4C**). However, the combination of β -HPV 8E6 expression and *TERT* expression allowed cells to sustain proliferation for months (presumably indefinitely) after cytokinesis failure and augmented genomic instability (**Fig. 4.4D**).

When comparing HFK and *TERT*-HFK cell lines some caution should be exercised as they were generated from different donors. However, phenotypes are frequently replicated across.

Keratinocytes from separate persons (White et al., 2012; Howie et al., 2011; Meyers et al., 2017). More specific to this study and these cells, the previously reported attenuation of the Hippo pathway kinase LATS activation by β -HPV 8E6 was conserved between both HFK and *TERT*-HFK cell lines (**Figure S4.1** and (Dacus et al., 2020)). These data are consistent with the established idea that telomerase activation promotes carcinogenesis and suggest that β -HPV infections may augment the transformative power of telomerase activation.

Our data also provides other, more specific insights. For instance, we found that β -HPV 8E6 made *TERT*-HFKs approximately 2.5 times more likely to be aneuploid (**Fig. 4.3C**). To our knowledge, this is the first report associating changes in ploidy with β -HPV 8E6. The observation is in line with reports from the Tommasino Lab that describe changes in ploidy in β -HPV 38 E6 and E7 immortalized keratinocytes (Gabet et al., 2008). Unlike our report, they demonstrated that ectopic *TERT* expression reduced aneuploidy, likely by reducing the chromosomal rearrangements, anaphase bridges, and multipolar mitoses associated with β -HPV 38 E6/E7 immortalization. This could be the result of differences between β -HPV 38 E6 and β -HPV 8E6 or they might be explained by the presence/absence of the β -HPV E7 protein (Tommasino, 2017; Howley and Pfister, 2015b).

In vitro studies on β -HPVs tend to examine the effects of stimuli over a short time interval (hours to days). However, the average β -HPV infection persists for six to eleven months (de Koning et al., 2007; Hampras et al., 2014). *TERT*-HFK cells provide a system to replicate lengthier conditions and our data demonstrates the utility of such an approach. By removing the restrictive nature of primary cell growth, we were able to describe the changes in ploidy stemming from failed cytokinesis. Based on our data, caution should be exercised when examining these systems as *TERT* expression can change the cellular response to genome destabilizing events.

Indeed, our data offers proof of principle that phenotypes associated with β -HPV E6 can change based on the genetic context of viral gene expression. There may be genetic environments where cutaneous papillomavirus infections promote cSCC and others where the same infections prevent cSCC. If this were true, it might help explain conflicting reports that describe these infections as oncogenic and oncopreventative (Howley and Pfister, 2015a; Aldabagh et al., 2013; Strickley et al., 2019; Hasche et al., 2018). Moving forward, it will be interesting to determine the ability of β -HPV E6 to synergize with other common mutations and the mechanism by which β -HPV 8E6 increases aneuploidy.

Material and methods

Cell culture

Primary HFK were derived from neonatal human foreskins. HFK and *TERT*-immortalized-HFK (obtained from Michael Underbrink, University of Texas Medical Branch) were grown in EpiLife medium supplemented with calcium chloride (60 μ M), human keratinocyte growth supplement (ThermoFisher Scientific), and penicillin-streptomycin. HPV genes were cloned, transfected, and confirmed as previously described (Wallace et al., 2014). In

order not to activate the Hippo pathway via contact inhibition, we carefully monitored the cell density in all experiments. Experiments were aborted if unintended differences in seeding resulted in cell densities that were more than 10% different among cell lines at the beginning of an experiment.

cBioPortal and gene ontology analysis

Software from (www.cbioportal.org) was used to recognize, analyze, and categorize mutations and transcriptomic data from cutaneous squamous cell carcinomas (Pickering et al., 2014; Li et al., 2015). Analysis of the squamous cell carcinoma samples was done at (<http://geneontology.org/>) powered by Protein ANalysis THrough Evolutionary Relationships (PANTHER) (The Gene Ontology Resourc, 2019; Ashburner et al., 2000).

H2CB recovery assay

6-well format: Cells were counted, then either 1.5×10^5 HFK or 5×10^4 *TERT*-HFK cells were seeded on a 6 well tissue culture plate and grown for 24 h. Cells were then treated with 4 μ M H2CB, refreshing the H2CB media every 2 days. After 6 days, the cells were washed with PBS and given fresh EpiLife. Once cells reached 90% confluency, they were counted then moved to new 6 wells. This process was continued until cells were no longer able to be passaged or cells could be moved to a 10 cm plate.

10 cm format: Cells were counted, then 3.0×10^5 cells were seeded on a 10 cm tissue culture plate and grown for 24 h. Cells were then treated with 4 μ M H2CB, refreshing the H2CB media every 2 days. After 6 days, the cells were washed with PBS and given fresh EpiLife. Once cells reached 90% confluency they were counted, then 9.0×10^4 cells were reseeded. This process was continued until cells were no longer able to be passaged or for 28 days.

RT-qPCR

Cells were lysed, isolated, reverse transcribed, and then RT-qPCR was performed as previously described (Dacus et al., 2020). The following probes (Thermo Scientific) were used: ACTB (Hs01060665_g1), STK4 (Hs00178979_m1), LATS2 (Referred to as LATS in the text) (Hs01059009_m1), YAP1 (Hs00902712_g1), CTGF (Hs00170014_m1), CYR61 (Hs00155479_m1), TEAD1 (Hs00173359_m1), CCND1 (Hs00765553_m1), AXL (Hs01064444_m1), SERPINE1 (Hs00167155_m1).

Immunoblotting

Cells were washed and lysed, then lysates were run, transferred, probed, and visualized as previously described (Dacus et al., 2020). The following antibodies were used: GAPDH (Santa Cruz Biotechnologies sc-47724), LATS2 (Referred to as LATS in the text, Cell Signaling Technologies D83D6), Phospho-LATS1/2 (Ser909) (Referred to as pLATS in the text) (Cell Signaling Technologies #9157), YAP (Cell Signaling Technologies 4912S), Phospho-YAP (Ser127) (Referred to pYAP in the text) (Cell Signaling Technologies 4911S), AXL (Cell Signaling Technologies 8661S, p300 (Santa Cruz Biotechnologies sc-584).

Senescence-associated β -galactosidase staining

Cells were seeded onto three 6-well plates and treated with H2CB then stained as previously described (Dacus et al., 2020).

Chromosome counts via metaphase spread

‘Before’ and after cells recovered from H2CB exposure *TERT*-immortalized HFK cells were grown to 80% confluency then chromosomes were detected and counted as previously described (Howe et al., 2014).

Statistical analysis

Unless otherwise noted, statistical significance was determined by a paired Student t-test and was confirmed when appropriate by a two-way analysis of variance (ANOVA) with Turkey's correction. Only P values less than 0.05 were reported as significant.

Acknowledgments:

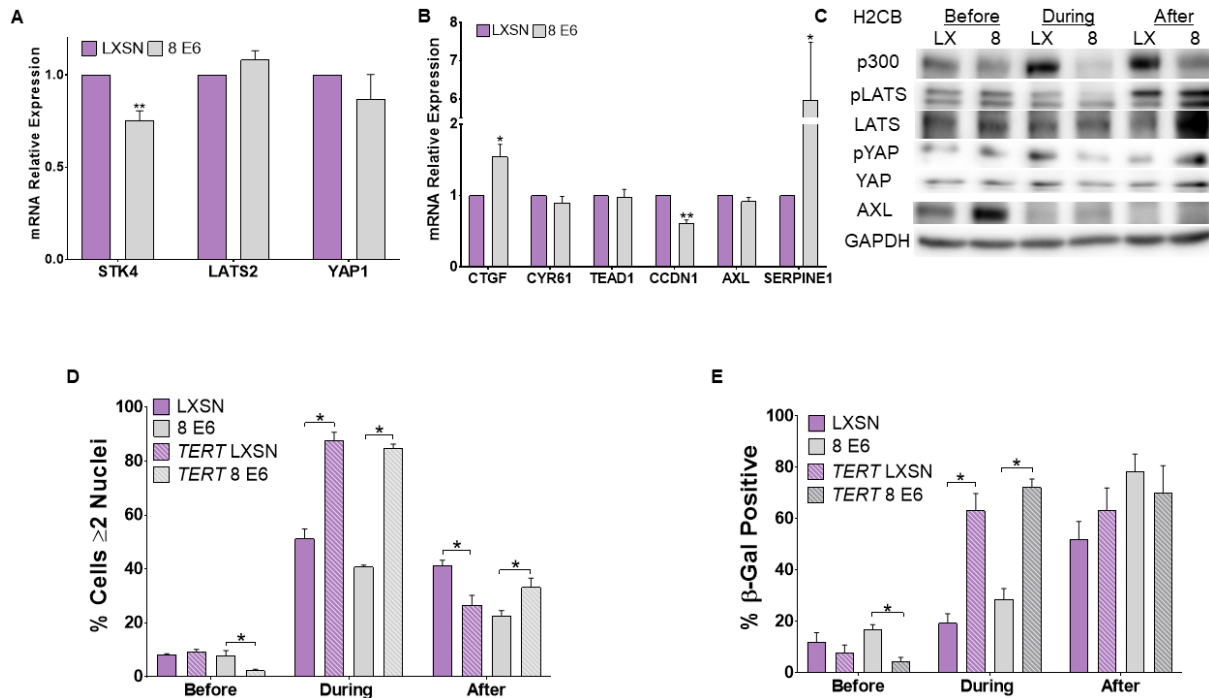
We thank and acknowledge Jocelyn A. McDonald for assisting with our metaphase spread imaging. Michael Underbrink for providing the *TERT*-immortalized-HFK. Jazmine A. Snow and Emily Burghardt for constructive criticism of the manuscript.

This work was supported by the Department of Defense CMDRP PRCRP CA160224 (NW) and made possible through generous support from the Les Clow family and the Johnson Cancer Research Center at Kansas State University. Declarations of interest: none.

Supplementary data

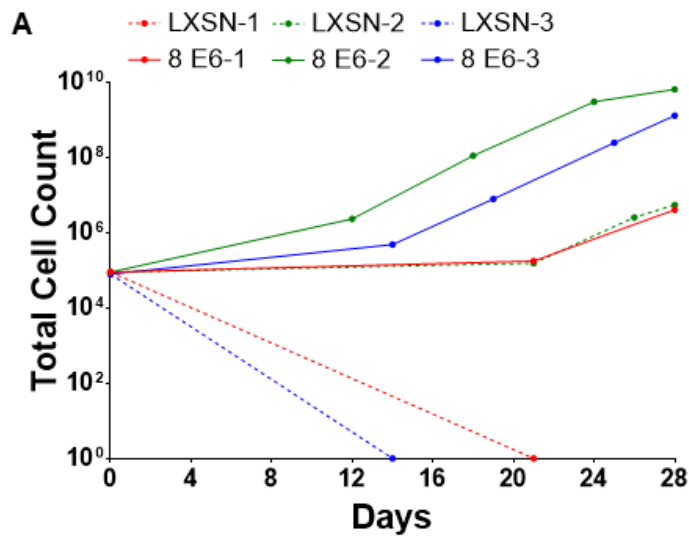
Data Set S4.1

[Download : Download spreadsheet \(378KB\)](#)



Figures S 4.1. Responses to H2CB-induced failed cytokinesis in TERT-HFK.

Expression of (A) canonical HP genes and (B) TEAD-regulated genes in *TERT*-HFKs measured by RT-qPCR and normalized to β -actin mRNA. (C) Representative immunoblot of HP proteins in *TERT*-HFK cells before, during, and after H2CB exposure. (D) Quantification of cells with more than 1 nucleus before, during, and after H2CB exposure. (E) Quantification of SA β -Gal staining in HFK cells vs *TERT*-HFK before, during, and after H2CB treatment. Figures depict means \pm standard error of the mean. $n \geq 3$. * denotes significant difference between indicated samples * denotes $p \leq 0.05$, ** denotes $p \leq 0.01$. (Student's *t*-test).



Figures S 4.2. *TERT*-HFK recovering from H2CB-induced cytokinesis failure.

(A) Three growth curves (one of 2 additional 10 cm biological replicates) comparing *TERT*-HFK-LXSN and β -HPV 8E6 once recovered from 6 days of H2CB exposure in 10 cm tissue culture plates. LXSN (dashed) and β -HPV 8E6 (solid) data with the same color and number (red, 1; green, 2; and blue, 3) were treated in parallel.

References

- Alam, M., Ratner, D., 2001. Cutaneous squamous-cell carcinoma. *N. Engl. J. Med.* 344, 975–983. <https://doi.org/10.1056/NEJM200103293441306>
- Aldabagh, B., Angeles, J.G.C., Cardones, A.R., Arron, S.T., 2013. Cutaneous Squamous Cell Carcinoma and Human Papillomavirus: Is There An Association? *Dermatol. Surg. Off. Publ. Am. Soc. Dermatol. Surg.* 39, 1–23. <https://doi.org/10.1111/j.1524-4725.2012.02558.x>

- Alonso-Lecue, P., de Pedro, I., Coulon, V., Molinuevo, R., Lorz, C., Segrelles, C., Ceballos, L., López-Aventín, D., García-Valtuille, A., Bernal, J.M., Mazorra, F., Pujol, R.M., Paramio, J., Ramón Sanz, J., Freije, A., Toll, A., Gandarillas, A., 2017. Inefficient differentiation response to cell cycle stress leads to genomic instability and malignant progression of squamous carcinoma cells. *Cell Death Dis.* 8, e2901–e2901. <https://doi.org/10.1038/cddis.2017.259>
- Ashburner, M., Ball, C.A., Blake, J.A., Botstein, D., Butler, H., Cherry, J.M., Davis, A.P., Dolinski, K., Dwight, S.S., Eppig, J.T., Harris, M.A., Hill, D.P., Issel-Tarver, L., Kasarskis, A., Lewis, S., Matese, J.C., Richardson, J.E., Ringwald, M., Rubin, G.M., Sherlock, G., 2000. Gene Ontology: tool for the unification of biology. *Nat. Genet.* 25, 25–29. <https://doi.org/10.1038/75556>
- Atlas, S.J., Lin, S., 1978. Dihydrocytochalasin B. Biological effects and binding to 3T3 cells. *J. Cell Biol.* 76, 360–370.
- Boxman, I.L.A., Berkhout, R.J.M., Mulder, L.H.C., Wolkers, M.C., Bavinck, J.N.B., Vermeer, B.J., ter Schegget, J., 1997. Detection of Human Papillomavirus DNA in Plucked Hairs from Renal Transplant Recipients and Healthy Volunteers. *J. Invest. Dermatol.* 108, 712–715. <https://doi.org/10.1111/1523-1747.ep12292090>
- Boyle, J., Briggs, J.D., Mackie, RonaM., Junor, B.J.R., Aitchison, T.C., 1984. CANCER, WARTS, AND SUNSHINE IN RENAL TRANSPLANT PATIENTS: A Case-control Study. *The Lancet*, Originally published as Volume 1, Issue 8379 323, 702–705. [https://doi.org/10.1016/S0140-6736\(84\)92221-9](https://doi.org/10.1016/S0140-6736(84)92221-9)
- Cerami, E., Gao, J., Dogrusoz, U., Gross, B.E., Sumer, S.O., Aksoy, B.A., Jacobsen, A., Byrne, C.J., Heuer, M.L., Larsson, E., Antipin, Y., Reva, B., Goldberg, A.P., Sander, C., Schultz, N., 2012. The cBio Cancer Genomics Portal: An Open Platform for Exploring Multidimensional Cancer Genomics Data. *Cancer Discov.* 2, 401–404. <https://doi.org/10.1158/2159-8290.CD-12-0095>
- Chahoud, J., Semaan, A., Chen, Y., Cao, M., Rieber, A.G., Rady, P., Tying, S.K., 2016. Association Between β -Genus Human Papillomavirus and Cutaneous Squamous Cell Carcinoma in Immunocompetent Individuals—A Meta-analysis. *JAMA Dermatol.* 152, 1354–1364. <https://doi.org/10.1001/jamadermatol.2015.4530>
- Cheng, K.A., Kurtis, B., Babayeva, S., Zhuge, J., Tantchou, I., Cai, D., Lafaro, R.J., Fallon, J.T., Zhong, M., 2015. Heterogeneity of TERT promoter mutations status in squamous cell carcinomas of different anatomical sites. *Ann. Diagn. Pathol.* 19, 146–148. <https://doi.org/10.1016/j.anndiagpath.2015.03.005>
- Dacus, D., Cotton, C., McCallister, T.X., Wallace, N.A., 2020. β -HPV 8E6 Attenuates LATS Phosphorylation After Failed Cytokinesis. *J. Virol.* <https://doi.org/10.1128/JVI.02184-19>
- Davoli, T., Denchi, E.L., de Lange, T., 2010. Persistent telomere damage induces bypass of mitosis and tetraploidy. *Cell* 141, 81–93. <https://doi.org/10.1016/j.cell.2010.01.031>

- de Koning, M.N.C., Struijk, L., Bavinck, J.N.B., Kleter, B., ter Schegget, J., Quint, W.G.V., Feltkamp, M.C.W., 2007. Betapapillomaviruses frequently persist in the skin of healthy individuals. *J. Gen. Virol.* 88, 1489–1495. <https://doi.org/10.1099/vir.0.82732-0>
- Deady, S., Sharp, L., Comber, H., 2014. Increasing skin cancer incidence in young, affluent, urban populations: a challenge for prevention. *Br. J. Dermatol.* 171, 324–331. <https://doi.org/10.1111/bjd.12988>
- Dickson, M.A., Hahn, W.C., Ino, Y., Ronfard, V., Wu, J.Y., Weinberg, R.A., Louis, D.N., Li, F.P., Rheinwald, J.G., 2000. Human Keratinocytes That Express hTERT and Also Bypass a p16INK4a-Enforced Mechanism That Limits Life Span Become Immortal yet Retain Normal Growth and Differentiation Characteristics. *Mol. Cell. Biol.* 20, 1436–1447.
- Fahradyan, A., Howell, A.C., Wolfswinkel, E.M., Tsuha, M., Sheth, P., Wong, A.K., 2017. Updates on the Management of Non-Melanoma Skin Cancer (NMSC). *Healthcare* 5. <https://doi.org/10.3390/healthcare5040082>
- Gabet, A.-S., Accardi, R., Bellopede, A., Popp, S., Boukamp, P., Sylla, B.S., Londoño-Vallejo, J.A., Tommasino, M., 2008. Impairment of the telomere/telomerase system and genomic instability are associated with keratinocyte immortalization induced by the skin human papillomavirus type 38. *FASEB J.* 22, 622–632. <https://doi.org/10.1096/fj.07-8389com>
- Ganem, N.J., Cornils, H., Chiu, S.-Y., O'Rourke, K.P., Arnaud, J., Yimlamai, D., Théry, M., Camargo, F.D., Pellman, D., 2014. Cytokinesis Failure Triggers Hippo Tumor Suppressor Pathway Activation. *Cell* 158, 833–848. <https://doi.org/10.1016/j.cell.2014.06.029>
- Ganem, N.J., Storchova, Z., Pellman, D., 2007. Tetraploidy, aneuploidy and cancer. *Curr. Opin. Genet. Dev.* 17, 157–162. <https://doi.org/10.1016/j.gde.2007.02.011>
- Gao, J., Aksoy, B.A., Dogrusoz, U., Dresdner, G., Gross, B., Sumer, S.O., Sun, Y., Jacobsen, A., Sinha, R., Larsson, E., Cerami, E., Sander, C., Schultz, N., 2013. Integrative Analysis of Complex Cancer Genomics and Clinical Profiles Using the cBioPortal. *Sci. Signal.* 6, p11. <https://doi.org/10.1126/scisignal.2004088>
- Genders, R.E., Mazlom, H., Michel, A., Plasmeijer, E.I., Quint, K.D., Pawlita, M., van der Meijden, E., Waterboer, T., de Fijter, H., Claas, F.H., Wolterbeek, R., Feltkamp, M.C.W., Bouwes Bavinck, J.N., 2015. The presence of betapapillomavirus antibodies around transplantation predicts the development of keratinocyte carcinoma in organ transplant recipients: a cohort study. *J. Invest. Dermatol.* 135, 1275–1282. <https://doi.org/10.1038/jid.2014.456>
- Griewank, K.G., Murali, R., Schilling, B., Schimming, T., Möller, I., Moll, I., Schwamborn, M., Sucker, A., Zimmer, L., Schadendorf, D., Hillen, U., 2013. TERT Promoter Mutations Are Frequent in Cutaneous Basal Cell Carcinoma and Squamous Cell Carcinoma. *PLoS ONE* 8. <https://doi.org/10.1371/journal.pone.0080354>

- Hampras, S.S., Giuliano, A.R., Lin, H.-Y., Fisher, K.J., Abrahamsen, M.E., Sirak, B.A., Iannacone, M.R., Gheit, T., Tommasino, M., Rollison, D.E., 2014. Natural History of Cutaneous Human Papillomavirus (HPV) Infection in Men: The HIM Study. *PLOS ONE* 9, e104843. <https://doi.org/10.1371/journal.pone.0104843>
- Hampras, S.S., Rollison, D.E., Giuliano, A.R., McKay-Chopin, S., Minoni, L., Sereeday, K., Gheit, T., Tommasino, M., 2017. Prevalence and Concordance of Cutaneous Beta Human Papillomavirus Infection at Mucosal and Cutaneous Sites. *J. Infect. Dis.* 216, 92–96. <https://doi.org/10.1093/infdis/jix245>
- Hasche, D., Vinzón, S.E., Rösl, F., 2018. Cutaneous Papillomaviruses and Non-melanoma Skin Cancer: Causal Agents or Innocent Bystanders? *Front. Microbiol.* 9. <https://doi.org/10.3389/fmicb.2018.00874>
- Hayashi, M.T., Karlseder, J., 2013. DNA damage associated with mitosis and cytokinesis failure. *Oncogene* 32, 4593–4601. <https://doi.org/10.1038/onc.2012.615>
- Hollestein, L.M., de Vries, E., Aarts, M.J., Schrotten, C., Nijsten, T.E.C., 2014. Burden of disease caused by keratinocyte cancer has increased in The Netherlands since 1989. *J. Am. Acad. Dermatol.* 71, 896–903. <https://doi.org/10.1016/j.jaad.2014.07.003>
- Howe, B., Umrigar, A., Tsien, F., 2014. Chromosome Preparation From Cultured Cells. *J. Vis. Exp. JoVE.* <https://doi.org/10.3791/50203>
- Howie, H.L., Koop, J.I., Weese, J., Robinson, K., Wipf, G., Kim, L., Galloway, D.A., 2011. Beta-HPV 5 and 8 E6 Promote p300 Degradation by Blocking AKT/p300 Association. *PLoS Pathog.* 7. <https://doi.org/10.1371/journal.ppat.1002211>
- Howley, P.M., Pfister, H.J., 2015a. Beta Genus Papillomaviruses and Skin Cancer. *Virology* 0, 290–296. <https://doi.org/10.1016/j.virol.2015.02.004>
- Howley, P.M., Pfister, H.J., 2015b. Beta Genus Papillomaviruses and Skin Cancer. *Virology* 0, 290–296. <https://doi.org/10.1016/j.virol.2015.02.004>
- Hufbauer, M., Akgül, B., 2017. Molecular Mechanisms of Human Papillomavirus Induced Skin Carcinogenesis. *Viruses* 9. <https://doi.org/10.3390/v9070187>
- Lens, S.M.A., Medema, R.H., 2019. Cytokinesis defects and cancer. *Nat. Rev. Cancer* 19, 32–45. <https://doi.org/10.1038/s41568-018-0084-6>
- Li, Y.Y., Hanna, G.J., Laga, A.C., Haddad, R.I., Lorch, J.H., Hammerman, P.S., 2015. Genomic analysis of metastatic cutaneous squamous cell carcinoma. *Clin. Cancer Res. Off. J. Am. Assoc. Cancer Res.* 21, 1447–1456. <https://doi.org/10.1158/1078-0432.CCR-14-1773>
- Lin, S., Lin, D.C., Flanagan, M.D., 1978. Specificity of the effects of cytochalasin B on transport and motile processes. *Proc. Natl. Acad. Sci.* 75, 329–333. <https://doi.org/10.1073/pnas.75.1.329>

- Lin, S., Spudich, J.A., 1974. Biochemical studies on the mode of action of cytochalasin B. Cytochalasin B binding to red cell membrane in relation to glucose transport. *J. Biol. Chem.* 249, 5778–5783.
- Lomas, A., Leonardi-Bee, J., Bath-Hextall, F., 2012. A systematic review of worldwide incidence of nonmelanoma skin cancer. *Br. J. Dermatol.* 166, 1069–1080. <https://doi.org/10.1111/j.1365-2133.2012.10830.x>
- Martincorena, I., Roshan, A., Gerstung, M., Ellis, P., Loo, P.V., McLaren, S., Wedge, D.C., Fullam, A., Alexandrov, L.B., Tubio, J.M., Stebbings, L., Menzies, A., Widaa, S., Stratton, M.R., Jones, P.H., Campbell, P.J., 2015. High burden and pervasive positive selection of somatic mutations in normal human skin. *Science* 348, 880–886. <https://doi.org/10.1126/science.aaa6806>
- McLaughlin-Drubin, M.E., 2015. Human papillomaviruses and non-melanoma skin cancer. *Semin. Oncol.* 42, 284–290. <https://doi.org/10.1053/j.seminoncol.2014.12.032>
- Meyers, J.M., Uberoi, A., Grace, M., Lambert, P.F., Munger, K., 2017. Cutaneous HPV8 and MmuPV1 E6 Proteins Target the NOTCH and TGF- β Tumor Suppressors to Inhibit Differentiation and Sustain Keratinocyte Proliferation. *PLoS Pathog.* 13. <https://doi.org/10.1371/journal.ppat.1006171>
- Mi, H., Huang, X., Muruganujan, A., Tang, H., Mills, C., Kang, D., Thomas, P.D., 2017. PANTHER version 11: expanded annotation data from Gene Ontology and Reactome pathways, and data analysis tool enhancements. *Nucleic Acids Res.* 45, D183–D189. <https://doi.org/10.1093/nar/gkw1138>
- Nunes, E.M., Talpe-Nunes, V., Sicheo, L., 2018. Epidemiology and biology of cutaneous human papillomavirus. *Clinics* 73. <https://doi.org/10.6061/clinics/2018/e489s>
- Orth, G., 2008. Host defenses against human papillomaviruses: lessons from epidermodysplasia verruciformis. *Curr. Top. Microbiol. Immunol.* 321, 59–83. https://doi.org/10.1007/978-3-540-75203-5_3
- Patel, A.S., Karagas, M.R., Perry, A.E., Nelson, H.H., 2008. Exposure Profiles and Human Papillomavirus Infection in Skin Cancer: An Analysis of 25 Genus β -Types in a Population-Based Study. *J. Invest. Dermatol.* 128, 2888–2893. <https://doi.org/10.1038/jid.2008.162>
- Pickering, C.R., Zhou, J.H., Lee, J.J., Drummond, J.A., Peng, S.A., Saade, R.E., Tsai, K.Y., Curry, J.L., Tetzlaff, M.T., Lai, S.Y., Yu, J., Muzny, D.M., Doddapaneni, H., Shinbrot, E., Covington, K.R., Zhang, J., Seth, S., Caulin, C., Clayman, G.L., El-Naggar, A.K., Gibbs, R.A., Weber, R.S., Myers, J.N., Wheeler, D.A., Frederick, M.J., 2014. Mutational landscape of aggressive cutaneous squamous cell carcinoma. *Clin. Cancer Res. Off. J. Am. Assoc. Cancer Res.* 20, 6582–6592. <https://doi.org/10.1158/1078-0432.CCR-14-1768>

- Pópulo, H., Boaventura, P., Vinagre, J., Batista, R., Mendes, A., Caldas, R., Pardal, J., Azevedo, F., Honavar, M., Guimarães, I., Manuel Lopes, J., Sobrinho-Simões, M., Soares, P., 2014. TERT Promoter Mutations in Skin Cancer: The Effects of Sun Exposure and X-Irradiation. *J. Invest. Dermatol.* 134, 2251–2257. <https://doi.org/10.1038/jid.2014.163>
- Rollison, D.E., Viarisis, D., Amorrortu, R.P., Gheit, T., Tommasino, M., 2019. An Emerging Issue in Oncogenic Virology: the Role of Beta Human Papillomavirus Types in the Development of Cutaneous Squamous Cell Carcinoma. *J. Virol.* 93, e01003-18. <https://doi.org/10.1128/JVI.01003-18>
- Scott, G.A., Laughlin, T.S., Rothberg, P.G., 2014. Mutations of the *TERT* promoter are common in basal cell carcinoma and squamous cell carcinoma. *Mod. Pathol.* 27, 516–523. <https://doi.org/10.1038/modpathol.2013.167>
- Storchova, Z., Kuffer, C., 2008. The consequences of tetraploidy and aneuploidy. *J. Cell Sci.* 121, 3859–3866. <https://doi.org/10.1242/jcs.039537>
- Strickley, J.D., Messerschmidt, J.L., Awad, M.E., Li, T., Hasegawa, T., Ha, D.T., Nabeta, H.W., Bevins, P.A., Ngo, K.H., Asgari, M.M., Nazarian, R.M., Neel, V.A., Jenson, A.B., Joh, J., Demehri, S., 2019. Immunity to commensal papillomaviruses protects against skin cancer. *Nature* 575, 519–522. <https://doi.org/10.1038/s41586-019-1719-9>
- The Gene Ontology Resource: 20 years and still GOing strong, 2019. *Nucleic Acids Res.* 47, D330–D338. <https://doi.org/10.1093/nar/gky1055>
- Tommasino, M., 2017. The biology of beta human papillomaviruses. *Virus Res., Human Papillomaviruses* 231, 128–138. <https://doi.org/10.1016/j.virusres.2016.11.013>
- Uetake, Y., Sluder, G., 2004. Cell cycle progression after cleavage failure: mammalian somatic cells do not possess a “tetraploidy checkpoint.” *J. Cell Biol.* 165, 609–615. <https://doi.org/10.1083/jcb.200403014>
- Underbrink, M.P., Howie, H.L., Bedard, K.M., Koop, J.I., Galloway, D.A., 2008. E6 proteins from multiple human betapapillomavirus types degrade Bak and protect keratinocytes from apoptosis after UVB irradiation. *J. Virol.* 82, 10408–10417. <https://doi.org/10.1128/JVI.00902-08>
- Urquidí, V., Tarin, D., Goodison, S., 2000. Role of Telomerase in Cell Senescence and Oncogenesis. *Annu. Rev. Med.* 51, 65–79. <https://doi.org/10.1146/annurev.med.51.1.65>
- Viccorelli, S., Passos, J.F., 2017. Telomeres and Cell Senescence - Size Matters Not. *EBioMedicine* 21, 14–20. <https://doi.org/10.1016/j.ebiom.2017.03.027>
- Wallace, N.A., Robinson, K., Galloway, D.A., 2014. Beta Human Papillomavirus E6 Expression Inhibits Stabilization of p53 and Increases Tolerance of Genomic Instability. *J. Virol.* 88, 6112–6127. <https://doi.org/10.1128/JVI.03808-13>

- Wang, J., Dupuis, C., Tyring, S.K., Underbrink, M.P., 2016. Sterile α Motif Domain Containing 9 Is a Novel Cellular Interacting Partner to Low-Risk Type Human Papillomavirus E6 Proteins. *PLoS ONE* 11. <https://doi.org/10.1371/journal.pone.0149859>
- Weissenborn, S.J., De Koning, M.N.C., Wieland, U., Quint, W.G.V., Pfister, H.J., 2009. Intrafamilial transmission and family-specific spectra of cutaneous betapapillomaviruses. *J. Virol.* 83, 811–816. <https://doi.org/10.1128/JVI.01338-08>
- Weissenborn, S.J., Nindl, I., Purdie, K., Harwood, C., Proby, C., Breuer, J., Majewski, S., Pfister, H., Wieland, U., 2005. Human papillomavirus-DNA loads in actinic keratoses exceed those in non-melanoma skin cancers. *J. Invest. Dermatol.* 125, 93–97. <https://doi.org/10.1111/j.0022-202X.2005.23733.x>
- Wendel, S.O., Wallace, N.A., 2017. Loss of Genome Fidelity: Beta HPVs and the DNA Damage Response. *Front. Microbiol.* 8. <https://doi.org/10.3389/fmicb.2017.02250>
- White, E.A., Kramer, R.E., Tan, M.J.A., Hayes, S.D., Harper, J.W., Howley, P.M., 2012. Comprehensive Analysis of Host Cellular Interactions with Human Papillomavirus E6 Proteins Identifies New E6 Binding Partners and Reflects Viral Diversity. *J. Virol.* 86, 13174–13186. <https://doi.org/10.1128/JVI.02172-12>
- Winer, R.L., Gheit, T., Cherne, S., Lin, J., Stern, J.E., Poljak, M., Feng, Q., Tommasino, M., 2017. Prevalence and correlates of beta human papillomavirus detection in fingernail samples from mid-adult women. *Papillomavirus Res.* 5, 1–5. <https://doi.org/10.1016/j.pvr.2017.11.002>

Chapter 5 - Beta HPV8 E6 Induces Micronuclei Formation and Promotes Chromothripsis

Dalton Dacus¹, Steven Stancic², Sarah R. Pollina¹, Elizabeth Riforgiate¹, Rachel Palinski^{2,3},
Nicholas A. Wallace^{1*}

1 - Division of Biology, Kansas State University, Manhattan, KS

2 - Veterinary Diagnostic Laboratory, Kansas State University, Manhattan, KS

3 - Diagnostic Medicine/Pathobiology, Kansas State University, Manhattan, KS

* Denotes the corresponding author

Submitted as: Dacus D, Stancic S, Pollina SR, Riforgiate E, Palinski R, Wallace NA. 2022. Beta HPV8 E6 Induces Micronuclei Formation and Promotes Chromothripsis. *J Virol*

Abstract

Cutaneous beta genus human papillomaviruses (β -HPV) are suspected to promote the development of non-melanoma skin cancer (NMSC) by destabilizing the host genome. Multiple studies have established the genome destabilizing capacities of β -HPV proteins E6 and E7 as a co-factor with UV. However, the E6 protein from β -HPV8 (HPV8 E6) induces tumors in mice without UV exposure. Here, we examined a UV-independent mechanism of HPV8 E6-induced genome destabilization. We showed that HPV8 E6 reduced the abundance of anaphase bridge resolving helicase, Bloom syndrome protein (BLM). The diminished BLM was associated with increased segregation errors and micronuclei. These HPV8 E6-induced micronuclei had disordered micronuclear envelopes yet retained replication and transcription competence. HPV8 E6 decreased antiproliferative responses to micronuclei and time-lapse imaging revealed HPV8 E6 promoted cells with micronuclei to complete mitosis. Finally, whole genome sequencing revealed that HPV8 E6 induced chromothripsis in 9 chromosomes. These data provide insight into mechanisms by which HPV8 E6-induces genome instability independent of UV exposure.

Importance

Some beta genus human papillomaviruses (β -HPVs) may promote skin carcinogenesis by inducing mutations in the host genome. Supporting this, the E6 protein from β -HPV8 (8E6) promotes skin cancer in mice with or without UV exposure. Many mechanisms by which 8E6 increases mutations caused by UV have been elucidated, but less is known about how 8E6 induces mutations without UV. We address that knowledge gap by showing 8E6 causes mutations stemming from mitotic errors. Specifically, 8E6 reduces the abundance of BLM, a helicase that resolves and prevents anaphase bridges. This hinders anaphase bridge resolution and increases their frequency. 8E6 makes the micronuclei that can result from anaphase bridges

more common. These micronuclei often have disrupted envelopes yet retain localization of nuclear-trafficked proteins. 8E6 promotes the growth of cells with micronuclei and causes chromothripsis, a mutagenic process where hundreds to thousands of mutations occur in a chromosome.

Introduction

Non-melanoma skin cancer (NMSC) is the most prevalent type of cancer and more occurrences are noted each year (1–4). While not often deadly, the cost of treating NMSC in the United States alone is \$4.8 billion annually (5). Environmental factors play an outsized role in NMSC development, with UV exposure acknowledged as the main etiological agent (6). Age and immunosuppression also contribute (7, 8). An increase in risk associated with immunosuppression indicates that an infectious agent can promote NMSC (9). Among possible infectious agents, some members of the beta genus human papillomaviruses (β -HPV) are considered likely candidates because they promote NMSC development in people with a genetic disorder (epidermodysplasia verruciformis) or undergoing immunosuppressive therapy (10–12). However, the extent that β -HPV infections contribute to NMSC development in the general population is unclear.

The association between β -HPV infections and NMSC is supported by in vitro systems, epidemiological studies, and animal models (13–15). These data were most compelling for a subset of β -HPVs (HPV5, HPV8, and HPV38). They also demonstrated that β -HPV infections rarely persist. However, β -HPV viral loads peak early in NMSC development before becoming dramatically reduced in NMSC cells (16). These observations caused speculation that β -HPV infections introduce tumorigenic mutations that are capable of independently driving tumorigenesis without continued viral gene expression (17, 18). In vitro and in vivo studies have

shown that the E6 protein from HPV5, HPV8, and HPV38 hinder DNA repair after UV exposure, suggesting the hypothesized role of β -HPV in NMSC is feasible (19, 20). However, other studies have indicated a broader role for β -HPV proteins by showing HPV8 E6 (8 E6) causes tumors in mice without UV exposure (21–25). This suggests that 8 E6 can introduce genome destabilization without an exogenous stimulus.

Genome integrity is also at-risk during mitosis, as cellular DNA must be replicated and segregated faithfully to avoid mutations. We have shown that 8 E6 attenuates cellular responses that protect genome integrity during mitosis and increases the frequency of aneuploidy (26–28). Aneuploidy results from the unequal segregation of chromosomes suggest that 8 E6 may cause other types of genome instability caused by segregation errors. Micronuclei are one type of destabilization associated with segregation errors. These small enveloped extra-nuclear structures can form when a chromosome gets caught between the nuclei of forming daughter cells in a structure known as an anaphase bridge (29–31). Mutations in micronuclear DNA is common because micronuclear envelopes are unstable which limits the ability to localize cellular factors necessary for replication, transcription, nuclear protein localization, and DNA repair (32–34). It is further mutagenic for a cell to enter mitosis with unrepaired micronuclear DNA. When this occurs, the micronuclear DNA is prone to undergo chromothripsis, where hundreds to thousands of clustered mutations occur over a single cell cycle (35–39). If 8 E6 promotes chromothripsis, it would provide a plausible mechanism by which β -HPV infections as brief as one cell cycle could cause enough mutations to drive NMSC development. Notably, chromothripsis-like events have been identified in NMSCs although there was no attempt to determine if they were caused by a β -HPV infection (40, 41).

Here, we show that 8 E6 hinders chromosomes segregation causing increases in anaphase bridge formation and impeding their resolution. We link this increase to a reduction of Bloom syndrome protein (BLM) and a reduced ability to localize to anaphase bridges. BLM helicase prevents anaphase bridge formation and is critical for their resolution (42, 43). Mechanistically, we provide evidence that the reduction in BLM is the result of reduced ATR-Chk1 kinase activity that stabilizes BLM by blocking cullin-3-mediated degradation (44). These data expand the significance of previous work demonstrating that 8 E6 reduces ATR-Chk1 activation (45–47). Although only a partial decrease in BLM abundance, we identified a significant impact from the BLM reduction as 8 E6 increases the frequency of segregation errors and micronuclei. We go on to characterize these micronuclei, showing that they are more likely to have disordered micronuclear envelopes and that 8 E6 makes it less likely that a cell undergoes antiproliferative responses to micronuclei (i.e., p53 accumulation, caspase activation, and senescence). 8 E6 also increases the frequency that cells with micronuclei undergo mitosis. Finally, we use whole-genome sequencing to demonstrate that 8 E6 causes chromothripsis.

Results

p300-dependent BLM reduction correlates with loss of ATR and Chk1 abundance.

Because HPV8 E6 (8 E6) reduces activation of the ATR-Chk1 signaling pathway that facilitates BLM stabilization, we hypothesized that 8 E6 decreased BLM abundance (45–47). To evaluate this, we compared BLM abundance in vector control (iHFK LXS_N) and HA-tagged 8 E6 expressing (iHFK 8 E6) hTERT-immortalized keratinocytes cells. 8 E6 expression was confirmed by probing for the HA-tag (**Fig. S5.1A**). As expected, 8 E6 reduced ATR-Chk1 signaling (**Fig. 5.1A**). Consistent with our hypothesis, 8 E6 also decreased BLM abundance. To determine if the reduced BLM required TERT immortalization, we repeated this experiment in

primary foreskin keratinocyte cells (HFK LXS_N and HFK 8 E6). Expression of 8 E6 in these cells was previously confirmed (27). We also detected p300 by immunoblot as further confirmation of 8 E6 expression (**Fig. S5.1B**). Examination of these cell lines demonstrated that the reduction in BLM levels did not require TERT immortalization (**Fig. 5.1B**). Further, these cell lines were from different donors indicating that the phenotype is conserved in at least two genetic backgrounds. We take this approach of dual confirmation throughout this manuscript with the goal of similarly probing the requirement of TERT immortalization and the conservation of phenotypes between donors.

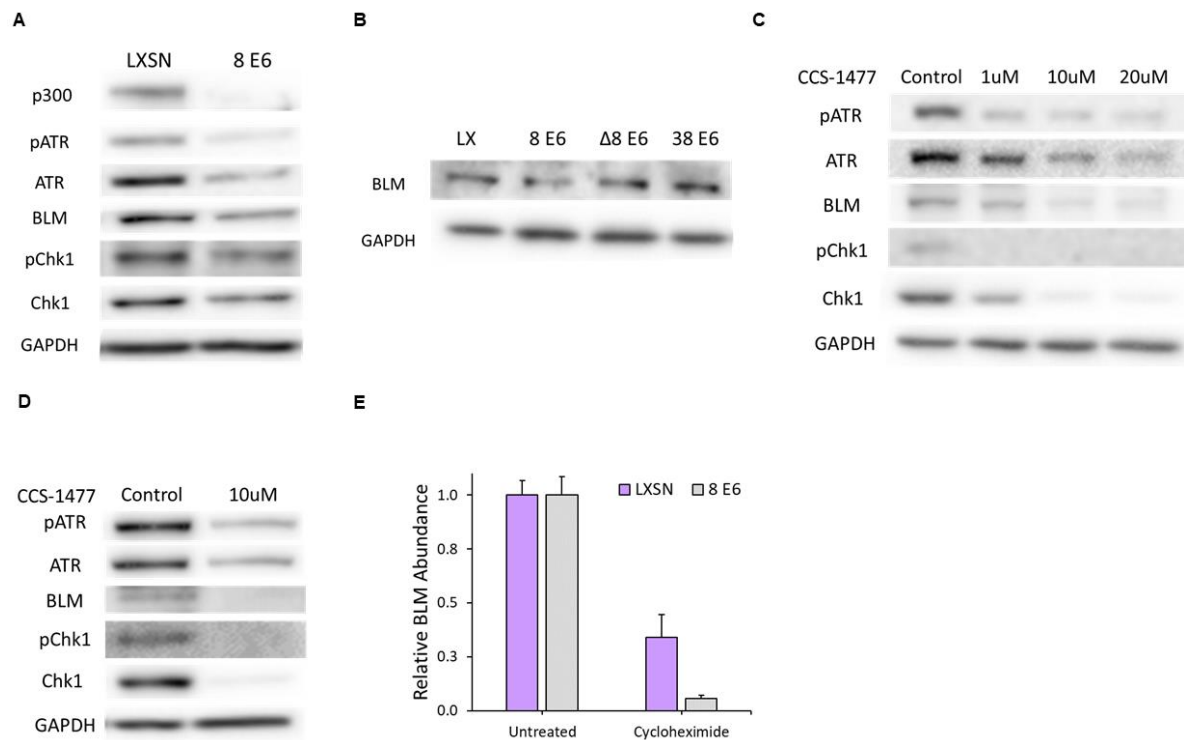


Figure 5.1. HPV8 E6 reduces BLM abundance.

(A) Immunoblots of whole cell lysates from iHFK cells expressing LXS_N and 8 E6. (B) Immunoblots of whole cell lysates HFK cells expressing LXS_N and the indicated E6 genes (C) Immunoblots of whole cell lysates from iHFK LXS_N cells treated with increasing amounts of CCS-1477 for 24 hrs. (D) Immunoblot of whole cell lysates from HFK LXS_N cells following 24 hr CCS-1477 treatment. (E) Densitometry of in iHFK LXS_N and iHFK 8 E6 cells treated 50

$\mu\text{g/ml}$ cycloheximide for 30 hrs. The graph depicts the mean \pm standard error of the mean from three independent experiments. Immunoblots are representative of at least three independent experiments. In $\Delta 8$ E6, residues 132 to 136 were deleted from 8 E6.

8 E6 disrupts ATR-Chk1 signaling by binding and destabilizing p300 (47), leading us to hypothesize that 8 E6 decreased BLM levels by binding p300. To test this hypothesis, we determined whether the residues responsible for p300 binding were required for 8E6 to reduce BLM abundance by expressing a mutant 8 E6 without the p300 binding site (HFK 8 E6 $\Delta 132$ -136) in primary human foreskin keratinocytes. Expression of this mutated 8 E6 in these cells was validated previously, but could not be confirmed by immunoblotting for p300 as HFK 8 E6 $\Delta 132$ -136 does not degrade p300 (27). BLM levels were not significantly reduced in HFK 8 E6 $\Delta 132$ -136 cells compared to HFK LXS cells. To further probe the role of p300 binding in BLM reduction, we expressed HPV38 E6 in primary foreskin keratinocytes (HFK 38 E6). Expression of 38 E6 in these cells has also been confirmed and is not amenable to indirect validation by detecting p300 as 38 E6 weakly binds p300 and does not destabilize p300 (27, 48). Consistent with the requirement for robust binding a p300, 38 E6 also did not reduce BLM abundance (**Fig. 5.1B**). Deletion of the p300 binding domain disrupts other functions of 8 E6 (23), so we verified the requirement of p300 for optimal BLM abundance by treating iHFK LXS cells with a small molecule inhibitor of p300 (CCS-1477; (49)). CCS-1477 reduced BLM and ATR-CHK1 activation in a dose-dependent manner (**Fig. 5.1C**; (47)). CCS-1477 similarly reduced BLM abundance and ATR-Chk1 signaling in HFK cells (**Fig. 5.1D**). Because Chk1 increases BLM abundance by stabilizing the protein, we hypothesized that 8 E6 decreased BLM stability. To test this, we determine the impact of cycloheximide (protein synthesis inhibitor) on BLM abundance in iHFK LXS and iHFK 8 E6 cells. Cycloheximide resulted in a greater reduction in BLM

abundance in iHFK 8 E6 cells compared to iHFK LXS cells, consistent with our hypothesis (Fig. 5.1E). However, the difference did not reach statistical significance ($p=0.11$).

8 E6 reduces BLM at anaphase bridges increasing unresolved bridge frequency

Because BLM is required for faithful chromosome segregation (42–44), we hypothesized that 8 E6 increased the frequency of segregation errors. To test this, iHFK cells were synchronized by thymidine block and released to enrich for cells in anaphase. Then, we used immunofluorescent microscopy to identify anaphase cells and determine if they had segregation errors. When identified, segregation errors were grouped into established categories. CENP-A, a centromere marker, was used to distinguish between acentric and lagging chromosomes (Fig. 5.2A). 8 E6 increased the frequency of segregation errors in general and anaphase bridges more specifically (Fig. 5.2B). To determine if 8 E6 reduced the amount of BLM that localized to these bridges, we compared BLM staining intensity at chromatin bridges between iHFK LXS and iHFK 8 E6 cells (Fig. 5.2C). 8 E6 decreased BLM staining at chromatin bridges (Fig. 5.2D). Because BLM is required for anaphase bridge resolution, we hypothesized that 8 E6 increased the time it takes to resolve anaphase bridges. To test this, we compared anaphase bridge duration by time-lapse imaging between iHFK LXS and iHFK 8 E6 cells expressing a mCherry-tagged H2B for DNA visualization (Movie S1, S2, and Fig. S5.2A). Anaphase bridges were more persistent in iHFK 8 E6 cells with one bridge lasting the duration of the observed 30 hours (Fig. 5.2E). However, difficulty in observing these rare events by time-lapse imaging prevented us from collecting enough data to establish statistical significance ($p=0.36$).

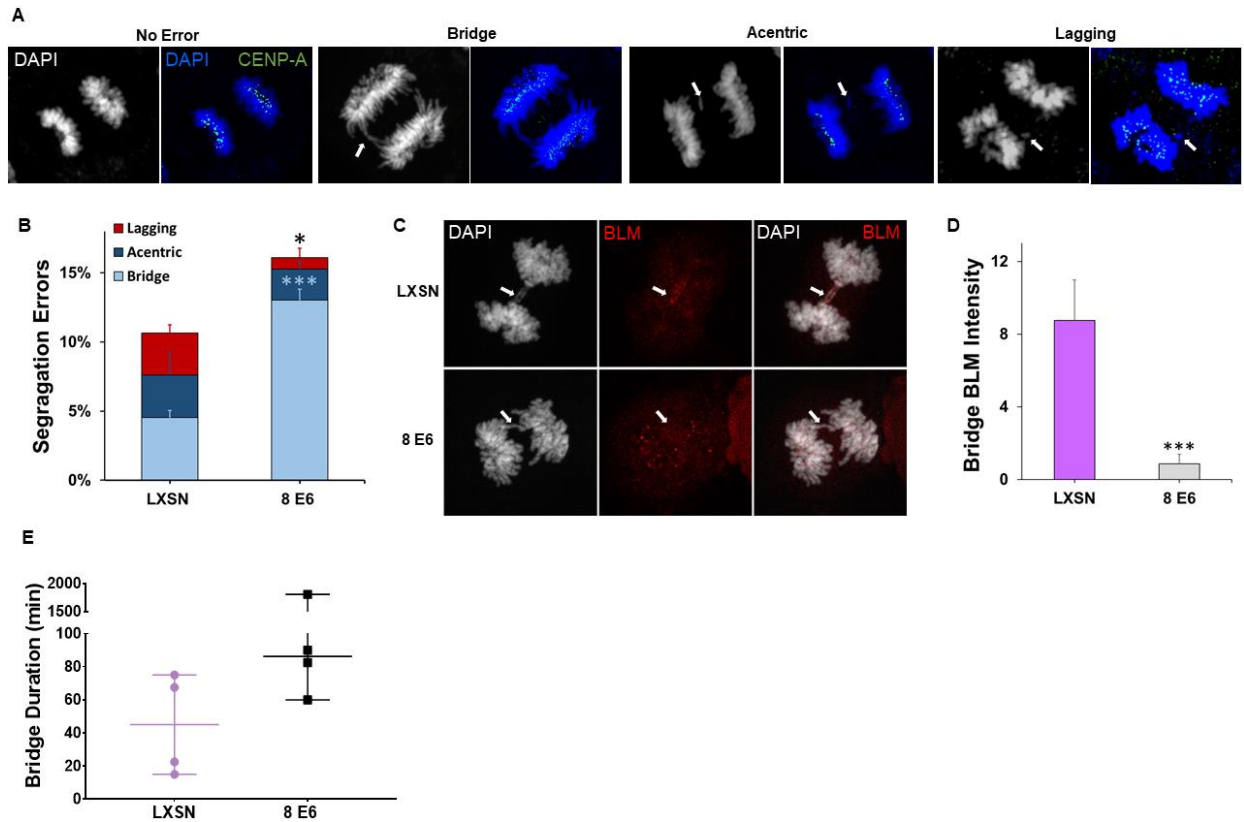


Figure 5.2. HPV8 E6 augments segregation error rate independent of p300.

(A) Images of iHFK cells displaying anaphases with no error (left), a chromatin bridge (left middle), acentric DNA (right middle), and a lagging chromosome (right) stained with DAPI (white and blue) and CENP-A (green); each indicated by arrows. (B) Quantification of segregation errors in iHFK cells after synchronization by thymidine block and released to enrich for mitotic cells. $n =$ at least 221 micronuclei from three experiments. (C) Representative images of BLM (red) localization to chromatin bridges stained with DAPI (white) in iHFK LXSN and 8 E6 cells. Arrows indicate the location of anaphase bridge (D) Mean intensity of BLM staining at chromatin bridges in iHFK LXSN and 8 E6 cells after being synchronized by thymidine block and released to enrich for mitotic cells. $n =$ at least 39 bridges from three experiments. (E) Quantification of time-lapse anaphase bridge duration in iHFK cells. $n = 4$ across three independent experiments. Graphs (B&D) depict mean \pm standard error of the mean from three independent experiments except. Graph E depicts the median with a 95% confidence interval from three independent experiments. Asterisks denote significant differences relative to LXSN. * = $p \leq 0.05$ and *** = $p \leq 0.001$ (Student's t -test).

8 E6 increases micronuclei frequency, in part through BLM reduction.

Because segregation errors associated with reduced BLM availability can result in the formation of micronuclei (37, 50–53), we hypothesized that 8 E6 expression increased the frequency of micronuclei. To test this, micronuclei were identified using immunofluorescence microscopy (**Fig. 5.3A**). Micronuclei were more common in both HFK 8 E6 and iHFK 8 E6 cells compared with their LXS cells counterparts (**Fig. 5.3B and 3C**). To provide mechanistic insight, we examined the p300 dependence of the increase in micronuclei. Compared to HFK LXS cells, both HFK 8 E6 Δ 132-136 and HFK 38 E6 cells had a higher frequency of micronuclei. However, micronuclei were significantly more common in HFK 8 E6 compared to HFK 8 E6 Δ 132-136 cells.

To determine the extent that reduced BLM abundance contributed to the elevated frequency of micronuclei, we exogenously expressed a GFP-tagged BLM or GFP alone (transfection control) in U2OS 8 E6 cells. We were unable to test the BLM-dependence of 8 E6-induced micronuclei formation in HFK or iHFK cells as these cell lines were not amenable to BLM transfection. We also confirmed the ability of 8 E6 to increase the prevalence of micronuclei in these cells (**Fig. S5.3A**). Cells were fixed 72 hours post-transfection and DAPI stained to detect micronuclei. This allowed the exogenous BLM to be expressed as cells pass through mitosis 1 to 3 times. We only examined cells expressing GFP to ensure that only transfected cells were considered. Exogenous GFP-BLM expression reduced the frequency of micronuclei in U2OS 8 E6 cells (**Fig. 5.3D**).

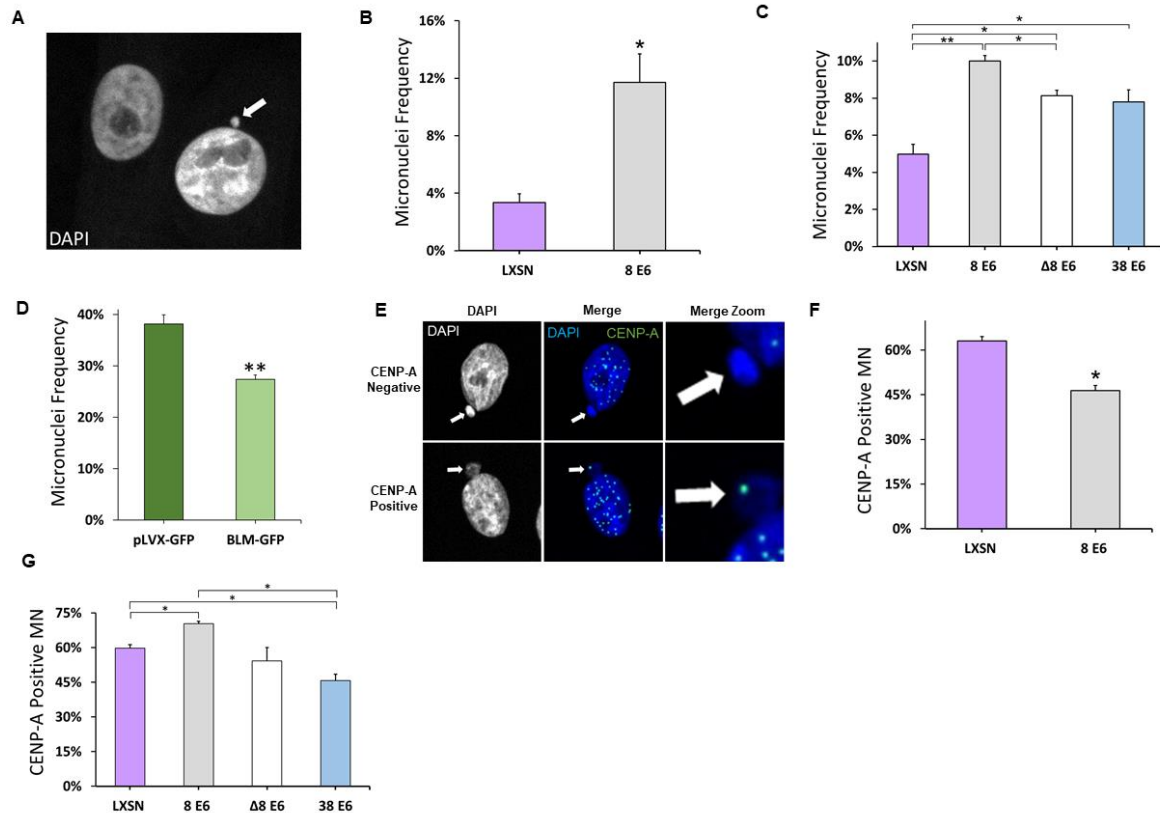


Figure 5.3. HPV8 E6 increases micronuclei frequency.

(A) Representative images of DAPI (white) stained HFK cells, one with (indicated by arrow) and one without a micronucleus. Micronuclei frequency of (B) iHFK and (C) HFK cells. (D) Micronuclei frequency of U2OS 8 E6 cells 72 hours post-transfection with BLM-GFP and pLVX-GFP. >150 cells/cell line were quantified for micronuclei frequency across three independent experiments. (E) Representative images of CENP-A-positive and -negative micronuclei (indicated by arrows) stained for DAPI (white and blue) and CENP-A (green). Percentage of micronuclei with at least one CENP-A foci in (F) iHFK and (G) HFK LXSN and β -HPV E6 cells. At least 250 micronuclei/cell line were quantified for CENP-A frequency across three independent experiments. Graphs depict mean \pm standard error of the mean; $n \geq 3$. Asterisks denote significant difference relative to LXSN unless specified with a bar. * = $p \leq 0.05$ and ** = $p \leq 0.01$ (Student's *t*-test). In $\Delta 8$ E6, residues 132 to 136 were deleted from 8 E6.

Micronuclei contain either whole (centric) or partial (acentric) chromosomes depending on how they form (54–57). Unrepaired DSBs lead to smaller acentric micronuclei (58), whereas

segregation errors result in larger centric micronuclei (59, 60). Our group and others have shown that 8 E6 attenuates DSB repair (19). Here, we demonstrate that 8 E6 can cause segregation errors (**Fig. 5.2B**). Therefore, we hypothesize 8 E6 caused both acentric and centric micronuclei. To test this we probed for CENP-A, a widely used marker for centric micronuclei, by immunofluorescence microscopy (61). 8 E6 caused acentric and centric micronuclei in iHFK and HFK cells (**Fig. 5.3E-G**). Micronuclei produced by 8 E6 were on average significantly smaller than vector control (**Fig. S5.4A**). This, along with 8 E6 micronuclei containing a DSB marker (γ H2AX) are consistent with some of these micronuclei forming because of impaired DSB repair (**Fig. S5.4B and S5.4C**).

8 E6 reduces Lamin B1 integrity of micronuclei

Anaphase bridges tend to produce micronuclei lacking micronuclear envelope integrity (62). Therefore, we hypothesized that 8 E6-induced micronuclei would more frequently have unstable micronuclear envelopes. To evaluate micronuclear envelope integrity, we used immunofluorescent microscopy to group micronuclei based on Lamin B1 morphology into established categories (32). First, micronuclei were placed into two large groups based on whether Lamin B1 staining displayed clear peripheral localization around the micronucleus (intact) or not (disordered). Micronuclei with intact membranes were further segregated based on whether they had a continuous (no holes) or discontinuous (one or more holes) nuclear Lamin B1 staining (**Fig. 5.4A**; top two panels). Micronuclei with disordered micronuclear membranes were also further split based on whether nuclear Lamin B1 staining appeared collapsed or was absent (**Fig. 5.4A**; bottom two panels). The ratio of intact to disordered micronuclear membranes in iHFK LXSN cells were similar to prior reports in other cell lines (**Fig. 5.4B**) (32, 63). In contrast, micronuclear membranes in iHFK 8 E6 cells were more often disordered, with a specific

increase in micronuclei without a membrane (**Fig. 5.4B**). Disordered membranes typically prevent nuclear factors from being imported from the cytoplasm (32, 51, 64). To characterize the impact of micronuclear membrane integrity on the localization of nuclear proteins, we generated iHFK LXSN and iHFK 8 E6 cells that stably expressed a fusion gene consisting of two RFP proteins and a nuclear localization signal (RFP-NLS). We examined Lamin B1 morphology and RFP staining in these cells and found RFP localized to micronuclei with intact envelopes (**Fig. 5.4C**). 8 E6 increased the proportion of RFP-positive micronuclei with discontinuous envelopes. This suggests 8 E6 disrupts envelope integrity but retains loss of nuclear localization when the envelope becomes disordered.

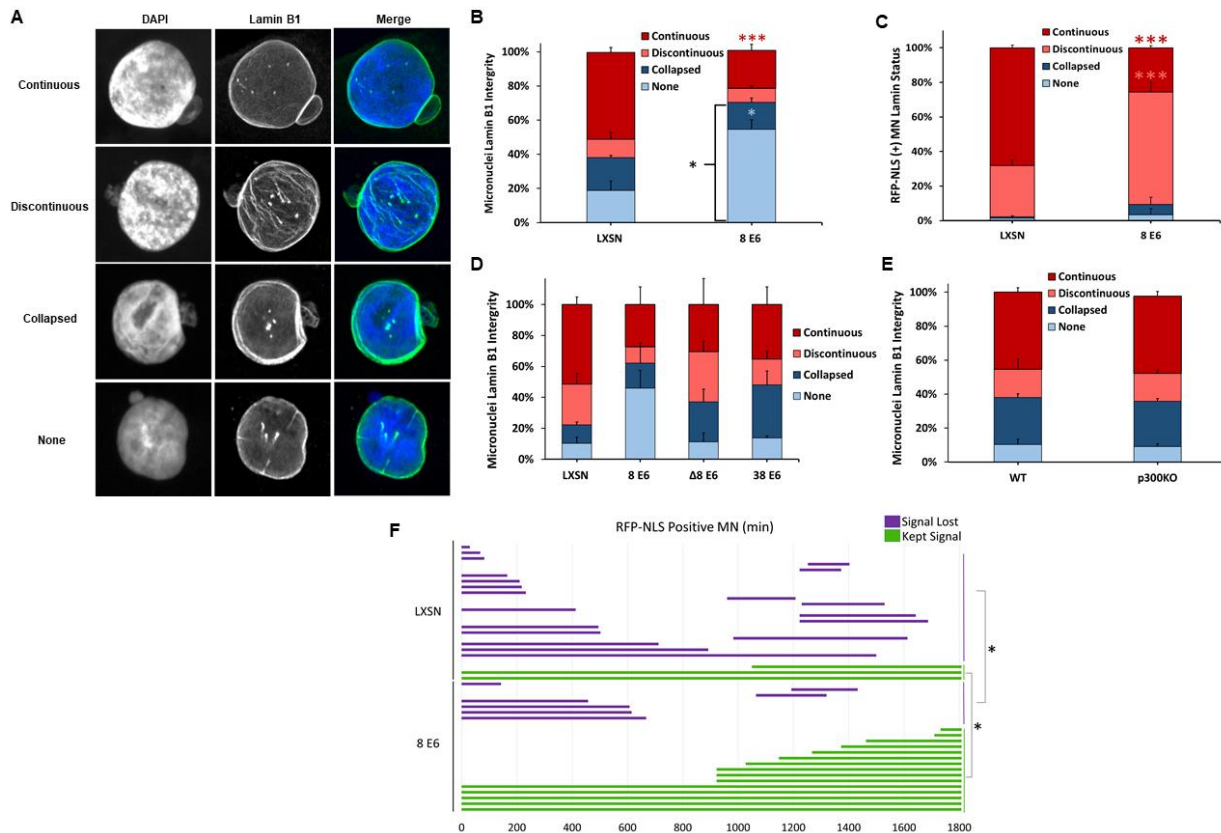


Figure 5.4. HPV8 E6 reduces Lamin B1 integrity of micronuclei.

(A) Representative images of cells with intact (continuous and discontinuous) and disordered (collapsed and none) micronuclear envelopes. DNA is stained with DAPI (blue) and nuclear

membranes were detected with antibodies against Lamin B1 (green). (B) Quantification of Lamin B1 micronuclear morphology in asynchronous iHFK cells. $n \geq 234$ micronuclei from three independent experiments. (C) Quantification of RFP-NLS-positive micronuclei segregated by micronuclear morphology (as determined by Lamin B1 staining) in iHFK cells. (D) Quantification of Lamin B1 micronuclear morphology in asynchronous HFK cells. $n =$ at least 146 micronuclei from three experiments. Same as (B) but in HCT 116 cells. Quantification of Lamin B1 micronuclear morphology in asynchronous iHFK cells. $n \geq 200$ micronuclei from three independent experiments. (F) Length of time (min) in which RFP-NLS-positive micronuclei in iHFK RFP-NLS cells persisted for 30 hours. Red, salmon, and blue asterisks denote a significant difference from LXS_N in respect to continuous, discontinuous, and none Lamin B1 morphologies, respectively. Graphs depict the mean \pm standard error of the mean from three independent experiments. Asterisks denote significant differences relative to LXS_N. * = $p \leq 0.05$ and *** = $p \leq 0.001$ (Student's *t*-test). In $\Delta 8$ E6, residues 132 to 136 were deleted from 8 E6.

To determine if 8 E6 could reduce micronuclear membrane stability in HFK cells, we examined micronuclear members by immunofluorescence microscopy. While not statistically significant ($p=0.079$), these data were similar to the observations in iHFK cells (**Fig. 5.D**). To determine the extent that p300 destabilization contributed to this phenotype, we compared membrane integrity between HFK 8 E6, HFK 8 E6 $\Delta 132-136$, and HFK 38 E6 cells, but they did not demonstrate a role for p300. The frequency of micronuclei without membranes in these cells were like the frequency in HFK LXS_N (**Fig. 5.4D**). However, the prevalence of collapsed micronuclear membranes was elevated in HFK 8 E6 $\Delta 132-136$, and HFK 38 E6 cells. These differences did not reach statistical significance. We also did not find a difference in micronuclear envelope integrity when comparing HCT 116 cells with or without p300 (**Fig. 5.4E**). Thus, we were unable to draw a conclusion about the role of p300 destabilization in 8 E6-mediated disruption of micronuclear membranes.

Notably, 8 E6 increased the frequency of RFP-NLS-positive micronuclei with discontinuous envelopes, but there was negligible RFP in micronuclei with disordered envelopes (**Fig. 5.4C**). Because discontinuous micronuclear envelopes are prone to become disordered with time (25), we hypothesized that 8 E6 increased the chance that cells lost nuclear RFP localization over time. To test this, we used time-lapse imaging to track RFP-NLS status of micronuclei (retained or lost) for 30 hours in iHFK LXS_N and 8 E6 cells (**Movie S3 and S4**). Instead, 8 E6 increased the retention of nuclear localization (**Fig. 5.4F**). Together, these data indicate that 8 E6 promotes nuclear localization despite more frequently having damaged micronuclear envelopes.

8 E6 promotes some nuclear function despite disrupted micronuclear envelopes

Membrane integrity is critical for the localization of proteins involved in nuclear functions (replication, transcription, and DNA damage repair). Failure to localize nuclear factors to micronuclei increases the likelihood that micronuclei contain damaged DNA (32, 51, 65). We used immunofluorescence microscopy to characterize these processes in the micronuclei of HFK LXS_N and HFK 8 E6 cells. We first evaluated active transcription and replication in these micronuclei using histone H3 acetylated at K27 (H3K27ac) and BrdU incorporation as respective markers. Consistent with previous results (32), transcription and replication were reduced in micronuclei with disordered membranes in HFK LXS_N cells (**Fig. 5.5A and 5.5B**, and **Fig. S 5.5A and S5.5B**). 8 E6 did not cause robust changes in transcription or replication in micronuclei with intact membranes. However, 8 E6 allowed both replication and transcription to occur significantly more frequently in micronuclei without envelopes. To evaluate the DDR in micronuclei, we exposed cells to a radiomimetic (zeocin) and assessed the formation of DSB repair foci (53bp1). Consistent with previous reports (32, 33) we found the DDR response is

attenuated in micronuclei with disordered envelopes in HFK LXS_N and HFK 8 E6 cells (**Fig. 5.5C** and **Fig. S5.5C**).

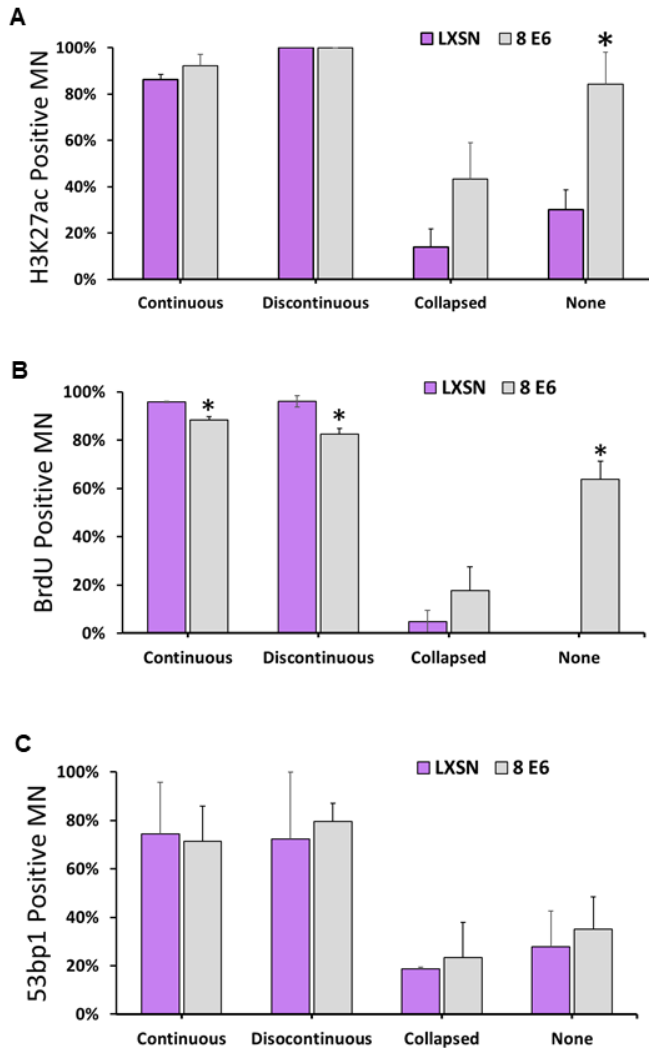


Figure 5.5. Some micronuclear functions changed by HPV8 E6.

Frequency of iHFK cells with (A) acetylated H3K27-positive, (B) 53bp1-positive, and (C) BrdU-positive micronuclei. At least 150 micronuclei/cell line were quantified across three independent experiments. Graphs depict mean \pm standard error of the mean; Asterisks denotes significant difference relative to LXS_N. * = $p \leq 0.05$ (Student's *t*-test). Micronuclei is abbreviated as MN.

8 E6 reduces apoptosis and senescence in response to micronuclei

Micronuclei induce apoptosis and senescence (66, 67). Because HPV replication requires cellular proliferation, we hypothesized that 8 E6 and 38 E6 impeded apoptosis and senescence in response to micronuclei. As p53 can facilitate these responses, we compared p53 staining intensity in HFK LXS_N, HFK 8 E6, HFK 8 E6 Δ 132-136, and HFK 38 E6 cells that did and did not have micronuclei (**Fig. 5.6A**). The presence of a micronucleus similarly increased p53 staining intensity in HFK LXS_N, HFK 8 E6, and HFK 8 E6 Δ 132-136 cells (**Fig. 5.6B**). HFK 38 E6 cells had significantly increased p53 intensity compared to all other HFK cells.

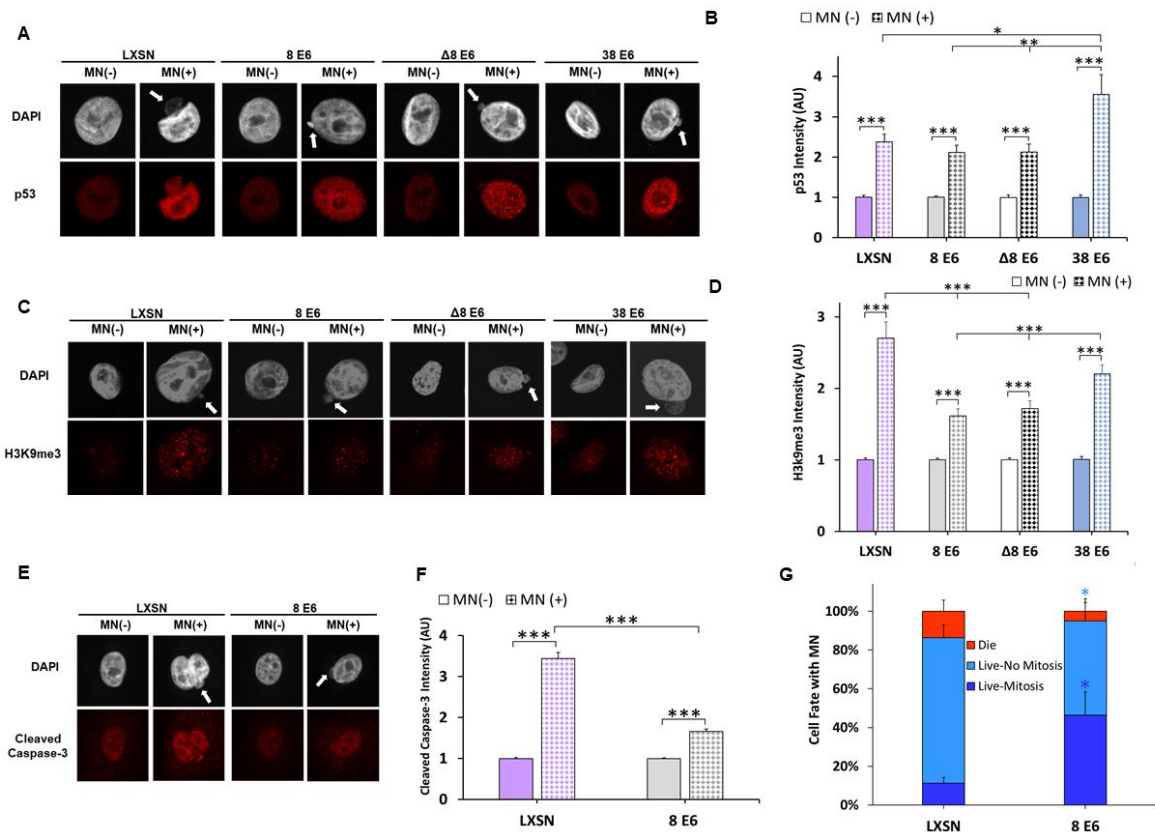


Figure 5.6. HPV8 E6 reduces a cell's apoptotic and senescent response to micronuclei. (A) Representative images of HFK cells stained for p53 (red) and DNA (DAPI, white) with (indicated by white arrow) and without a micronucleus. (B) Quantification of normalized p53 intensity in HFK cells with and without micronuclei. (C) Representative images of methylated

H3K9- (red) and DAPI (white)-stained HFK cells with (indicated by white arrow) and without a micronucleus. (D) Quantification of normalized methylated H3k9 intensity in HFK cells with and without micronuclei. At least 200 cells/cell line were quantified across three independent experiments. (E) Representative images of HFK cells stained for cleaved caspase-3- (red) and DAP (white) with (indicated by white arrow) and without a micronucleus. (F) Quantification of normalized cleaved caspase 3 intensity in iHFK cells with and without micronuclei. ≥ 550 cells/cell line were quantified across 4 independent experiments. (G) Quantification of cell fate imaging micronuclei-positive iHFK LaminB1-GFP H2B-RFP cells for 30 hrs. Light and dark blue asterisks denote a significant difference between 'Live-no mitosis' and 'Live-mitosis' to LXSNS, respectively. Graphs depict mean \pm standard error of the mean; Asterisks denotes significant difference relative to LXSNS unless specified with a bar. * = $p \leq 0.05$ and ** = $p \leq 0.01$ (Student's *t*-test). In $\Delta 8$ E6, residues 132 to 136 were deleted from 8 E6. Micronuclei is abbreviated as MN.

We next used similar approaches to examine markers of senescence (histone H3 methylated at K9; H3K9me3) and apoptosis (cleaved caspase-3). H3K9me3 staining intensity was increased by micronuclei in all cell lines (**Fig. 5.6D**). However, this increase was significantly reduced in HFK 8 E6 and HFK 8 E6 $\Delta 132-136$ cells compared to HFK LXSNS cells (**Fig. 5.6C-D**). H3K9me3 staining in HFK 38 E6 cells more closely resembled the intensity found in HFK LXSNS cells. Cleaved caspase-3 staining was likewise elevated in all iHFK cell lines with micronuclei (**Fig. 5.6E-F**). However, 8 E6 significantly attenuated the increase in cleaved caspase-3 staining in cells with micronuclei (**Fig. 5.6E-F**). Because 8 E6 attenuates the accumulation of apoptosis and senescent markers in cells with micronuclei, we hypothesized that 8 E6 increased the frequency that cells with micronuclei underwent mitosis. To test this, we transduced LXSNS and 8E6 iHFK cells with mCherry-tagged histone H2B to visualize DNA and used time-lapse imaging to track the fate of cells with micronuclei over 30 hours. 8 E6 made it

significantly more likely that a cell with a micronucleus completed mitosis (**Fig. 5.6G** and **Movie S5-6**).

8 E6 promotes chromothripsis events

Micronuclear DNA is at risk of chromothripsis if the cell containing them completes mitosis (34, 36, 39). Because 8 E6 increases the frequency of micronuclei and promotes proliferation (**Fig 5.3B and 5.6G**), we hypothesized that 8 E6 caused chromothripsis. To detect chromothripsis, we performed whole genome sequencing on passaged-matched iHFK LXS and 8 E6 cells. Raw reads were trimmed for quality and analyzed using a standard pipeline, using the vector mutations as a control (Methods, **Fig. S5.6**). Shatterseek software (68) was used to determine chromothripsis by analyzing copy number changes (CN) and structural variant (SV) differences between cell lines. We identified 9 chromosomes with chromothripsis mutations and 7 others with high numbers of structural variants (**Fig. 5.7A-B**). Significant instability was not found in eight other chromosomes. We found smaller chromosomes were less likely to have instability following mitosis, however, did have an observed decrease in copy number changes and an increase in structural variants per nucleotide (**Fig 5.7C**).

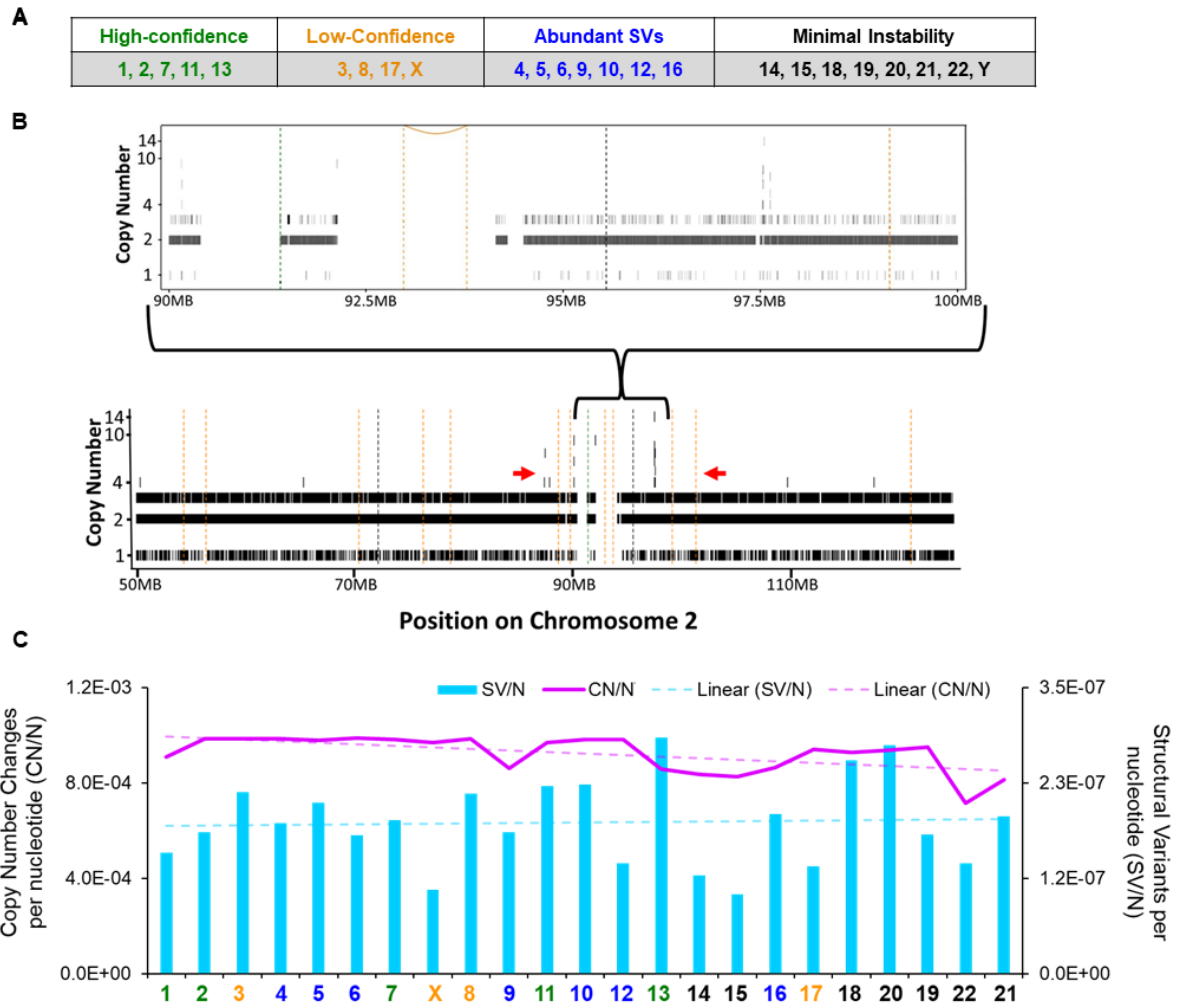


Figure 5.7. HPV8 E6 promotes non-canonical chromothripsis.

(A) Table summarizing the chromothripsis status of iHFK 8 E6 chromosomes analyzed when compared to iHFK LXSIN (vector-control) chromosomes. (B) Chromothripsis analysis from chromosome 2. Vertical hashed bars show deletion-like events (orange), head-to-head inversions (black), and tail-to-tail inversions (green). Copy number (CN) variations are indicated by solid black bars ranging from 1-14. The red arrows denote an area with Shatterseek-defined chromothripsis. (C) Total copy number variations per nucleotide (CN/N) and structural variants per nucleotide (SV/N) per chromosome in iHFK 8 E6 cells. The purple line represents CN/N and the blue bars represent SV/N. Chromosome color corresponds to chromothripsis status from.

Discussion

β -HPV research often focuses on the ability of the β -HPV proteins to facilitate the accumulation of UV-induced mutations (69, 70). However, a growing body of evidence has demonstrated 8 E6 also hinders genome integrity independent of UV exposure (26–28). In this study, we show 8 E6 causes anaphase bridges by reducing BLM abundance. (**Fig. 5.1-2**). In turn, this leads to an increased frequency of micronuclei (**Fig. 5.3**). These micronuclei are less likely to have intact membranes, but surprisingly retain the localization of nuclear proteins and processes (**Fig. 5.4-5**). 8 E6 attenuates the antiproliferative responses that typically accompany the micronuclei that it causes which allow cells to complete mitosis (**Fig. 5.6**). Our whole genome sequencing data suggest that culminates in significant genome destabilization in the form of chromothripsis (**Fig. 5.7**).

Among HPVs, HPV8 is not alone in its ability to induce genomic instability in association with mitotic defects and micronuclei. In fact, this capability spans across two HPV genera (alpha and beta) (71, 72). The E6 oncoprotein from the alpha genus human papillomavirus 16 (HPV16 E6) also promotes micronuclei and anaphase bridges (73, 74). Micronuclei are also associated with alpha HPV oncogene expression in human tissues, where they can distinguish between HPV-positive and HPV-negative tumors (75, 76). HPV16 oncoprotein E7 (HPV16 E7) exacerbates HPV16 E6-induced anaphase bridges and micronuclei (73, 74, 77). Notably, the combined expression of HPV38 E6 and E7 has previously been shown to promote genomic instability associated with increased anaphase bridges (71). Our data show that HPV38 E6 can increase the frequency of micronuclei without E7 (**Fig. 5.3C**). This is consistent with other published data that demonstrate multiple β -HPV E6s can extensively alter the cellular environment without co-expression of their corresponding E7s (19, 69). While the

ability of HPV16 E6/E7 and HPV38 E6/E7 to increase chromosomal instability and anaphase bridge prevalence is impaired by telomerase expression, we show that the ability of 8 E6 to cause similar phenotypes was not altered by telomerase expression (71, 73). It is unclear whether the differences should be attributed to the lack of 8 E7 in our experimental system or whether they represent differences in 8 E6 and other HPV E6s.

Albeit via differing mechanisms, a common phenotype between HPV16, HPV38 and HPV8 are their capacities to promote cell proliferation despite inhibitory stimuli from the cell (23, 78, 79). This is likely an evolutionarily conserved phenotype due to the requirement that host cells remain proliferatively active for the completion of HPV's lifecycle. Micronuclei can trigger these inhibitory stimuli, resulting in apoptosis and senescence (80–82). To the best of our knowledge, how HFKs respond to micronuclei had not yet been determined. We show that micronuclei (or the damage associated with them) elicit apoptotic and senescent responses in vector control keratinocytes (**Fig. 5.6**). HPV8 E6 attenuates cellular responses to micronuclei, promoting entry and completion of mitosis (**Fig. 5.6G**). This is notable because completion of mitosis greatly increases the risk of chromothripsis (36, 39). If a second mitosis occurs, the chromatin trapped inside the micronucleus often becomes missegregated, resulting in further anaphase bridges and/or micronuclei (83, 84).

The increases in micronuclei and chromothripsis are likely caused by 8 E6-mediated reductions in BLM. BLM mutations cause a predisposition to cancer (85). BLM is an essential genome stabilizer due to its regulation of DNA recombination, replication, and both homologous and non-homologous double-strand break repair pathways (86). We hypothesize that the 8 E6-induced BLM reduction results in yet unreported defects in DNA repair. This could include increased sister chromatid intertwines that result in the anaphase bridges reported here. Another

interesting observation from this work is the ability of 8 E6 to promote replication and transcription in micronuclei without envelopes. Whether 8 E6 is actively involved in recruiting nuclear factors or causes this localization indirectly is unclear.

Our whole genome sequencing analysis is the first to directly compare two passage-matched hTERT-immortalized primary cells lines. This is important because we can directly compare and describe the genomic changes following HPV8 E6 exposure. This approach could improve the existing knowledge of HPV16-induced chromothripsis (72) or of mutations that promote chromothripsis. Finally, when compared to previous chromothripsis reports, the frequency of copy number oscillations with 8 E6 expression is higher, and the changed fragment sizes are smaller (68, 87). This observation suggests either the use of immortalized primary cells lines coupled with the matched passages changes the landscape of chromothripsis calling during analysis and/or tumors caused by HPV8 infection have a distinct mutation pattern.

Further, comparisons between passage-matched non-immortalized primary cell lines are needed to determine the extent that hTERT immortalization is required for 8 E6 to induce chromothripsis. There are other remaining questions as well. Is p300 degradation required for 8 E6 to cause chromothripsis? Do other β -HPV E6s cause chromothripsis? Are the unusual copy number oscillations found in NMSCs?

Material and Methods

Cell culture

U2OS and HCT 116 cells were maintained in Dulbecco modified Eagle medium (DMEM) supplemented with 10% fetal bovine serum (FBS) and penicillin-streptomycin. Primary HFK cells were derived from neonatal human foreskins. hTERT-immortalized-HFK (iHFK cells were obtained from Michael Underbrink, University of Texas Medical Branch).

HFK and iHFK cells were grown in EpiLife medium supplemented with calcium chloride (60 μ M), human keratinocyte growth supplement (Thermo Fisher Scientific), or Keratinocyte Growth Medium 2 (PromoCell) supplemented with calcium chloride (60 μ M), SupplementMix, and penicillin-streptomycin. HPV genes were cloned, transfected, and confirmed as previously described (27).

Plasmids

2 \times RFP-NLS (RFP-NLS) was a gift from Emily Hatch and previously described (32) and contains mCherry-TagRFP-NLS in the Gateway vector pDONOR20. GFP-BLM was a gift from Nathan Ellis (Addgene plasmid # 80070 ; <http://n2t.net/addgene:80070>; RRID: Addgene_80070) pLV-LaminB1-GFP/H2B-mCherry was purchased from VectorBuilder and is detailed here (<https://en.vectorbuilder.com/vector/VB210611-1255jkx.html>). (88)

Immunoblotting

After being washed with ice-cold phosphate-buffered saline (PBS), cells were lysed with radioimmunoprecipitation assay (RIPA) lysis buffer (VWR Life Science) supplemented with phosphatase inhibitor cocktail 2 (Sigma) and protease inhibitor cocktail (Bimake). The Pierce bicinchoninic acid (BCA) protein assay kit (Thermo Scientific) was used to determine protein concentration. Equal protein lysates were run on Novex 4-12% Tris-Glycine WedgeWell mini gels (Invitrogen) and transferred to Immobilon-P membranes (Millipore). Membranes were then probed with the following primary antibodies: glyceraldehyde-3-phosphate dehydrogenase (GAPDH) (Santa Cruz Biotechnologies; catalog no. sc-47724), pATR (Thr1989) (58014S, Cell Signaling Technology), ATR (2790S, Cell Signaling Technology), pCHK1 (Ser345) (133D3) (2348S, Cell Signaling Technology), CHK1 (2G1D5) (2360S, Cell Signaling Technology), p300 (Santa Cruz Biotechnologies; catalog no. sc-584), BLM (2742S, Cell Signaling Technology)

and after exposure to the matching horseradish peroxidase (HRP)-conjugated secondary antibody, cells were visualized using SuperSignal West Femto maximum sensitivity substrate (Thermo Scientific).

Immunofluorescence microscopy

Cells were seeded onto either 96-well glass-bottom plates (Cellvis) or etched-coverslips and grown overnight. Cells were fixed with 4% formaldehyde. Then, 0.1% Triton-X solution in PBS was used to permeabilize the cells, followed by blocking with 3% bovine serum albumin in PBS for 30 min. Cells were then incubated with the following: alpha-tubulin (Abcam; catalog no. ab18251), α -tubulin (3873S, Cell Signaling Technology), p53 (2527S, Cell Signaling Technology), BLM (gift from Matthew Weitzman, Children's Hospital of Philadelphia), CENP-A (3-19) (GTX13939, GeneTex), Lamin B1 (C-12) (sc-365214), Santa Cruz Biotechnology), phospho-Histone H2AX (Ser139) (20E3) (9718S, Cell Signaling Technology), 53bp1 (4937S, Cell Signaling Technology), Histone H3 (acetyl K27) (ab4729, Abcam), Tri-methyl-Histone H3 (Lys9) (D4W1U) (13969T, Cell Signaling Technology), Cleaved Caspase-3 (Asp175) (9661S, Cell Signaling Technology). The cells were washed and stained with the appropriate secondary antibodies: Alexa Fluor 594 goat anti-rabbit (Thermo Scientific; catalog no. A11012) and Alexa Fluor 488 goat anti-mouse (Thermo Scientific A11001). After washing, the cells were stained with 2 μ M 4',6-diamidino-2-phenylindole (DAPI) in PBS and visualized with the Zeiss LSM 770 microscope. Images were analyzed using ImageJ techniques previously described in reference (89).

Detection of BrdU incorporation

Detection of BrdU was performed the same as immunofluorescent cells with the addition of a 30 min incubation with 1.5 M HCl for 30 min between Triton-X and 3% bovine serum

albumin. Primary antibodies as indicated and stained with Alexa Fluor 594 anti-BrdU (BU1/75 (ICR1)) (ab20076, Abcam). After washing, the cells were stained with 2 μ M 4',6-diamidino-2-phenylindole (DAPI) in PBS and visualized with the Zeiss LSM 770 microscope. Images were analyzed using ImageJ techniques previously described in reference (89).

53bp1 detection

Cells were seeded onto etched coverslips and grown overnight. Cells were exposed to 10 μ g/ml of zeocin for 10 min and then washed. 1 hr post zeocin cells were fixed and stained following immunofluorescent microscopy steps above.

Segregation error

Cells were arrested in G1/S phase by culture in 2mM thymidine for 16 hours, washed to release, and grown for 9 hr 10 min in the absence of thymidine to enhance mitotic cells. Cells were shaken into the media, concentrated, and cytocentrifuged onto glass coverslips. Cells were fixed with 4% formaldehyde. Then, 0.1% Triton-X solution in PBS was used to permeabilize the cells, followed by blocking with 3% bovine serum albumin in PBST supplemented with 300mM Glycine for 1 hr. Primary and secondary antibodies were stained for 16 hr and 1 hr 20 min, respectively. After washing, the cells were stained with 2 μ M 4',6-diamidino-2-phenylindole (DAPI) in PBS and visualized with the Zeiss LSM 770 microscope. Images were analyzed using ImageJ techniques previously described in reference (89)

Establishment of RFP-NLS and LaminB1-GFP/H2B-RFP expressing cells and transient expression of BLM-GFP

RFP-NLS expressing iHFK cells were generated by transfecting with the RFP-NLS expression plasmids using Xfect transfection reagent (Takara Bio; 631317). Cells containing RFP-NLS plasmids were selected using 1 μ g/ml puromycin. Drug resistant colonies were pooled

after 10 days. LaminB1-GFP/H2B-RFP expressing iHFK cells were generated by transducing with LaminB1-GFP/H2B-RFP lentivirus according to the manufacturer's protocol then selected with 1 µg/ml puromycin until mock transfected cells ceased proliferation.

Time-Lapse Imaging

Cells were plated into 6-well glass bottom plates (Cellvis) and imaged on a BioTek LionheartFX Automated Microscope with a 20x air objective at 37°C and 5% CO₂ for 30 hrs. Images were captured using Gen5 software (Biotek). Videos were cropped and adjusted for brightness and contrast using ImageJ.

Whole genome mate-pair sequencing

Passage-matched iHFK LXS_N and 8 E6 cells were subjected to whole genome sequencing. DNA was extracted from cells using the Qiagen High Molecular Weight (HMW) DNA extraction kit, library prepped using the Illumina DNA prep library prep kit, and sequenced on an Illumina Novaseq using an SP 250PE v1.5 cartridge, by the manufacturer's specification. The average coverages were 53x and 75x for iHFK LXS_N and 8 E6 cells, respectively. The raw reads were analyzed using a validated pipeline with some modifications (87). Most notably mutations in 8 E6 expressing HFK cells were identified by comparison to the sequencing from vector control cells rather than the reference genome (87). Raw reads were trimmed with trimmomatic v0.40, aligned with BWA v0.7.17 to Genbank reference GRCh37 (RefSeq # GCF_000001405.25), and copy numbers (CN) were calculated with Xcavator, using default parameters (90). The alignment was subjected to structural variant (SV) calling in sVABA using a log odds ratio of 4 and quality score above 30 (91). CN and SV variants were used to determine the likelihood of chromothripsis in Shatterseek with default parameters (68). Confidence was called for each chromosome based on the number of coinciding structural and copy number

variants, the location of genomic breakpoints, and the frequency of all three parameters coinciding.

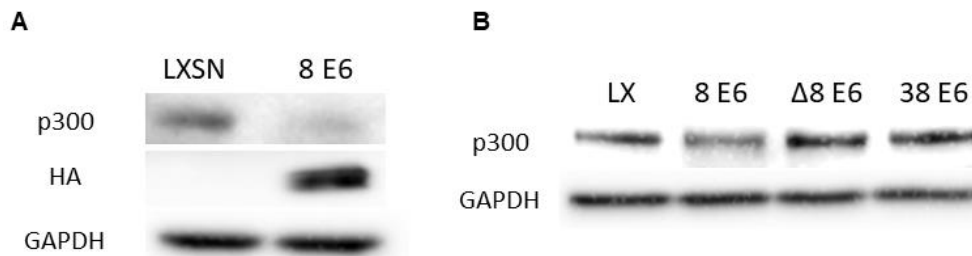
Measurement of protein half-life

iHFK LXSN and 8 E6 cells were grown in 6-well plates until ~80% confluency. Cells were treated with 50 $\mu\text{g/ml}$ cycloheximide for indicated times and whole cell lysates for all time points were harvested together. Western blot analysis same as above.

Statistical analysis.

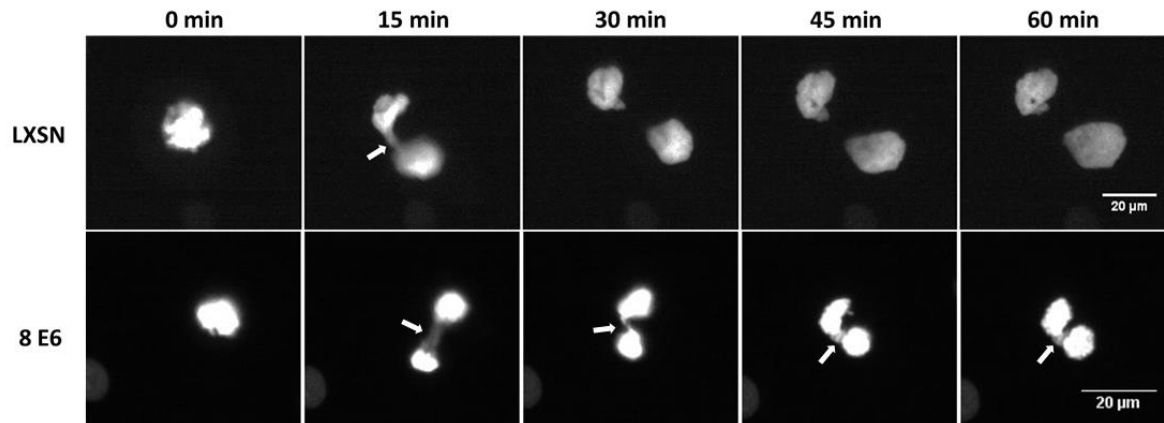
Unless otherwise noted, statistical significance was determined by an unpaired Student's t-test and was confirmed when appropriate by two-way analysis of variance (ANOVA) with Turkey's correction. Only p values of less than 0.05 were reported as significant.

Supplementary Data



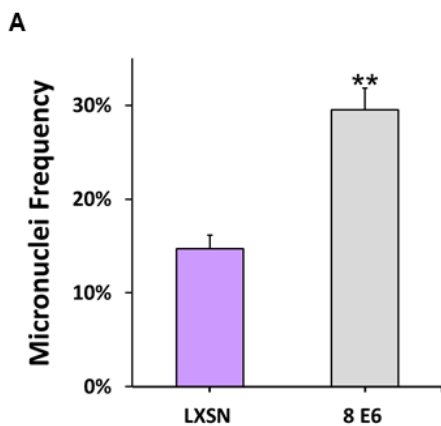
Figures S 5.1. p300 level detected by immunoblot.

(A) Immunoblots of HA-tagged 8 E6 and corresponding p300 staining in iHFK LXSN and 8 E6 cells. (B) Immunoblot analysis of p300 abundance in HFK cells.



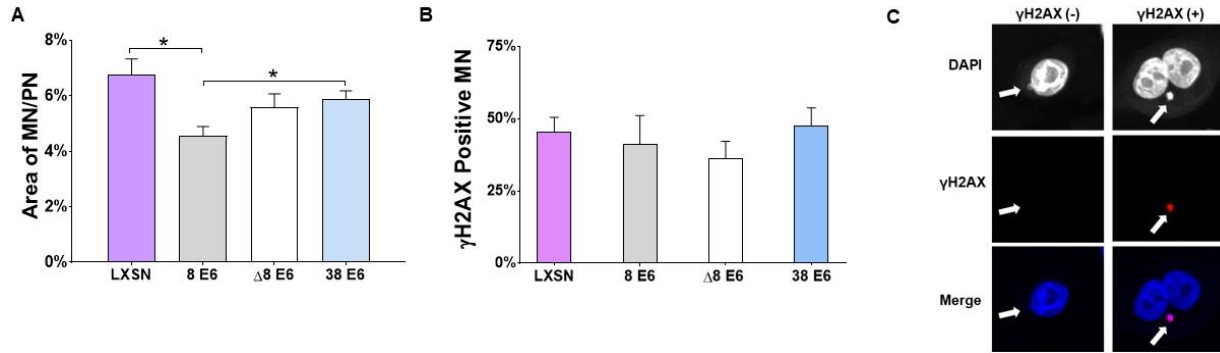
Figures S 5.2. Time-lapse images of anaphase bridge duration.

(A) Representative time-lapse images of chromatin bridge resolution in iHFK LXSN and 8 E6 cells transduced with H2B-mCherry (white). Arrows indicate the presence of an anaphase bridge.



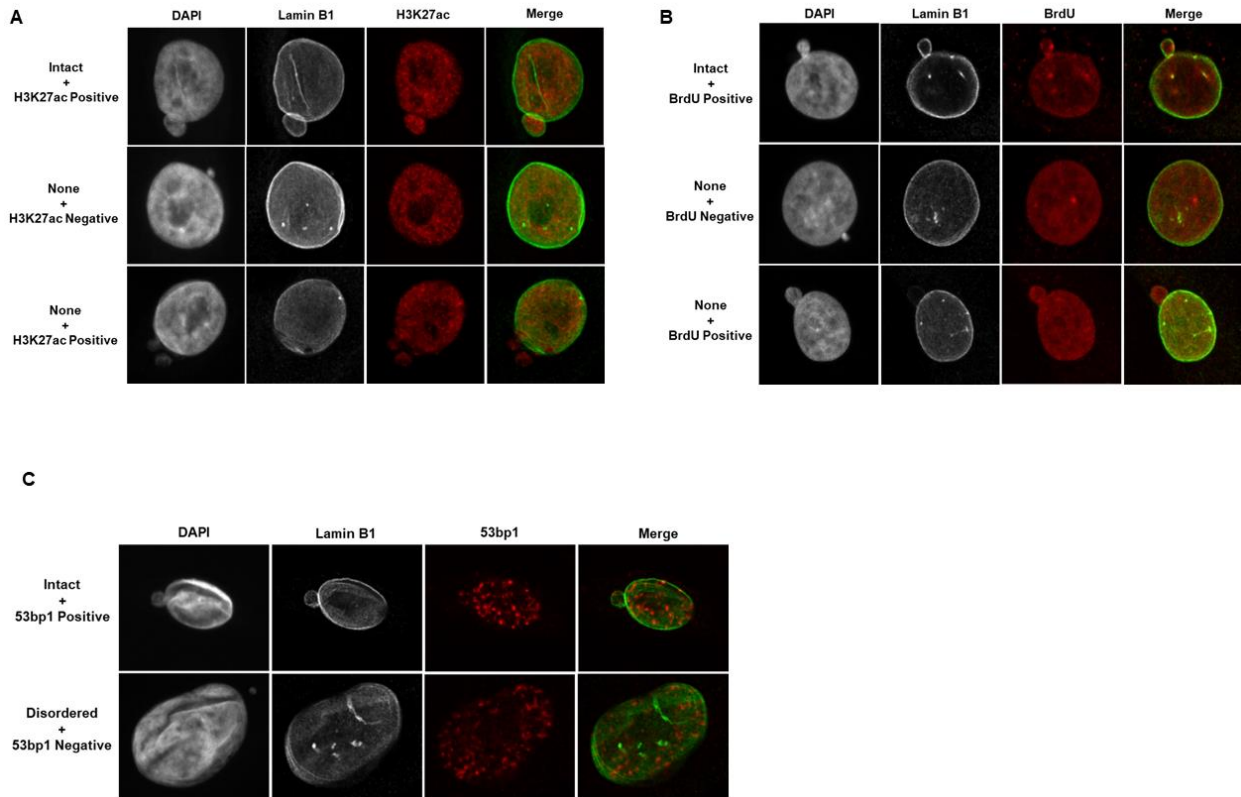
Figures S 5.3. 8 E6 increases micronuclei frequency in U2OS cells.

(A) Micronuclei frequency of U2OS cells. >136 cells/cell line were quantified for micronuclei frequency across three independent experiments. The graph depicts the mean \pm standard error of the mean; Asterisks denotes significant difference relative to LXSN. ** = $p \leq 0.01$ (Student's *t*-test).



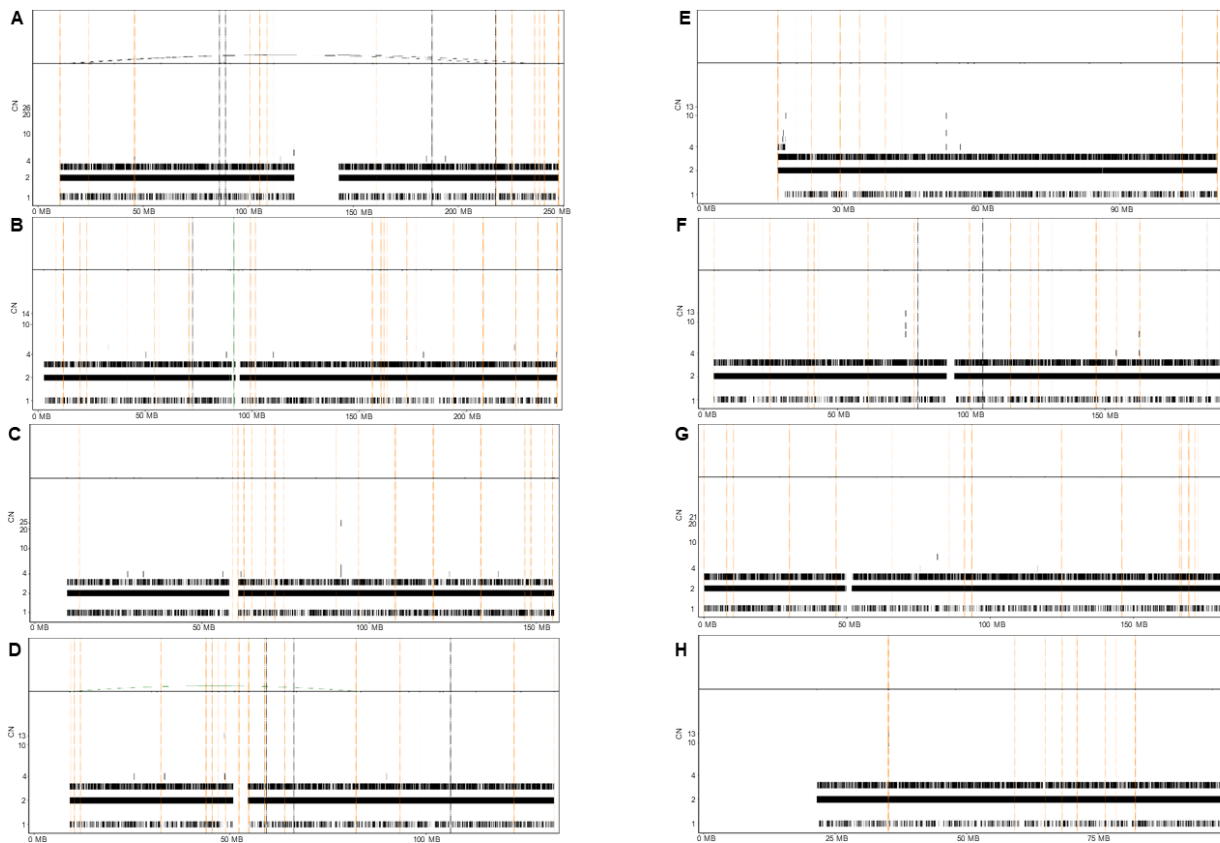
Figures S 5.4. Characteristics of micronuclei in E6 expression HFK cells.

(A) Percentage of micronuclear area normalized to area of primary nucleus in HFK cells expressing β -HPV E6 proteins. At least 150 micronuclei/cell line were quantified across three independent experiments. (B) Percentage of γ H2AX-positive micronuclei in HFK β -HPV E6 cells. At least 75 micronuclei/cell line were quantified across three independent experiments. (C) Representative images of DAPI (blue) stained HFK micronuclei with or without γ H2AX (red). The graph depicts mean \pm standard error of the mean, * = $p \leq 0.05$ (Student's *t*-test). In $\Delta 8$ E6, residues 132 to 136 were deleted. Micronuclei is abbreviated as MN.



Figures S 5.5. Representative images of nuclear activity in micronuclei of varying envelope status.

Representative images iHFK micronuclei (A) with or without acetylated H3K27 (H3K27ac; red) staining and (B) with or without BrdU staining in iHFK cells grouped by micronuclear envelope morphology as determined by Lamin B1 (green) staining. DNA was stained with DAPI (white). (C) Representative images of DAPI (white) stained iHFK micronuclei with or without 53bp1 (red) in cells with indicated micronuclear membrane morphologies as determined by Lamin B1 (green) staining.



Figures S 5.6. Representative chromothripsis plots for each chromothripsis category.

Chromothripsis plots that represent the four clusters from the chromothripsis analysis: High-confidence, Low-confidence, Abundant SVs, and Minimal Instability. All High-confidence chromosomes are shown A) 1, B) 2, C) 7, D) 11, and E) 13. Additionally, one chromosome from each other group is displayed as a representative. Chromosomes F) 3 (Low-confidence), G) 4 (Abundant SVs) and H) 14 (Minimal Instability). Vertical hashed bars show deletion-like events

(orange), head-to-head inversions (black), and tail-to-tail inversions (green). Copy number (CN) variations are indicated by solid black bars ranging from 1-26 as indicated on the y-axis.

Supplementary Movie 1

This movie shows a representative iHFK LXS cell expressing H2B-mCherry that undergoes mitosis with an anaphase bridge lasting 22.5 min. Images were captured every 7.5 minutes.

Supplementary Movie 2

This movie shows a representative iHFK 8 E6 cell (center-right at the start) expressing H2B-mCherry that undergoes mitosis with an anaphase bridge lasting 82.5 min that results in micronuclei formation. Images were captured every 7.5 minutes.

Supplementary Movie 3

This movie shows a representative iHFK LXS cell (on the right) expressing RFP-NLS whose micronucleus loses RFP-NLS expression. Images were captured every 7.5 minutes.

Supplementary Movie 4

This movie shows an iHFK 8 E6 cell (bottommost cell) expressing RFP-NLS whose 2 micronuclei do not lose RFP-NLS expression. Images were captured every 7.5 minutes.

Supplementary Movie 5

This movie shows a representative iHFK LXS cell expressing H2B-mCherry with a micronucleus that does not enter mitosis. Images were captured every 7.5 minutes.

Supplementary Movie 6

This movie shows a representative iHFK 8 E6 cell expressing H2B-mCherry with a micronucleus that enters and completes mitosis. Images were captured every 7.5 minutes.

Acknowledgements

We appreciate KSU-CVM Confocal Core especially Joel Sanneman, for assisting with our immunofluorescence imaging, the Center on Emerging and Zoonotic Infectious Diseases for providing the live cell microscope, Michael Underbrink for providing hTERT-immortalized HFK cells, Emily Hatch for gifting the RFP-NLS plasmid.

Research reported in this publication was supported by the National Institute of General Medical Sciences (NIGMS) of the National Institutes of Health under award number P20 GM130448 and P20 GM103418, the Department of Defense CMDRP PRCRP CA160224, and made possible through generous support from the Johnson Cancer Research Center at Kansas State University. The content is solely the responsibility of the authors and does not necessarily represent the official views of the National Institutes of Health

References

1. Madan V, Lear JT, Szeimies R-M. 2010. Non-melanoma skin cancer. *The Lancet* 375:673–685.
2. Ciężyńska M, Kamińska-Winciorek G, Lange D, Lewandowski B, Reich A, Sławińska M, Pabianek M, Szczepaniak K, Hankiewicz A, Ułańska M, Morawiec J, Błasińska-Morawiec M, Morawiec Z, Piekarski J, Nejc D, Brodowski R, Zaryczańska A, Sobjanek M, Nowicki RJ, Owczarek W, Słowińska M, Wróbel K, Bieniek A, Woźniacka A, Skibińska M, Narbutt J, Niemczyk W, Ciężyński K, Lesiak A. 2021. The incidence and clinical analysis of non-melanoma skin cancer. *Sci Rep* 11:4337.
3. Sung H, Ferlay J, Siegel RL, Laversanne M, Soerjomataram I, Jemal A, Bray F. Global cancer statistics 2020: GLOBOCAN estimates of incidence and mortality worldwide for 36 cancers in 185 countries. *CA Cancer J Clin* n/a.
4. Bray F, Ferlay J, Soerjomataram I, Siegel RL, Torre LA, Jemal A. 2018. Global cancer statistics 2018: GLOBOCAN estimates of incidence and mortality worldwide for 36 cancers in 185 countries. *CA Cancer J Clin* 68:394–424.
5. Guy GP, Machlin SR, Ekwueme DU, Yabroff KR. 2015. Prevalence and Costs of Skin Cancer Treatment in the U.S., 2002–2006 and 2007–2011. *Am J Prev Med* 48:183–187.

6. Fahradyan A, Howell AC, Wolfswinkel EM, Tsuha M, Sheth P, Wong AK. 2017. Updates on the Management of Non-Melanoma Skin Cancer (NMSC). *Healthcare* 5.
7. Lubov J, Labbé M, Sioufi K, Morand GB, Hier MP, Khanna M, Sultanem K, Mlynarek AM. 2021. Prognostic factors of head and neck cutaneous squamous cell carcinoma: a systematic review. *J Otolaryngol - Head Neck Surg* 50:54.
8. Didona D, Paolino G, Bottoni U, Cantisani C. 2018. Non Melanoma Skin Cancer Pathogenesis Overview. 1. *Biomedicines* 6:6.
9. Kiviat NB. 1999. Papillomaviruses in non-melanoma skin cancer: epidemiological aspects. 6. *Semin Cancer Biol* 9:397–403.
10. Orth G. 2008. Host defenses against human papillomaviruses: lessons from epidermodysplasia verruciformis. *Curr Top Microbiol Immunol* 321:59–83.
11. Nunes EM, Talpe-Nunes V, Sichero L. 2018. Epidemiology and biology of cutaneous human papillomavirus. *Clinics* 73.
12. Bandolin L, Borsetto D, Fussey J, Mosto MCD, Nicolai P, Menegaldo A, Calabrese L, Tommasino M, Boscolo-Rizzo P. 2020. Beta human papillomaviruses infection and skin carcinogenesis. *Rev Med Virol* 30:e2104.
13. Tommasino M. 2017. The biology of beta human papillomaviruses. *Virus Res* 231:128–138.
14. Chahoud J, Semaan A, Chen Y, Cao M, Rieber AG, Rady P, Tyring SK. 2016. Association Between β -Genus Human Papillomavirus and Cutaneous Squamous Cell Carcinoma in Immunocompetent Individuals—A Meta-analysis. *JAMA Dermatol* 152:1354–1364.
15. Patel AS, Karagas MR, Perry AE, Nelson HH. 2008. Exposure Profiles and Human Papillomavirus Infection in Skin Cancer: An Analysis of 25 Genus β -Types in a Population-Based Study. *J Invest Dermatol* 128:2888–2893.
16. Weissenborn SJ, Nindl I, Purdie K, Harwood C, Proby C, Breuer J, Majewski S, Pfister H, Wieland U. 2005. Human papillomavirus-DNA loads in actinic keratoses exceed those in non-melanoma skin cancers. *J Invest Dermatol* 125:93–97.
17. Hufbauer M, Akgül B. 2017. Molecular Mechanisms of Human Papillomavirus Induced Skin Carcinogenesis. *Viruses* 9.
18. Howley PM, Pfister HJ. 2015. Beta Genus Papillomaviruses and Skin Cancer. *Virology* 0:290–296.
19. Wendel SO, Wallace NA. 2017. Loss of Genome Fidelity: Beta HPVs and the DNA Damage Response. *Front Microbiol* 8.

20. Meyers JM, Grace M, Uberoi A, Lambert PF, Munger K. 2018. Inhibition of TGF- β and NOTCH Signaling by Cutaneous Papillomaviruses. *Front Microbiol* 9.
21. Viarisio D, Müller-Decker K, Accardi R, Robitaille A, Dürst M, Beer K, Jansen L, Flechtenmacher C, Bozza M, Harbottle R, Voegelé C, Ardin M, Zavadil J, Caldeira S, Gissmann L, Tommasino M. 2018. Beta HPV38 oncoproteins act with a hit-and-run mechanism in ultraviolet radiation-induced skin carcinogenesis in mice. *PLoS Pathog* 14.
22. Dong W, Kloz U, Accardi R, Caldeira S, Tong W-M, Wang Z-Q, Jansen L, Dürst M, Sylla BS, Gissmann L, Tommasino M. 2005. Skin Hyperproliferation and Susceptibility to Chemical Carcinogenesis in Transgenic Mice Expressing E6 and E7 of Human Papillomavirus Type 38. *J Virol* 79:14899–14908.
23. Meyers JM, Uberoi A, Grace M, Lambert PF, Munger K. 2017. Cutaneous HPV8 and MmuPV1 E6 Proteins Target the NOTCH and TGF- β Tumor Suppressors to Inhibit Differentiation and Sustain Keratinocyte Proliferation. *PLoS Pathog* 13.
24. Marcuzzi GP, Hufbauer M, Kasper HU, Weißenborn SJ, Smola S, Pfister H. 2009. Spontaneous tumour development in human papillomavirus type 8 E6 transgenic mice and rapid induction by UV-light exposure and wounding. *J Gen Virol* 90:2855–2864.
25. Schaper ID, Marcuzzi GP, Weissenborn SJ, Kasper HU, Dries V, Smyth N, Fuchs P, Pfister H. 2005. Development of Skin Tumors in Mice Transgenic for Early Genes of Human Papillomavirus Type 8. *Cancer Res* 65:1394–1400.
26. Dacus D, Cotton C, McCallister TX, Wallace NA. 2020. Beta Human Papillomavirus 8E6 Attenuates LATS Phosphorylation after Failed Cytokinesis. *J Virol* 94.
27. Wallace NA, Robinson K, Galloway DA. 2014. Beta Human Papillomavirus E6 Expression Inhibits Stabilization of p53 and Increases Tolerance of Genomic Instability. *J Virol* 88:6112–6127.
28. Dacus D, Riforgiate E, Wallace NA. 2020. β -HPV 8E6 combined with TERT expression promotes long-term proliferation and genome instability after cytokinesis failure. *Virology* <https://doi.org/10.1016/j.virol.2020.07.016>.
29. Ye CJ, Sharpe Z, Alemara S, Mackenzie S, Liu G, Abdallah B, Horne S, Regan S, Heng HH. 2019. Micronuclei and Genome Chaos: Changing the System Inheritance. *Genes* 10.
30. Kisurina-Evgenieva OP, Sutiagina OI, Onishchenko GE. 2016. Biogenesis of micronuclei. *Biochem Mosc* 81:453–464.
31. Naim V, Rosselli F. 2009. The FANCD1 pathway and BLM collaborate during mitosis to prevent micro-nucleation and chromosome abnormalities. *Nat Cell Biol* 11:761–768.
32. Hatch EM, Fischer AH, Deerinck TJ, Hetzer MW. 2013. Catastrophic Nuclear Envelope Collapse in Cancer Cell Micronuclei. *Cell* 154:47–60.

33. Terradas M, Martín M, Hernández L, Tusell L, Genescà A. 2012. Nuclear envelope defects impede a proper response to micronuclear DNA lesions. *Mutat Res Mol Mech Mutagen* 729:35–40.
34. Zhang C-Z, Spektor A, Cornils H, Francis JM, Jackson EK, Liu S, Meyerson M, Pellman D. 2015. Chromothripsis from DNA damage in micronuclei. 7555. *Nature* 522:179–184.
35. Hatch EM, Hetzer MW. 2015. Linking Micronuclei to Chromosome Fragmentation. *Cell* 161:1502–1504.
36. Mammel AE, Hatch EM. 2021. Genome instability from nuclear catastrophe and DNA damage. *Semin Cell Dev Biol* <https://doi.org/10.1016/j.semcdb.2021.03.021>.
37. Crasta K, Ganem NJ, Dagher R, Lantermann AB, Ivanova EV, Pan Y, Nezi L, Protopopov A, Chowdhury D, Pellman D. 2012. DNA breaks and chromosome pulverization from errors in mitosis. *Nature* 482:53–58.
38. Terzoudi GI, Karakosta M, Pantelias A, Hatzi VI, Karachristou I, Pantelias G. 2015. Stress induced by premature chromatin condensation triggers chromosome shattering and chromothripsis at DNA sites still replicating in micronuclei or multinucleate cells when primary nuclei enter mitosis. *Mutat Res Toxicol Environ Mutagen* 793:185–198.
39. Ly P, Cleveland DW. 2017. Rebuilding Chromosomes After Catastrophe: Emerging Mechanisms of Chromothripsis. *Trends Cell Biol* 27:917–930.
40. Perry J, Ashford B, Thind AS, Gauthier M-E, Minaei E, Major G, Iyer NG, Gupta R, Clark J, Ranson M. 2020. Comprehensive Mutational and Phenotypic Characterization of New Metastatic Cutaneous Squamous Cell Carcinoma Cell Lines Reveal Novel Drug Susceptibilities. 24. *Int J Mol Sci* 21:9536.
41. Ashford BG. 2019. The mutational landscape of metastatic cutaneous squamous cell carcinoma. *Dr Philos Thesis Sch Chem Mol Biosci Univ Wollongong* 1–201.
42. Chan K-L, North PS, Hickson ID. 2007. BLM is required for faithful chromosome segregation and its localization defines a class of ultrafine anaphase bridges. *EMBO J* 26:3397–3409.
43. Ke Y, Huh J-W, Warrington R, Li B, Wu N, Leng M, Zhang J, Ball HL, Li B, Yu H. 2011. PICH and BLM limit histone association with anaphase centromeric DNA threads and promote their resolution. *EMBO J* 30:3309–3321.
44. Petsalaki E, Dandoulaki M, Morrice N, Zachos G. 2014. Chk1 protects against chromatin bridges by constitutively phosphorylating BLM serine 502 to inhibit BLM degradation. *J Cell Sci* 127:3902–3908.
45. Snow JA, Murthy V, Dacus D, Hu C, Wallace NA. 2019. β -HPV 8E6 Attenuates ATM and ATR Signaling in Response to UV Damage. *Pathogens* 8:267.

46. Hufbauer M, Cooke J, van der Horst GTJ, Pfister H, Storey A, Akgül B. 2015. Human papillomavirus mediated inhibition of DNA damage sensing and repair drives skin carcinogenesis. *Mol Cancer* 14:183.
47. Wallace NA, Robinson K, Howie HL, Galloway DA. 2012. HPV 5 and 8 E6 Abrogate ATR Activity Resulting in Increased Persistence of UVB Induced DNA Damage. *7. PLOS Pathog* 8:e1002807.
48. Howie HL, Koop JI, Weese J, Robinson K, Wipf G, Kim L, Galloway DA. 2011. Beta-HPV 5 and 8 E6 Promote p300 Degradation by Blocking AKT/p300 Association. *PLoS Pathog* 7.
49. Brooks N, Raja M, Young BW, Spencer GJ, Somerville TC, Pegg NA. 2019. CCS1477: A Novel Small Molecule Inhibitor of p300/CBP Bromodomain for the Treatment of Acute Myeloid Leukaemia and Multiple Myeloma. *Blood* 134:2560–2560.
50. Stephens PJ, Greenman CD, Fu B, Yang F, Bignell GR, Mudie LJ, Pleasance ED, Lau KW, Beare D, Stebbings LA, McLaren S, Lin M-L, McBride DJ, Varela I, Nik-Zainal S, Leroy C, Jia M, Menzies A, Butler AP, Teague JW, Quail MA, Burton J, Swerdlow H, Carter NP, Morsberger LA, Iacobuzio-Donahue C, Follows GA, Green AR, Flanagan AM, Stratton MR, Futreal PA, Campbell PJ. 2011. Massive Genomic Rearrangement Acquired in a Single Catastrophic Event during Cancer Development. *Cell* 144:27–40.
51. Liu S, Kwon M, Mannino M, Yang N, Renda F, Khodjakov A, Pellman D. 2018. Nuclear envelope assembly defects link mitotic errors to chromothripsis. *Nature* 561:551–555.
52. Vietri M, Schultz SW, Bellanger A, Jones CM, Petersen LI, Raiborg C, Skarpen E, Pedurupillay CRJ, Kjos I, Kip E, Timmer R, Jain A, Collas P, Knorr RL, Grellescheid SN, Kusumaatmaja H, Brech A, Micci F, Stenmark H, Campsteijn C. 2020. Unrestrained ESCRT-III drives micronuclear catastrophe and chromosome fragmentation. *Nat Cell Biol* 22:856–867.
53. Rosin MP, German J. 1985. Evidence for chromosome instability in vivo in bloom syndrome: Increased numbers of micronuclei in exfoliated cells. *Hum Genet* 71:187–191.
54. Guo X, Ni J, Liang Z, Xue J, Fenech MF, Wang X. 2019. The molecular origins and pathophysiological consequences of micronuclei: New insights into an age-old problem. *Mutat Res Mutat Res* 779:1–35.
55. Fenech M, Knasmueller S, Bolognesi C, Holland N, Bonassi S, Kirsch-Volders M. 2020. Micronuclei as biomarkers of DNA damage, aneuploidy, inducers of chromosomal hypermutation and as sources of pro-inflammatory DNA in humans. *Mutat Res Mutat Res* 786:108342.
56. Rosefort C, Fauth E, Zankl H. 2004. Micronuclei induced by aneugens and clastogens in mononucleate and binucleate cells using the cytokinesis block assay. *Mutagenesis* 19:277–284.

57. MacDonald KM, Benguerfi S, Harding SM. 2020. Alerting the immune system to DNA damage: micronuclei as mediators. *Essays Biochem* 64:753–764.
58. Terradas M, Martín M, Genescà A. 2016. Impaired nuclear functions in micronuclei results in genome instability and chromothripsis. *Arch Toxicol* 90:2657–2667.
59. Hatch EM, Hetzer MW. 2016. Nuclear envelope rupture is induced by actin-based nucleus confinement. *J Cell Biol* 215:27–36.
60. Hashimoto K, Nakajima Y, Matsumura S, Chatani F. 2010. An in vitro micronucleus assay with size-classified micronucleus counting to discriminate aneugens from clastogens. *Toxicol In Vitro* 24:208–216.
61. Marsh EK, Delury CP, Davies NJ, Weston CJ, Miah MAL, Banks L, Parish JL, Higgs MR, Roberts S. 2017. Mitotic control of human papillomavirus genome-containing cells is regulated by the function of the PDZ-binding motif of the E6 oncoprotein. *Oncotarget* 8:19491–19506.
62. Hoffelder DR, Luo L, Burke NA, Watkins SC, Gollin SM, Saunders WS. 2004. Resolution of anaphase bridges in cancer cells. *Chromosoma* 112:389–397.
63. Kneissig M, Keuper K, de Pagter MS, van Roosmalen MJ, Martin J, Otto H, Passerini V, Campos Sparr A, Renkens I, Kropveld F, Vasudevan A, Sheltzer JM, Kloosterman WP, Storchova Z. 2019. Micronuclei-based model system reveals functional consequences of chromothripsis in human cells. *eLife* 8:e50292.
64. Vargas JD, Hatch EM, Anderson DJ, Hetzer MW. 2012. Transient nuclear envelope rupturing during interphase in human cancer cells. *Nucleus* 3:88–100.
65. Hatch EM. 2018. Nuclear envelope rupture: little holes, big openings. *Curr Opin Cell Biol* 52:66–72.
66. Kwon M, Leibowitz ML, Lee J-H. 2020. Small but mighty: the causes and consequences of micronucleus rupture. 11. *Exp Mol Med* 52:1777–1786.
67. Gekara NO. 2017. DNA damage-induced immune response: Micronuclei provide key platform. *J Cell Biol* 216:2999–3001.
68. Cortés-Ciriano I, Lee JJ-K, Xi R, Jain D, Jung YL, Yang L, Gordenin D, Klimczak LJ, Zhang C-Z, Pellman DS, Park PJ. 2020. Comprehensive analysis of chromothripsis in 2,658 human cancers using whole-genome sequencing. *Nat Genet* 52:331–341.
69. Rollison DE, Viarisio D, Amorrortu RP, Gheit T, Tommasino M. 2019. An Emerging Issue in Oncogenic Virology: the Role of Beta Human Papillomavirus Types in the Development of Cutaneous Squamous Cell Carcinoma. *J Virol* 93.
70. Lambert PF, Münger K, Rösl F, Hasche D, Tommasino M. 2020. Beta human papillomaviruses and skin cancer. *Nature* 588:E20–E21.

71. Gabet A-S, Accardi R, Bellopede A, Popp S, Boukamp P, Sylla BS, Londoño-Vallejo JA, Tommasino M. 2008. Impairment of the telomere/telomerase system and genomic instability are associated with keratinocyte immortalization induced by the skin human papillomavirus type 38. *FASEB J* 22:622–632.
72. Schütze DM, Krijgsman O, Snijders PJF, Ylstra B, Weischenfeldt J, Mardin BR, Stütz AM, Korbel JO, Winter JP de, Meijer CJLM, Quint WGV, Bosch L, Wilting SM, Steenbergen RDM. 2016. Immortalization capacity of HPV types is inversely related to chromosomal instability. *Oncotarget* 7:37608–37621.
73. Plug-DeMaggio AW, Sundsvold T, Wurscher MA, Koop JI, Klingelhutz AJ, McDougall JK. 2004. Telomere erosion and chromosomal instability in cells expressing the HPV oncogene 16E6. *Oncogene* 23:3561–3571.
74. Duensing S, Münger K. 2002. The Human Papillomavirus Type 16 E6 and E7 Oncoproteins Independently Induce Numerical and Structural Chromosome Instability. *Cancer Res* 62:7075–7082.
75. Adam ML, Pini C, Túlio S, Cantalice JCLL, Torres RA, Correia MTDS. 2015. Assessment of the Association Between Micronuclei and the Degree of Uterine Lesions and Viral Load in Women with Human Papillomavirus. *Cancer Genomics - Proteomics* 12:67–71.
76. Cassel APR, Barcellos RB, da Silva CMD, de Matos Almeida SE, Rossetti MLR. 2014. Association between human papillomavirus (HPV) DNA and micronuclei in normal cervical cytology. *Genet Mol Biol* 37:360–363.
77. Marullo R, Werner E, Zhang H, Chen GZ, Shin DM, Doetsch PW. 2015. HPV16 E6 and E7 proteins induce a chronic oxidative stress response via NOX2 that causes genomic instability and increased susceptibility to DNA damage in head and neck cancer cells. *Carcinogenesis* 36:1397–1406.
78. 2000. E6 proteins from diverse cutaneous HPV types inhibit apoptosis in response to UV damage. 4. *Publ Online* 04 Febr 2000 Doi101038sjonc1203339 19.
79. Lanfredini S, Olivero C, Borgogna C, Calati F, Powell K, Davies K-J, De Andrea M, Harries S, Tang HKC, Pfister H, Gariglio M, Patel GK. 2017. HPV8 Field Cancerization in a Transgenic Mouse Model Is due to Lrig1+ Keratinocyte Stem Cell Expansion. *J Invest Dermatol* <https://doi.org/10.1016/j.jid.2017.04.039>.
80. Yang H, Wang H, Ren J, Chen Q, Chen ZJ. 2017. cGAS is essential for cellular senescence. *Proc Natl Acad Sci* 114:E4612–E4620.
81. Glück S, Guey B, Gulen MF, Wolter K, Kang T-W, Schmacke NA, Bridgeman A, Rehwinkel J, Zender L, Ablasser A. 2017. Innate immune sensing of cytosolic chromatin fragments through cGAS promotes senescence. *Nat Cell Biol* 19:1061–1070.

82. Maciejowski J, Hatch EM. 2020. Nuclear Membrane Rupture and Its Consequences. *Annu Rev Cell Dev Biol* 36:85–114.
83. Soto M, García-Santisteban I, Krenning L, Medema RH, Raaijmakers JA. 2018. Chromosomes trapped in micronuclei are liable to segregation errors. *J Cell Sci* 131.
84. He B, Gnawali N, Hinman AW, Mattingly AJ, Osimani A, Cimini D. 2019. Chromosomes missegregated into micronuclei contribute to chromosomal instability by missegregating at the next division. *Oncotarget* 10:2660–2674.
85. Babbe H, McMenamin J, Hobeika E, Wang J, Rodig SJ, Reth M, Leder P. 2009. Genomic instability resulting from BLM-deficiency compromises development, maintenance, and function of the B cell lineage. *J Immunol Baltim Md* 1950 182:347–360.
86. Kaur E, Agrawal R, Sengupta S. 2021. Functions of BLM Helicase in Cells: Is It Acting Like a Double-Edged Sword? *Front Genet* 12.
87. Voronina N, Wong JKL, Hübschmann D, Hlevnjak M, Uhrig S, Heilig CE, Horak P, Kreutzfeldt S, Mock A, Stenzinger A, Hutter B, Fröhlich M, Brors B, Jahn A, Klink B, Geldon L, Sieverling L, Feuerbach L, Chudasama P, Beck K, Kroiss M, Heining C, Möhrmann L, Fischer A, Schröck E, Glimm H, Zapatka M, Lichter P, Fröhling S, Ernst A. 2020. The landscape of chromothripsis across adult cancer types. *Nat Commun* 11:2320.
88. Hu P, Beresten S, van Brabant A, Ye T-Z, Pandolfi P-P, Johnson FB, Guarente L, Ellis NA. 2001. Evidence for BLM and Topoisomerase III α interaction in genomic stability. *Hum Mol Genet* 10:1287–1298.
89. Murthy V, Dacus D, Gamez M, Hu C, Wendel SO, Snow J, Kahn A, Walterhouse SH, Wallace NA. 2018. Characterizing DNA Repair Processes at Transient and Long-lasting Double-strand DNA Breaks by Immunofluorescence Microscopy. *JoVE J Vis Exp* e57653.
90. Magi A, Pippucci T, Sidore C. 2017. XCAVATOR: accurate detection and genotyping of copy number variants from second and third generation whole-genome sequencing experiments. *BMC Genomics* 18:747.
91. Wala JA, Bandopadhyay P, Greenwald NF, O'Rourke R, Sharpe T, Stewart C, Schumacher S, Li Y, Weischenfeldt J, Yao X, Nusbaum C, Campbell P, Getz G, Meyerson M, Zhang C-Z, Imielinski M, Beroukhim R. 2018. SvABA: genome-wide detection of structural variants and indels by local assembly. *Genome Res* 28:581–591.

Chapter 6 - Conclusions and Future Directions

Cutaneous squamous cell carcinoma (cSCC) is among the most prevalent types of cancer, with an increase in cases being reported every year (1–4). While survival rates are high, cSCC treatments cost the US \$4.8 billion annually (5). To ease the physical and economic harm caused by cSCCs, we must identify and mitigate factors that contribute to this disease. It is established that DNA damage from UV exposure is the main factor in cSCC development, but growing evidence suggests that beta genus papillomaviruses (β -HPVs) are associated with carcinogenic development. For example, recurrent β -HPV infections cause cSCC in patients with epidermodysplasia verruciformis (EV) and organ transplant recipients (6, 7). However, it is unclear whether transient β -HPV infections play a similar role in immunocompetent patients (8, 9), where infection is nearly ubiquitous among adults (10, 11). Due to their transient nature, β -HPV are thought to aid UV in facilitating mutations that drive carcinogenesis after viral gene expression ceases. However, several studies suggest that the E6 protein from type 8 β -HPVs (8 E6) may drive cSCC development independent of UV exposure (12–14). Determining the degree to which β -HPV gene expression induces genomic instability can guide the next steps in mitigating cSCC. This chapter focuses on how the data in this dissertation contributes to our understanding of β -HPV E6's role in genomic instability. It also aims to provide future directions based on the findings presented in this dissertation.

Chromosomal Instability After Cytokinesis Failure

In Chapters 3 and 4, we couple comprehensive in silico screens with classic molecular biology approaches to show that 8 E6 dysregulates several aspects of the Hippo pathway. We also demonstrate the contributions of a common cSCC mutation to 8 E6-induced genomic instability. Destabilization of p300 by 8 E6 augments pro-proliferative Hippo pathway gene

expression, leading to increased proliferation. Further, 8 E6-mediated p300 degradation attenuates Lats phosphorylation, causing decreased p53 and cell death after failed cytokinesis. Taken together, these findings support the notion that 8 E6 is capable of reprogramming cellular signaling to increase proliferation in both damaged (15, 16) and healthy cells (17–19). These data also expand our knowledge of p300 biology, establishing a connection to the Hippo pathway.

Binucleated cells are at increased risk of chromosomal instability if they continue to proliferate (20, 21). Despite 8 E6 reducing cell death after cytokinesis failure, it simultaneously leads to increased senescence, suggesting 8 E6 expression may be more mutagenic in certain backgrounds. Studies demonstrate that sun-exposed but physiologically “normal” skin contain a high burden of mutations, with many which are known to drive cSCC growth (22, 23). In silico screens on the most prevalent genes mutated in cSCC allowed us to identify a common cSCC mutation (TERT) that showed potential for overcoming the senescent response to failed cytokinesis. Expression of both TERT and 8 E6 significantly increased sustained proliferation after failed cytokinesis and increased chromosomal instability. These data demonstrate that 8 E6 phenotypes can be altered depending on the genetic background of viral gene expression. Determining which mutations or additional factors synergize or diminish 8 E6-induced phenotypes is an important next step in understanding β -HPV tumorigenicity. HPV8 E7 hyperphosphorylates the tumor suppressor pRb (24, 25), inhibiting its ability to prevent transcription of pro-proliferative genes (26). 8 E6 and E7 are expressed at the same time during infection, making E7 a likely candidate to overcome senescence caused by cytokinesis failure.

Consequences of BLM Reduction

The Bloom syndrome DNA helicase, BLM, is a key genome stabilizer involved in regulating numerous DNA damage repair (DDR) pathways, including resolving anaphase

bridges during mitosis (27). While investigating signaling targets downstream of p300 in Chapter 5, we discovered that 8 E6 reduced BLM abundance by destabilizing p300. Further, 8 E6-mediated BLM reduction led to increased frequency of micronuclei and anaphase bridges, both factors that promote genomic instability (28). Anaphase bridges result from unresolved sister chromatid intertwines (SCIs) that arise as a natural consequence of DNA replication (29). We found that 8 E6 reduced BLM intensity at anaphase bridges, suggesting that lack of bridge dissolution during mitosis is the mechanism behind increased bridge frequency. However, BLM also functions in earlier steps of the cell cycle, specifically in DNA repair and resolution of replication intermediates (30). This makes it unclear whether the increase in anaphase bridge frequency is due to BLM's mitotic role or a consequence of BLM functions earlier in the cell cycle. The latter can be determined by observing whether 8 E6's reduction of BLM increases sister chromatid exchange, a destabilizing consequence associated with a lack of resolving replication intermediates by BLM (31, 32). Either of these scenarios supports the idea that 8 E6 promotes genome destabilization by altering cell signaling independent of UV exposure.

Another genome protecting role of BLM is its involvement in the early stages of double-stranded break (DSB) repair pathway choice (27). Studies show that BLM protects against destabilizing events by preventing cells from choosing the error-prone alternative end-joining (A-EJ) DSB repair pathway (33, 34). Further, A-EJ is more likely to occur in the absence of functional canonical DSB repair pathways (35–37). A recent study from our lab demonstrates that 8 E6 disrupts canonical DSB repair pathways and causes a significant increase in genome instability after repair, suggesting the usage of an error-prone pathway (38). Taken together, these data suggest that 8 E6-mediated destabilization of p300 forces cells to switch to A-EJ by

disrupting canonical DSB repair and reducing BLM abundance, thereby promoting genomic instability.

Micronucleus Formation

Studies on BLM deficiency show that reduced BLM leads to a higher frequency of micronuclei (39, 40). We validate these findings, demonstrating that 8 E6's augmentation of micronuclei frequency can be at least partially rescued by exogenous BLM expression. However, despite 8 E6's p300-dependent reduction of BLM, the mutant 8 E6 (Δ 132-136) that can no longer bind and destabilize p300 also shows increased micronuclei frequency. This suggests that 8 E6 can cause micronuclei via multiple avenues and that at least one of them is independent of its ability to bind p300. Among the numerous routes that can lead to a micronucleus forming (over 15 of them) (41), 8 E6's promotion of abnormal centrosomes (42, 43) is the only phenotype that isn't entirely dependent on p300 destabilization.

Micronuclei are inherently prone to envelope rupture (28, 44). Envelope rupture allows the cytosolic DNA sensor, cGAS, to access micronuclear DNA (45, 46), prompting the activation of the cGAS-STING pathway and induction of apoptosis and senescence (47–50). We found 8 E6-induced micronuclei were more likely to lack micronuclear envelopes. However, 8 E6 reduced the accumulation of senescence and apoptosis markers in cells with micronuclei compared to vector control cells. Further time-lapse imaging demonstrated that 8 E6 expression allowed cells with micronuclei to complete mitosis more often. These data suggest that 8 E6 may be attenuating cGAS-STING signaling towards micronuclei. These findings, while noteworthy in and of themselves, raised several questions regarding 8 E6's promotion of micronuclei. What is the fate of 8 E6-induced micronuclei? How often do they persist as micronuclei rather than reincorporate into the primary nucleus? Do aspects like the size of micronucleus, content (whole

or piece of chromosome), and envelope status affect reincorporation, a necessary step in chromothripsis?

Mutational Signatures

We found that 8 E6 promoted chromothripsis in 9 chromosomes after performing whole genome sequencing on passage-matched 8 E6 and vector control immortalized keratinocytes. Of note is the high frequency of copy number oscillations and short length of changed fragments compared to previous chromothripsis results. This suggests that 8 E6 is either introducing a distinct virus-specific form of genome instability or that comparison of passage-matched cells changes how chromothripsis is determined during analysis. The few studies to use whole genome sequencing on cSCCs use a standard evaluation of copy number variation frequency (of certain regions) rather than oscillation frequency (51–53). Additionally, these studies show no record of recorded β -HPV status. Further studies are needed to both determine if an 8 E6 mutational signature exists and to determine if it occurs in cSCCs. A recent meta-analysis covering 105 cSCCs across 10 studies identified EP300 (the gene that encodes p300) loss-of-function mutations as a novel driver of cSCC (54). This supports the hypothesis that 8 E6-induced degradation of p300 promotes tumor formation.

Big Picture Ideas

The findings in this dissertation add to the field of knowledge surrounding 8 E6's ability to promote genomic instability without UV exposure. This, however, does not give a reason to remove UV from the equation. Rather, due to β -HPV's prevalence in sun-exposed areas of the skin (55) and connection with sun-exposed skin cancer (56), future research should identify whether the genome destabilizing phenotypes demonstrated in Chapters 3-5 persist, worsen, or cease with UV exposure. Many of the phenotypes presented here have been

dependent on 8 E6's binding and destabilization of p300. Sequence alignments in Chapter 2 suggest that other β -HPVs may also deregulate p300 activity. If β -HPVs are determined to pose a significant risk for cSCC development, then, it will need to be determined which β -HPVs represent the highest carcinogenic risk. This will help determine which β -HPVs might be chosen to be administered in a vaccine, the recommended way to prevent other types of HPV malignancies (57–59). Finally, the findings presented throughout are yet to be validated in organotypic rafts and/or animal models. These models are important because β -HPV's life cycle is dependent on the skin's differentiation.

References

1. Madan V, Lear JT, Szeimies R-M. 2010. Non-melanoma skin cancer. *The Lancet* 375:673–685.
2. Ciężyńska M, Kamińska-Winciorek G, Lange D, Lewandowski B, Reich A, Sławińska M, Pabianek M, Szczepaniak K, Hankiewicz A, Ułańska M, Morawiec J, Błasińska-Morawiec M, Morawiec Z, Piekarski J, Nejc D, Brodowski R, Zaryczańska A, Sobjanek M, Nowicki RJ, Owczarek W, Słowińska M, Wróbel K, Bieniek A, Woźniacka A, Skibińska M, Narbutt J, Niemczyk W, Ciężyński K, Lesiak A. 2021. The incidence and clinical analysis of non-melanoma skin cancer. *Sci Rep* 11:4337.
3. Sung H, Ferlay J, Siegel RL, Laversanne M, Soerjomataram I, Jemal A, Bray F. Global cancer statistics 2020: GLOBOCAN estimates of incidence and mortality worldwide for 36 cancers in 185 countries. *CA Cancer J Clin* n/a.
4. Bray F, Ferlay J, Soerjomataram I, Siegel RL, Torre LA, Jemal A. 2018. Global cancer statistics 2018: GLOBOCAN estimates of incidence and mortality worldwide for 36 cancers in 185 countries. *CA Cancer J Clin* 68:394–424.
5. Guy GP, Machlin SR, Ekwueme DU, Yabroff KR. 2015. Prevalence and Costs of Skin Cancer Treatment in the U.S., 2002–2006 and 2007–2011. *Am J Prev Med* 48:183–187.
6. Bouwes Bavinck JN, Feltkamp M, Struijk L, ter Schegget J. 2001. Human papillomavirus infection and skin cancer risk in organ transplant recipients. 3. *J Investig Dermatol Symp Proc* 6:207–211.
7. de Jong SJ, Imahorn E, Itin P, Uitto J, Orth G, Jouanguy E, Casanova J-L, Burger B. 2018. Epidermodysplasia Verruciformis: Inborn Errors of Immunity to Human Beta-Papillomaviruses. *Front Microbiol* 9.

8. Rollison DE, Viarasio D, Amorrortu RP, Gheit T, Tommasino M. 2019. An Emerging Issue in Oncogenic Virology: the Role of Beta Human Papillomavirus Types in the Development of Cutaneous Squamous Cell Carcinoma. *J Virol* 93:e01003-18.
9. Tommasino M. 2017. The biology of beta human papillomaviruses. *Virus Res* 231:128–138.
10. Antonsson A, Forslund O, Ekberg H, Sterner G, Hansson BG. 2000. The Ubiquity and Impressive Genomic Diversity of Human Skin Papillomaviruses Suggest a Commensalic Nature of These Viruses. *J Virol* 74:11636–11641.
11. de Koning MNC, Weissenborn SJ, Abeni D, Bouwes Bavinck JN, Euvrard S, Green AC, Harwood CA, Naldi L, Neale R, Nindl I, Proby CM, Quint WGV, Sampogna F, Ter Schegget J, Struijk L, Wieland U, Pfister HJ, Feltkamp MCW, The Epi-Hpv-Uv-Ca Group null. 2009. Prevalence and associated factors of betapapillomavirus infections in individuals without cutaneous squamous cell carcinoma. *J Gen Virol* 90:1611–1621.
12. Marcuzzi GP, Hufbauer M, Kasper HU, Weißenborn SJ, Smola S, Pfister H. 2009. Spontaneous tumour development in human papillomavirus type 8 E6 transgenic mice and rapid induction by UV-light exposure and wounding. *J Gen Virol* 90:2855–2864.
13. Hufbauer M, Lazić D, Reinartz M, Akgül B, Pfister H, Weissenborn SJ. 2011. Skin tumor formation in human papillomavirus 8 transgenic mice is associated with a deregulation of oncogenic miRNAs and their tumor suppressive targets. 1. *J Dermatol Sci* 64:7–15.
14. Andrea MD, Rittà M, Landini MM, Borgogna C, Mondini M, Kern F, Ehrenreiter K, Baccarini M, Marcuzzi GP, Smola S, Pfister H, Landolfo S, Gariglio M. 2010. Keratinocyte-Specific Stat3 Heterozygosity Impairs Development of Skin Tumors in Human Papillomavirus 8 Transgenic Mice. 20. *Cancer Res* 70:7938–7948.
15. Jackson S, Harwood C, Thomas M, Banks L, Storey A. 2000. Role of Bak in UV-induced apoptosis in skin cancer and abrogation by HPV E6 proteins. 23. *Genes Dev* 14:3065–3073.
16. Underbrink MP, Howie HL, Bedard KM, Koop JI, Galloway DA. 2008. E6 proteins from multiple human betapapillomavirus types degrade Bak and protect keratinocytes from apoptosis after UVB irradiation. *J Virol* 82:10408–10417.
17. Meyers JM, Uberoi A, Grace M, Lambert PF, Munger K. 2017. Cutaneous HPV8 and MmuPV1 E6 Proteins Target the NOTCH and TGF- β Tumor Suppressors to Inhibit Differentiation and Sustain Keratinocyte Proliferation. *PLoS Pathog* 13.
18. Taute S, Böhnke P, Sprissler J, Buchholz S, Hufbauer M, Akgül B, Steger G. 2019. The Protein Tyrosine Phosphatase H1 PTPH1 Supports Proliferation of Keratinocytes and is a Target of the Human Papillomavirus Type 8 E6 Oncogene. *Cells* 8.

19. Marthaler AM, Podgorska M, Feld P, Fingerle A, Knerr-Rupp K, Grässer F, Smola H, Roemer K, Ebert E, Kim Y-J, Bohle RM, Müller CSL, Reichrath J, Vogt T, Malejczyk M, Majewski S, Smola S. 2017. Identification of C/EBP α as a novel target of the HPV8 E6 protein regulating miR-203 in human keratinocytes. *PLoS Pathog* 13:e1006406.
20. Davoli T, de Lange T. 2011. The causes and consequences of polyploidy in normal development and cancer. *Annu Rev Cell Dev Biol* 27:585–610.
21. Ganem NJ, Storchova Z, Pellman D. 2007. Tetraploidy, aneuploidy and cancer. *Curr Opin Genet Dev* 17:157–162.
22. Martincorena I, Roshan A, Gerstung M, Ellis P, Loo PV, McLaren S, Wedge DC, Fullam A, Alexandrov LB, Tubio JM, Stebbings L, Menzies A, Widaa S, Stratton MR, Jones PH, Campbell PJ. 2015. High burden and pervasive positive selection of somatic mutations in normal human skin. *Science* 348:880–886.
23. Fowler JC, King C, Bryant C, Hall MWJ, Sood R, Ong SH, Earp E, Fernandez-Antoran D, Koeppl J, Dentre SC, Shorthouse D, Durrani A, Fife K, Rytina E, Milne D, Roshan A, Mahububani K, Saeb-Parsy K, Hall BA, Gerstung M, Jones PH. 2021. Selection of Oncogenic Mutant Clones in Normal Human Skin Varies with Body Site. *Cancer Discov* 11:340–361.
24. Caldeira S, Zehbe I, Accardi R, Malanchi I, Dong W, Giarrè M, de Villiers E-M, Filotico R, Boukamp P, Tommasino M. 2003. The E6 and E7 Proteins of the Cutaneous Human Papillomavirus Type 38 Display Transforming Properties. *J Virol* 77:2195–2206.
25. Cornet I, Bouvard V, Campo MS, Thomas M, Banks L, Gissmann L, Lamartine J, Sylla BS, Accardi R, Tommasino M. 2012. Comparative Analysis of Transforming Properties of E6 and E7 from Different Beta Human Papillomavirus Types. *J Virol* 86:2366–2370.
26. Dyson N. 1998. The regulation of E2F by pRB-family proteins. 15. *Genes Dev* 12:2245–2262.
27. Kaur E, Agrawal R, Sengupta S. 2021. Functions of BLM Helicase in Cells: Is It Acting Like a Double-Edged Sword? *Front Genet* 12.
28. Kwon M, Leibowitz ML, Lee J-H. 2020. Small but mighty: the causes and consequences of micronucleus rupture. 11. *Exp Mol Med* 52:1777–1786.
29. Finardi A, Massari LF, Visintin R. 2020. Anaphase Bridges: Not All Natural Fibers Are Healthy. 8. *Genes* 11:902.
30. Manthei KA, Keck JL. 2013. The BLM dissolvasome in DNA replication and repair. *Cell Mol Life Sci* 70:4067–4084.
31. Ellis NA, Lennon DJ, Proytcheva M, Alhadeff B, Henderson EE, German J. 1995. Somatic intragenic recombination within the mutated locus BLM can correct the high

- sister-chromatid exchange phenotype of Bloom syndrome cells. *Am J Hum Genet* 57:1019–1027.
32. Nguyen GH, Dexheimer TS, Rosenthal AS, Chu WK, Singh DK, Mosedale G, Bachrati CZ, Schultz L, Sakurai M, Savitsky P, Abu M, McHugh PJ, Bohr VA, Harris CC, Jadhav A, Gileadi O, Maloney DJ, Simeonov A, Hickson ID. 2013. A small molecule inhibitor of the BLM helicase modulates chromosome stability in human cells. *Chem Biol* 20:55–62.
 33. Grabarz A, Guirouilh-Barbat J, Barascu A, Pennarun G, Genet D, Rass E, Germann SM, Bertrand P, Hickson ID, Lopez BS. 2013. A Role for BLM in Double-Strand Break Repair Pathway Choice: Prevention of CtIP/Mre11-Mediated Alternative Nonhomologous End-Joining. *Cell Rep* 5:21–28.
 34. Gaymes TJ, North PS, Brady N, Hickson ID, Mufti GJ, Rassool FV. 2002. Increased error-prone non homologous DNA end-joining – a proposed mechanism of chromosomal instability in Bloom’s syndrome. *Oncogene* 21:2525–2533.
 35. Sallmyr A, Tomkinson AE. 2018. Repair of DNA double-strand breaks by mammalian alternative end-joining pathways. *J Biol Chem* 293:10536–10546.
 36. Boboila C, Yan C, Wesemann DR, Jankovic M, Wang JH, Manis J, Nussenzweig A, Nussenzweig M, Alt FW. 2010. Alternative end-joining catalyzes class switch recombination in the absence of both Ku70 and DNA ligase 4. *J Exp Med* 207:417–427.
 37. Ceccaldi R, Liu JC, Amunugama R, Hajdu I, Primack B, Petalcorin MIR, O’Connor KW, Konstantinopoulos PA, Elledge SJ, Boulton SJ, Yusufzai T, D’Andrea AD. 2015. Homologous-recombination-deficient tumours are dependent on Pol θ -mediated repair. 7538. *Nature* 518:258–262.
 38. Hu C, Bugbee T, Dacus D, Palinski R, Wallace N. 2022. Beta human papillomavirus 8 E6 allows colocalization of non-homologous end joining and homologous recombination repair factors. *PLOS Pathog* 18:e1010275.
 39. Rosin MP, German J. 1985. Evidence for chromosome instability in vivo in bloom syndrome: Increased numbers of micronuclei in exfoliated cells. *Hum Genet* 71:187–191.
 40. Naim V, Rosselli F. 2009. The FANC pathway and BLM collaborate during mitosis to prevent micro-nucleation and chromosome abnormalities. *Nat Cell Biol* 11:761–768.
 41. Guo X, Ni J, Liang Z, Xue J, Fenech MF, Wang X. 2019. The molecular origins and pathophysiological consequences of micronuclei: New insights into an age-old problem. *Mutat Res Mutat Res* 779:1–35.
 42. Cimini D, Fioravanti D, Salmon ED, Degrossi F. 2002. Merotelic kinetochore orientation versus chromosome mono-orientation in the origin of lagging chromosomes in human primary cells. *J Cell Sci* 115:507–515.

43. Wallace NA, Robinson K, Galloway DA. 2014. Beta Human Papillomavirus E6 Expression Inhibits Stabilization of p53 and Increases Tolerance of Genomic Instability. *J Virol* 88:6112–6127.
44. Hatch EM. 2018. Nuclear envelope rupture: little holes, big openings. *Curr Opin Cell Biol* 52:66–72.
45. Mackenzie KJ, Carroll P, Martin C-A, Murina O, Fluteau A, Simpson D, Olova N, Sutcliffe H, Rainger J, Robertson A, Osborn R, Wheeler A, Nowotny M, Gilbert N, Chandra T, Reijns MAM, Jackson AP. 2017. cGAS surveillance of micronuclei links genome instability to innate immunity. *Nature* 548:461–465.
46. Harding SM, Benci JL, Irianto J, Discher DE, Minn AJ, Greenberg RA. 2017. Mitotic progression following DNA damage enables pattern recognition within micronuclei. *Nature* 548:466–470.
47. Li C, Liu W, Wang F, Hayashi T, Mizuno K, Hattori S, Fujisaki H, Ikejima T. 2021. DNA damage-triggered activation of cGAS-STING pathway induces apoptosis in human keratinocyte HaCaT cells. *Mol Immunol* 131:180–190.
48. Yang H, Wang H, Ren J, Chen Q, Chen ZJ. 2017. cGAS is essential for cellular senescence. *Proc Natl Acad Sci* 114:E4612–E4620.
49. Chattopadhyay S, Marques JT, Yamashita M, Peters KL, Smith K, Desai A, Williams BRG, Sen GC. 2010. Viral apoptosis is induced by IRF-3-mediated activation of Bax. *EMBO J* 29:1762–1773.
50. Sun F, Liu Z, Yang Z, Liu S, Guan W. 2019. The emerging role of STING-dependent signaling on cell death. *Immunol Res* 67:290–296.
51. Mueller SA, Gauthier M-EA, Ashford B, Gupta R, Gayevskiy V, Ch'ng S, Palme CE, Shannon K, Clark JR, Ranson M, Cowley MJ. 2019. Mutational Patterns in Metastatic Cutaneous Squamous Cell Carcinoma. *J Invest Dermatol* 139:1449-1458.e1.
52. Thind AS, Ashford B, Strbenac D, Gupta R, Clark JR, Iyer NG, Mitchell J, Lee J, Mueller SA, Minaei E, Perry J, Ranson M. 2022. Whole genome analysis reveals the genomic complexity in metastatic cutaneous squamous cell carcinoma. medRxiv <https://doi.org/10.1101/2022.01.10.22269035>.
53. Inman GJ, Wang J, Nagano A, Alexandrov LB, Purdie KJ, Taylor RG, Sherwood V, Thomson J, Hogan S, Spender LC, South AP, Stratton M, Chelala C, Harwood CA, Proby CM, Leigh IM. 2018. The genomic landscape of cutaneous SCC reveals drivers and a novel azathioprine associated mutational signature. 1. *Nat Commun* 9:3667.
54. Chang D, Shain AH. 2021. The landscape of driver mutations in cutaneous squamous cell carcinoma. 1. *Npj Genomic Med* 6:1–10.

55. Hampras SS, Rollison DE, Giuliano AR, McKay-Chopin S, Minoni L, Sereday K, Gheit T, Tommasino M. 2017. Prevalence and Concordance of Cutaneous Beta Human Papillomavirus Infection at Mucosal and Cutaneous Sites. *J Infect Dis* 216:92–96.
56. Howley PM, Pfister HJ. 2015. Beta Genus Papillomaviruses and Skin Cancer. *Virology* 0:290–296.
57. McClung NM, Gargano JW, Park IU, Whitney E, Abdullah N, Ehlers S, Bennett NM, Scahill M, Niccolai LM, Brackney M, Griffin MR, Pemmaraju M, Querec TD, Cleveland AA, Unger ER, Markowitz LE, HPV-IMPACT Working Group. 2019. Estimated Number of Cases of High-Grade Cervical Lesions Diagnosed Among Women - United States, 2008 and 2016. *MMWR Morb Mortal Wkly Rep* 68:337–343.
58. Drolet M, Bénard É, Pérez N, Brisson M, HPV Vaccination Impact Study Group. 2019. Population-level impact and herd effects following the introduction of human papillomavirus vaccination programmes: updated systematic review and meta-analysis. *Lancet Lond Engl* 394:497–509.
59. Patel C, Brotherton JM, Pillsbury A, Jayasinghe S, Donovan B, Macartney K, Marshall H. 2018. The impact of 10 years of human papillomavirus (HPV) vaccination in Australia: what additional disease burden will a nonavalent vaccine prevent? *Eurosurveillance* 23:1700737.